AN INVESTIGATION OF TRANSITION METAL CATALYSTS FOR CYANOHYDRIN HYDRATION: THE INTERFACE OF HOMOGENEOUS AND HETEROGENOUS CATALYSIS

by

EMMA LEIGH DOWNS

A DISSERTATION

Presented to the Department of Chemistry and Biochemistry
and the Graduate School of the University of Oregon
in partial fulfillment of the requirements
for the degree of
Doctor of Philosophy

June 2014

DISSERTATION APPROVAL PAGE

Student: Emma Leigh Downs

Title: An Investigation of Transition Metal Catalysts for Cyanohydrin Hydration: The Interface of Homogeneous and Heterogeneous Catalysis

This dissertation has been accepted and approved in partial fulfillment of the requirements for the Doctor of Philosophy degree in the Department of Chemistry and Biochemistry by:

Dr. Victoria J. DeRose	Chairperson
Dr. David R. Tyler	Advisor
Dr. Darren W. Johnson	Core Member
Dr. Mark H. Reed	Institutional Representative

and

Kimberly Andrews Espy	Vice President for Research and Innovation; Dean of the Graduate School

Original approval signatures are on file with the University of Oregon Graduate School.

Degree awarded June 2014

DISSERTATION ABSTRACT

Emma Leigh Downs

Doctor of Philosophy

Department of Chemistry and Biochemistry

June 2014

Title: An Investigation of Transition Metal Catalysts for Cyanohydrin Hydration: The Interface of Homogeneous and Heterogeneous Catalysis

Acrylic monomers are important materials that represent a large portion of the economy. The current industrial synthesis hydrates cyanohydrins with sulfuric acid, a process which results in large amounts of waste and significant energy costs. A transition metal catalyzed, acid free hydration of cyanohydrins would be beneficial from both economic and environmental standpoints. However, this reaction is challenging, as many catalysts are poisoned by the cyanide released when cyanohydrins degrade. Therefore the development of a catalyst that is resistant to cyanide poisoning is the ideal method to circumvent these difficulties.

This dissertation describes several cyanohydrin hydration catalysts, with an emphasis on nanoparticle catalysts. These are at the interface between the homogeneous and heterogeneous catalysts that have been explored previously for this reaction. Chapter I surveys previous studies on nanoparticle catalysts for nitrile hydration and their implications for the hydration of cyanohydrins.

Chapter II reports on the homogeneous platinum catalysts $[PtHCl(P(NMe_2)_3)_2]$ and $[PtH_2(P(NMe_2)_3)_2]$, exploring secondary coordination sphere effects to enhance nitrile hydration. Chapter III describes another example of this type of complex,

$[PtH_2(P(OMe)_3)_2]$, that forms catalytically active nanoparticles under reaction conditions. Explorations of the reactivity of this catalyst with nitriles and cyanohydrins are also described in this chapter.

Chapter IV investigates a silver nanoparticle catalyst with a water soluble phosphine (1,3,5-triaza-7-phosphaadamantane) ligand for its activity towards the hydration of nitriles and cyanohydrins. The results of the degradation of the nanoparticles in the presence of cyanide are also described. Chapter V reports on the preparation and examination of a solid supported nickel catalyst for cyanohydrin hydration. Finally, Chapter VI describes how these investigations have made progress towards the development of a cyanide resistant nitrile hydration catalyst.

This dissertation includes previously published and unpublished co-authored material.

CURRICULUM VITAE

NAME OF AUTHOR: Emma Leigh Downs

GRADUATE AND UNDERGRADUATE SCHOOLS ATTENDED:

University of Oregon, Eugene
University of Massachusetts, Amherst

DEGREES AWARDED:

Doctor of Philosophy, Chemistry, 2014, University of Oregon
Master of Science, Chemistry, 2010, University of Oregon
Bachelor of Science, Chemistry, 2009, University of Massachusetts
Bachelor of Arts, English, 2009, University of Massachusetts

AREAS OF SPECIAL INTEREST:

Nanoparticles
Catalysis
Green and Sustainable Chemistry

PROFESSIONAL EXPERIENCE:

Graduate Teaching Fellow, Department of Chemistry and Biochemistry, University of Oregon, Eugene, 2009-2010, 2011-2014

Graduate Research Assistant, Department of Chemistry and Biochemistry, University of Oregon, Eugene, 2010-2011

Outreach Intern, New England Water Pollution Control Commission, Lowell, Massachusetts, 2007-2009

GRANTS, AWARDS, AND HONORS:

University of Oregon Chemistry Department Travel Award, 2013

Undergraduate Award in Analytical Chemistry, American Chemical Society, 2008

Commonwealth College Scholarship, Commonwealth College, University of Massachusetts, 2005-2009

Chandler Award for Chemistry Majors, University of Massachusetts, 2008

PUBLICATIONS:

Sherbow, T.J.; Downs, E.L.; Sayler, R.I.; Razink, J.J.; Juliette, J.J.; Tyler, D.R. "Investigation of PTA Stabilized Silver Nanoparticles as Catalysts for the Hydration of Nitriles and Cyanohydrins" Submitted, *ACS Catalysis*, Manuscript Under Review

Downs, E. L. and Tyler, D.R. "Nanoparticle Catalysts for Nitrile Hydration" Submitted, *Coordination Chemistry Reviews*

ACKNOWLEDGMENTS

There are too many people to thank. Thanks to DT for his advice and support throughout my grad school career. I couldn't ask for a better mentor, and I will always remember the adventures in China and the Irish coffees. To all of the Tyler lab members, for keeping up a great environment of intellectual cooperation, while still keeping it fun. Charlie, Jen, Brandy, Spring, Sarah, Chantal, Bryan, Alex, Justin, and Adrian, it was great. Thanks especially to Bryan, my buddy through sixth term, China, and thesis writing. Also to Justin, for always being ready to grab a beer. There were days when that meant a lot.

There were several undergraduates who did great work on this project. Thanks to Rick Sayler and Catherine McKenas, and especially to Toby Sherbow, for all their effort.

Thanks to everyone who aided in my research, especially those who helped me navigate the world of nanoparticles. The Hutch lab: Rick, Ed, ZK, and Adam, thanks for helping me figure it all out. To Mike Strain, Josh Razink, and Lev Zakharov for their knowledge and assistance.

Thank you to all members of BEAM DOWN, original and new. To Lena for always being there with advice, scientific and otherwise, and just always being there. To Michelle for helping me stay sane. To Seth and Alex for reminding me that there is a world outside of the chemistry department. And to all the other awesome friends I've made during my time in Oregon, and everyone who played with me on the Specific Heat. I wouldn't have made it if it weren't for all of you.

Thanks to 16 Tons Café for keeping me fueled during the writing process.

And, of course, to my family. Thanks to you most of all. To my parents, who have always believed in and supported me, even when it meant me moving across the country. To Bizzy and Perry, and Alyssa, you are the people closest to me, even when we live a continent apart. I carry your heart(s) in my heart. I could not have done it without you.

“Aim for the stars. You might miss, but at least you won’t shoot your foot off.”

TABLE OF CONTENTS

Chapter Page

Chapter Page

Chapter Page

Chapter Page

LIST OF FIGURES

Figure .....Page

CHAPTER IV

CHAPTER V

LIST OF TABLES

Table Page

CHAPTER V

LIST OF SCHEMES

Scheme Page

CHAPTER IV

CHAPTER V

CHAPTER I

A REVIEW OF NANOPARTICLE CATALYSTS FOR NITRILE HYDRATION

1.1. Introduction

The catalytic hydration of nitriles to amides is an efficient, atom economical route to amides, which are important synthetic building blocks with a variety of applications. Amide bond formation is a key step in many pharmaceutical syntheses as well as numerous industrial applications.[1] The greatest potential for impact from the greener production of amides comes from the industrial production of acrylate monomers. These amides, esters, and acids are used to make an assortment of commercial polymeric products.[2]

Acrylate monomers such as acrylamide are produced in large quantities every year. In 2011, over two hundred thousand metric tons were produced, and the market is projected to continue increasing at a rate of 3.5% per year.[3] Acrylamide is often converted to acrylic acids and esters, which are used in water treatment as well as a variety of hygiene products, most commonly as the absorbent polymer in diapers. When combined with other alkyl acrylates, they can be used to generate paints and coatings.[2]

Polymethacrylates are in even higher demand, with millions of tons produced per year. A variety of consumer goods are generated from these remarkable polymers. Due to the rigidity imparted by the methyl groups, these hard plastics can be used for commercial products such as windshields, signs, and safety glasses. One particularly ubiquitous example of this class of polymers is poly(methyl methacrylate) (PMMA), marketed as Plexiglas™, of which six million pounds are generated per year.[4]

Acrylic monomers are clearly an important part of our economy. The commonly used industrial processes of converting nitriles to amides, however, presents multiple problems such as high energy demands, waste products, and harsh conditions.[4] Hydration with a weak acid or base is possible, but often results in hydrolysis of the amide bond to form a carboxylic acid side product, as the latter process is more energetically favorable (Scheme 1).[5] The resulting acid lowers the amide yield and necessitates more difficult purification steps before the desired product is obtained.

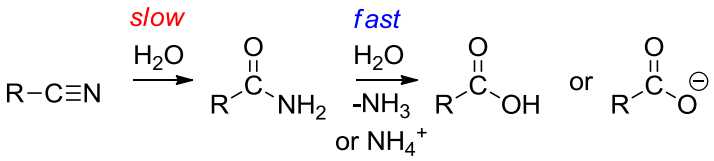

Scheme 1. Hydrolysis of nitriles to carboxylic acids.

Thus the industrial process for the production of methacrylate monomers involves hydration with concentrated sulfuric acid, which does not generate the unwanted acid (Scheme 2). Due to the strongly acidic conditions, however, the amide sulfate salt is formed. Treatment with ammonia affords the desired amide and ammonium sulfate,

which can be sold as fertilizer or recycled to sulfuric acid (Scheme 2, Line 3). The latter route is often used for methacrylic monomers, but requires high temperature pyrolysis and accordingly a large amount of energy.[4]

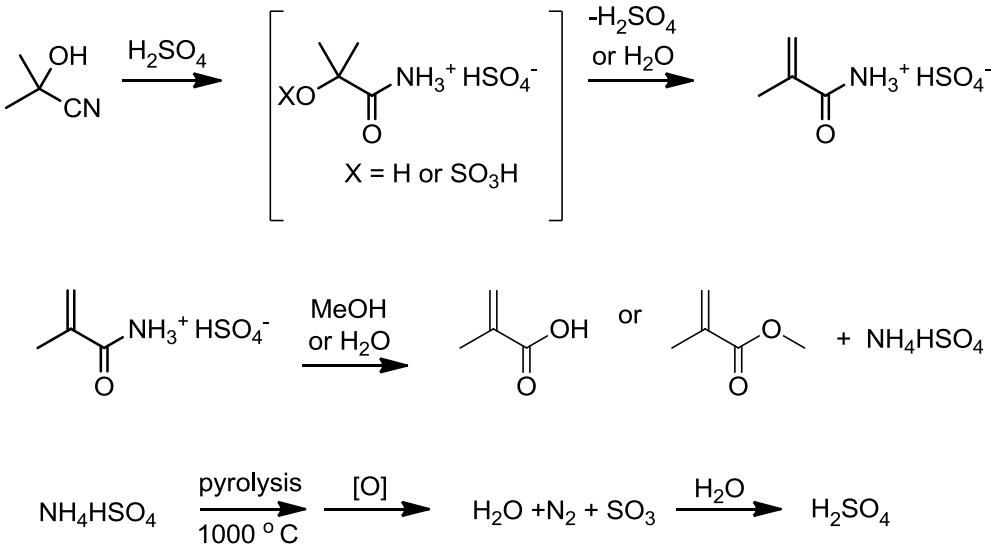

Scheme 2. The acetone cyanohydrin process for the production of methyl methacrylate.

1.1.1. Catalytic Strategies for the Production of Acrylic Monomers

1.1.1.1. Cu Catalysts for Acrylamide Production

For the preparation of acrylamide, efficient Cu transition metal catalysts (Raney Cu, mixed metal Cu oxides, and Cu(I) and Cu(II) salts) have been developed, eliminating the need for concentrated acid.[2,6–8] These Cu catalysts require extensive preparation as well as separation of the acrylamide from the metal, adding unnecessary cost to the process. Additionally, the Cu catalysts are not practical for the hydration of acetone cyanohydrin (ACH), and thus not useful for the production of methacrylates.

1.1.1.2. Enzymatic Hydration

Another alternative process used for acrylonitrile hydration involves nitrile hydratase (an enzyme containing non-heme low spin Fe(III) or non-corrinoid low spin Co(III)) immobilized in a cationic acrylamide based polymer. This process offers high selectivity and greatly lowers energy input.[9] However the efficacy of this catalyst varies greatly for different cyanohydrins, and therefore the technology is not yet practical for large-scale development.

1.1.1.3. The Mitsubishi Process for Acid-free ACH Hydration

MnO_2 has been used for the hydration of ACH, in an acid free process developed by the Mitsubishi Gas Chemical Company.[4,10,11] Instead of discarding the nitrogen of the cyano group in the AHS waste produce, this approach instead recycles that atom to regenerate HCN. ACH is hydrated to 3-hydroxyisobutyramide (HIBAM) in a slurry of MnO_2 with water and acetone. HIBAM is then converted to the methyl ester using methyl formate, generating methyl formamide as a byproduct (Scheme 4). Heating this to high temperatures regenerates HCN and water. This process reduces the cost of MMA production in two ways: 1) a new molecule of HCN is no longer required for each molecule of MMA; and 2) the cost of recycling AHS is removed. Yet the MnO_2 must be pretreated to optimize its structure for activity, adding to the overall cost.[12] Even with treatment, the catalyst efficacy and thus the yield vary between batches. The reasons for this deviation are unknown, and as mechanistic studies with heterogeneous catalysts are not trivial, the reactivity with cyanohydrins has not been well explored. Overall, this new ACH process is less cost effective than the current industrial process.

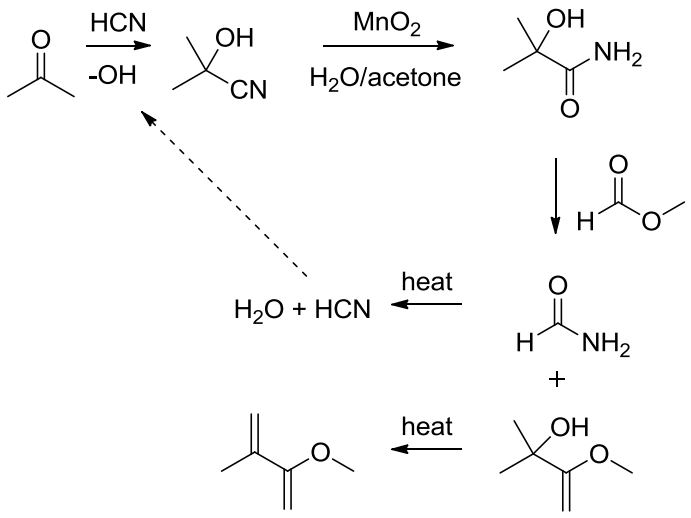

Scheme 3. The overall Mitsubishi Process for MMA production.

1.2 Studies of Nitrile Hydration Catalysts

Small improvements in the production of acrylic monomers could generate large savings in production costs as well as decrease the environmental and health risks. As such, significant progress has been made towards finding an efficient regioselective transition metal catalyst for hydrating acrylonitrile and α-hydroxy nitriles (cyanohydrins) to their respective amides.[1,2,5] Much of this work has been devoted to the development of homogeneous catalysts and elucidation of their mechanisms. Several advantages come with this type of catalysis, such as ease of kinetic studies, unhindered contact between the substrate and all catalyst active sites, and the ability to tailor chemical properties.[13]

1.2.1. Homogeneous Catalysts

Homogenous transition metal catalysts of platinum,[14–19] ruthenium, [20–32] molybdenum, [18,33–36] nickel, [37–39] gold, [40,41]osmium,[42–44] cobalt,[45–49] rhodium,[50–52]

palladium,[53–55] irridium,[52,56] and zinc, [57]among others, have been reported for nitrile hydration; however none of these has yet proven practically useful. The few homogeneous catalysts tested for the hydration of cyanohydrins have shown a susceptibility to cyanide poisoning. As ACH is in an equilibrium with acetone and HCN (Scheme 4), even those particularly active catalysts such as $[PtH\{P(PMe_2O)_2\}\{PMe_2OH\}]$[18] and $[RuCl_2(\eta^6\text{-}p\text{-cymene})\{P(NMe_2)_3\}]$[26] cannot be used in the ACH hydration process. Furthermore, these catalysts are often air sensitive and require the use of air-free techniques, as well as organic solvents. Finally, to be an industrially viable catalyst requires high turnover numbers (TON) and thus recyclability. Although homogeneous catalysts often display higher turnover frequencies (TOF) compared to heterogeneous ones, separation of these complexes from the products presents a daunting challenge, which would greatly increase costs.

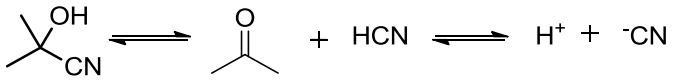

Scheme 4. Equilibrium of ACH and acetone.

1.2.2. Heterogeneous Catalysts

Similarly, an array of heterogeneous catalysts has been tested. These include multiple metal oxides which have been used to great effect, such as MnO_2,[58–62] cobalt spinels (Co_3O_4),[59,63] and CeO_2.[64,65] Several solid supported Ru catalysts have been reported as well.[28] These include $Ru(OH)_x/Al_2O_3$[66], Ru supported hydroxyapatite

($RuCl_2Ca_8(PO_4)_6(OH)_2$)[67], and Ru on Nafion and Amberlite solid resins[68,69] Heterogeneous catalysts are, by nature, easier to separate and recycle than many homogeneous nitrile hydration catalysts. Yet in general they require harsher conditions (e.g. higher temperatures and pressures). Also, since not all active sites are accessible to the substrate with this type of catalyst, larger amounts of the active transition metals, often precious materials such as Ru, could be required, thus the catalysts often display lower TOFs. This could be prohibitive for industrial scale implementation of such catalysts.

1.2.3. Nanocatalysis

Nanocatalysis represents a bridge between heterogeneous and homogeneous catalysis, offering unique opportunities for the development of new nitrile hydration catalysts.[70] Nanoparticles (NPs) are often insoluble (or can easily be made so), and thus easily separated from reaction media, solving one of the largest problems faced with homogeneous catalysts. Yet the high surface area offered by these structures also mimics the high availability of active sites of homogeneous catalysts, often mitigating the low TOFs suffered by heterogeneous catalysts.[13] Furthermore, by changing the size, shape, and stabilizing agent (or support) of NP catalysts, the properties can be tuned.[71] While NP catalysts have been used to catalyze a variety of reactions, only a handful of NP nitrile hydration catalysts have been reported (Table 1).[72–81] To the best of our knowledge, no examples of cyanohydrin hydration with NP catalysts have been reported.

1.3. An Overview of Nanoparticle Nitrile Hydration Catalysts

This review is intended to provide an in depth look at existing NP nitrile hydration catalysts, with an emphasis on how they might be used for the hydration of cyanohydrins. A discussion of the various catalysts and their beneficial properties is undertaken, along with suggestions for the design of a new generation of cyanohydrin hydration catalysts.

A list comparing the catalytic activity of the available examples of NP nitrile hydration catalysts has been compiled (Table 1). As the hydration of benzonitrile to benzamide is often used as a model reaction for these catalysts, this reaction was used for evaluation. In many cases, TOF values were not available, and for these examples the values listed in the table were calculated from available data. Calculating TOF values is often complicated for NP catalysts, as it can be difficult to determine the number of active sites available for catalysis. Therefore the most appropriate way to determine the TOF values is taking into account the total amount of metal used. These entries provide data on how metal, size, stabilizing agents, and other factors affect catalytic activity.

A final note: This overview focuses on *intentional* nanoparticle catalysts for nitrile hydration reactions. There are many examples of supposed homogeneous catalysts where the active species is, in fact, a nanoparticle catalyst. No examples of this type of reactivity are known for nitrile hydration catalysts, and thus such reactions are not discussed here.

Table 1. Summary of selected data available for benzonitrile hydration with nanoparticle nitrile hydration catalysts.

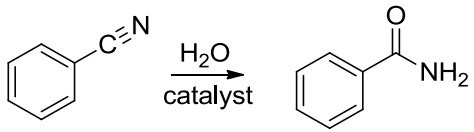

Entry	Metal	Stabilization	Size (nm)	Temperature	Mol % catalyst	TOF (mol/mol catalyst h)	Comments	Hydrate aliphatics?	Reference
1	Palladium	poly(N-vinyl-2-pyrrolidone) (PVP) (ligand)	1.8	180	5	1.2	Only functional in the presence of an oxygen containing copper compound (CuO, $CuSO_4$).	propionitrile	73
2	Platinum	PVP (ligand)	1.5	180	5	0.46	Only functional with copper compounds (CuO, $CuSO_4$)	Not tested	73
3	Palladium	Carbon (solid support)	6.5	120	2	1.8	Only functions in the presence of O_2	Pentanonitrile, hexanonitrile	78
Entry	Metal	Stabilization	Size	Temperature	Mol % catalyst	TOF (mol/mol	Comments	Hydrate aliphatics?	Reference

			(nm)			catalyst h)			
4	Nickel	Hydrotalcite ($Mg_6Al_2(CO_3)(OH)_{16} \cdot 4H_2O$)	1-4	120	5	1.7		acrylonitrile	79
5	Silver	hydroxy-apatite ($Ca_5(PO_4)_3(OH)$) (solid support)	7.6	140	3	11	Airfree conditions required.	no	73
6	Silver	PVP (ligand)	100	150	0.3	333	Toluene cosolvent	no	74
7	Silver	SiO_2 (support)	17	160	3	0.38	Oxygen atoms adsorbed to the surface enhance catalytic activity	Pentanonitrile, hexanonitrile	81

Entry	Metal	Stabilization	Size (nm)	Temperature	Mol % catalyst	TOF (mol/mol catalyst h)	Comments	Hydrate aliphatics?	Reference

8	Silver	PTA (ligand)	4	90	0.5	0.86	Form active $Ag(CN)_2$ complexes in the presence of cyanohydrins	no	Chapter IV
9	Silver	Fe_3O_4 microspheres (NP support)	12	150	3	5.6	Also used for reduction of nitro compounds	Acetonitrile, acrylonitrile	75
10	Gold	TiO_2 (support)	1.7	60	1	25	Usable at room temperature	yes	80
11	Ru(OH)	On magnetic silica NPs (NP support)	15-30	100	3	44	Reaction done under microwave radiation.	Acetonitrile, acrylonitrile	77

1.3.1. Group 10

1.3.1.1. Palladium and Platinum

The first reported example of nitrile hydration by a nanoparticle catalyst is from a short letter published by Oshiki and co-workers in the Japanese journal *Chemistry Letters*.[72] They prepared water soluble palladium and platinum nanoparticles with a water soluble polymer, poly(N-vinyl-2-pyrrolidone) (PVP), as a stabilizer (Figure 1).

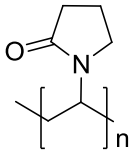

Figure 1. Poly(N-vinyl-2-pyrrolidone) (PVP), a water soluble polymer commonly used as a nanoparticle stabilizer.

The polyol method (ethylene glycol reduction) was used to prepare the catalysts from palladium acetate and platinic acid as metal sources, generating NPs of 1.8 and 1.5 nm, respectively. The particles themselves affected little or no hydration as catalysts, however in the presence of copper compounds containing an oxygen atom ($Cu(acac)_2$, CuO, and $Cu(SO_4)_2$), reasonable hydration of benzonitrile was achieved. The palladium particles had a maximum turnover number (TON) of 19.6 and a turnover frequency (TOF) of 1.2 h^{-1} when the reaction was conducted at 180 ˚C with $CuSO_4$ as a promoter. Other copper sources ($Cu(acac)_2$, CuO, $CuCO_3{\cdot}Cu(OH)_2$) led to reduced yields.

The platinum NPs with $Cu(acac)_2$ as a promoter were far less active, with a TON of 7.4 and a TOF of 0.46 h^{-1}. No explanation was given as to why $CuSO_4$, which was the

most active promoter for the Pd NPs, was not tried as a promoter with the Pt NPs. The reduced activity of the Pt catalysts is possibly due to stronger binding with either the nitriles or the substrate by the Pt surface. Alternatively, the Pt catalyst could be more sensitive to oxidation than its Pd counterpart. Our group has observed that Pt nanoparticles are susceptible to degradation under catalytic conditions (See chapter 3). No recycling studies were conducted on either nanoparticle catalyst.

Copper sources containing a chloride (CuCl, $CuCl_2$) resulted in severe inhibition of the hydration reaction. It is possible that rather than the copper acting as an activator, the anions containing oxygen result in oxygen species adsorbed to the surface of the NPs, creating the potential for a bifucntional mechanism.

Shimzu *et a.l* suggested such a bifucntional mechanism for their Pd NP catalysts on solid carbon supports.[78] In this proposal, the nitrile is activated by the metal surface, while an oxygen atom adsorbed to the metal surface acts as a binding site for water (Scheme 5). This encourages water dissociation and the formation of a hydroxide. As nucleophilic attack on the nitrile carbon is generally considered the slow step in the hydration mechanism, the generation of the more nucleophilic hydroxide results in significant rate acceleration.

Based on the fact that silver surfaces show higher reactivity for water dissociation than clean silver surfaces, Shimzu, *et al.* assumed that a similar increase in reactivity would occur with Pd nanoparticles and allow for hydration of nitriles to amides. The catalyst was prepared through the reduction of Pd/C by H_2 at 500 ˚C. This material was then exposed to air to generate the oxygen adsorbed (O_{ad}) sites to form Pd/$C500_{ox}$. The

particle size was estimated to be 6.5 nm. Particles of similar sizes were prepared with reduction temperatures of 100 and 300 ˚C. The oxygen coverage on the particle surface was estimated through the reaction of CO and O_{ad} to form CO_2.

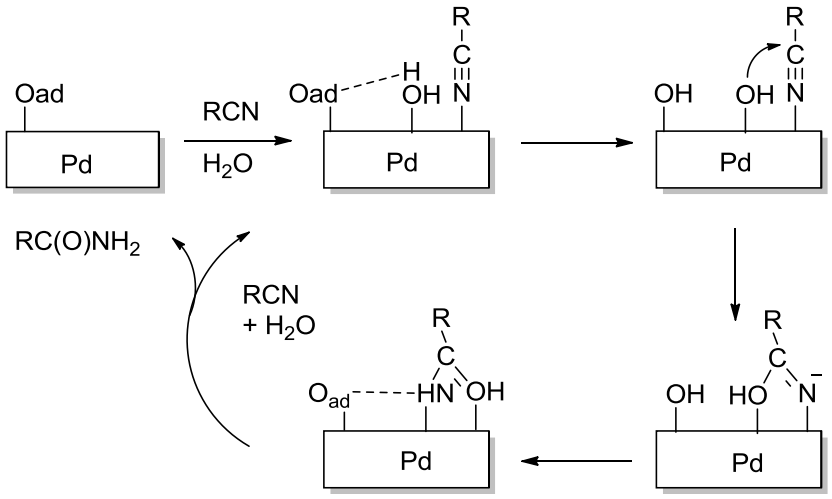

Scheme 5. Proposed reaction mechanism for nitrile hydration on a Pd surface with adsorbed oxygen atoms

It was found that the surface coverage of O_{ad} decreases with the reduction temperature. The authors hypothesize the reduced coverage is a result of lower crystallinity when the reduction occurs at a lower temperature.

These catalysts were tested for activity towards the initial hydration (up to 15%) of acetonitrile to acetamide. The clean Pd surface under air-free conditions was nearly inactive for nitrile hydration, while a surface with both O_{ad} and Pd^0 sites results in increased catalytic activity (Table 2). When the surface coverage of O_{ad} becomes too high, however, the low concentration of Pd^0 sites causes a decrease in conversion. This suggests that the active site involves both species, which was later corroborated by DFT calculations.

Table 2. Comparison of TOFs for Pd/C catalysts based on size and surface coverage of oxygen atoms.

Entry	Catalyst	Size (nm)	O_{ad} coverage ($[O_{ad}]/[Pd_{surf}]$)	TOF (h^{-1})
1	Pd/C-500H	6.5	0	0
2	Pd/C-500ox	6.5	0.5	80
3	Pd/C-300ox	5.3	1	50
4	Pd/100ox	6.1	1.8	15

The most active catalyst, Pd/C-500_{ox}, was tested for the hydration of several different nitrile substrates. It was active for aliphatic nitriles (acetonitrile and propionitrile) as well as aromatic nitriles and highly coordinating heteroaromatic nitriles. For benzonitrile, the TOF was 1.8 h^{-1} over 24h at 135 ˚C. Construction of a Hammett plot revealed that nitriles with an electron withdrawing group in the *para* position were hydrated more quickly than those with an electron donating group, as is common for nitrile hydration catalysts. This result suggests that the rate limiting step of the mechanism is the nucleophilic attack on the nitrile carbon.

Recycling studies were conducted on the Pd/C-500_{ox} catalyst for the hydration of *n*-pentanonitrile to *n*-pentanamide. After reacting at 120 ˚C for 24h the catalyst was separated from the product and retrieved by centrifugation, and an isolated yield of 89% was obtained. After a second portion of nitrile was added, the yield for the same time and

temperature was decreased to 75%. This lower yield was attributed to increased adsorption of oxygen onto the catalyst surface, which reduced the number of active sites available. Catalytic activity was regenerated, however, by again reducing the Pd/C-500_{ox} with H_2 at 500 ˚C.

1.3.1.2. Nickel

While Pd (and to a lesser extent Pt) NPs are effective catalysts for nitrile hydration, these metals are scarcer and more expensive than nickel, their first row counterpart. Subramanian and Pitchumani prepared Ni NPs supported on cheap and easily synthesized hydrotalcite clay ($Mg_6Al_2(CO_3)(OH)_{16} \cdot 4H_2O$).[79] The material (Ni NPs/HT) was characterized by TEM and energy dispersive x-ray analysis (EDX), indicating the nickel content was 5 atom % and the size of the particles ranged from 1-4 nm. Reaction parameters were optimized using benzonitrile as a substrate, and a variety of controls were run. While some amount of hydration was achieved with the hydrotalcite support as well as other heterogeneous nickel catalysts, the yields of benzamide were larger when the nickel nanoparticles are present (23 % and 35%, respectively, vs. 85% at 120 ˚C for 10 h) . The catalyst was inactive at temperatures less than 80 ˚C.

At 120 ˚C, the TON and TOF were 17 and 1.7, respectively, with an 85% yield. Reasonable yields and TONs were afforded for a variety of aromatic nitriles. Acrylonitrile was also hydrated selectively to acrylamide. Notably, heteroaromatic nitriles were hydrated in excellent yields. Strong coordination to the metal center often leads to lower reaction rates with these species due to the difficulty in the dissociation step. However, as is commonly reported with NP nitrile hydration catalysts, these nitriles

were hydrated with comparable rates to the normally more reactive aromatic nitriles. The Ni NPs/HT catalyst was able to be recycled up to three times with minimal loss of activity (TON drops from 17 to 15).

The authors claimed the nitrile binding mode on the NP surface for catalysis is an example of η-2n side-on binding across the nitrile bond, rather than the usual end on binding through donation of the nitrogen lone pair (Figure 2). This binding motif has been observed previously in Ni(0)-nitrile complexes[37] and select other complexes, [82–84]and studies of nitrile coordination complexes suggest that side on nitrile binding instead results in a large shift (200-500 wavenumbers) to a lower frequency.[85] However, in this case, the shift of the CN stretching frequency in the IR spectrum is higher than observed for free CN. Although x-ray photoelectron spectroscopy (XPS) could further elucidate the binding mode of the nitrile, no such study was undertaken.[86]

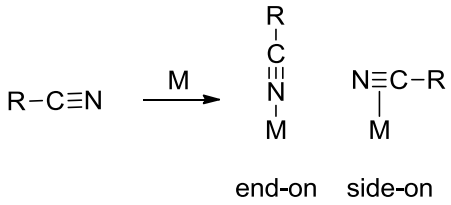

Figure 2. Possible modes of nitrile binding to a metal center.

1.3.2. Group 11

1.3.2.1. Silver

Silver nanoparticles are well characterized, and have a convenient spectroscopic handle in the UV-vis spectrum, with a characteristic absorbance at 400 nm resulting from

the surface plasmon resonance (SPR) of the particle.[87] Additionally, they are relatively inexpensive and easily synthesized. As a result, the most commonly studied NPs catalysts for nitrile hydration are silver.[73–75,81] Another early report of nitrile hydration by nanocatalysis is the hydroxyapatite (HAP) supported silver NP catalyst published by Mitsudome, *et al.* in 2009.[73]

HAP ($Ca_5(PO_4)_3(OH)$) was treated with $AgNO_3$ and subsequently reduced with KBH_4 to generate the AgHAP catalyst, with Ag wt% of 3.3 %. TEM showed Ag NPs with a mean diameter of 7.6 nm with a narrow size distribution on the surface of the HAP. This catalyst was tested for the hydration of benzonitrile to benzamide. Benzamide was produced quantitatively at 140 ˚C in 3 h for a TOF of 11 h^{-1} and a TON of 33. Ag NPs were prepared on other supports but did not give as good results. TiO_2 supported AgNPs resulted in good yields of benzamide, but over-hydrolysis occurred to form the carboxylic acid. MgO, SiO_2, and C supported Ag NPs were less active.

AgHAP was used to hydrate a variety of substituted aromatic nitriles in good yields. Nitriles with electron withdrawing groups in the *para* position were hydrated faster than those with electron withdrawing groups, as is common for nitrile hydration catalyst due to the increased electrophilicity of the nitrile carbon (Scheme 6). Cinnamonitrile, which contains an alkene group, was hydrated selectively with the alkene bond intact. Hydration of aliphatic nitriles was unsuccessful, however. The increased electron density of the Ag(0) surface compared to a complex in a higher oxidation state is likely not activating enough for the hydration of aliphatic nitriles, where the electrophilicity of the carbon is greatly decreased by the electron donating groups. Another drawback to this catalyst system is the air-free conditions necessary for its

activity. Nonetheless, the catalyst was able to be recycled four times with no loss in activity.

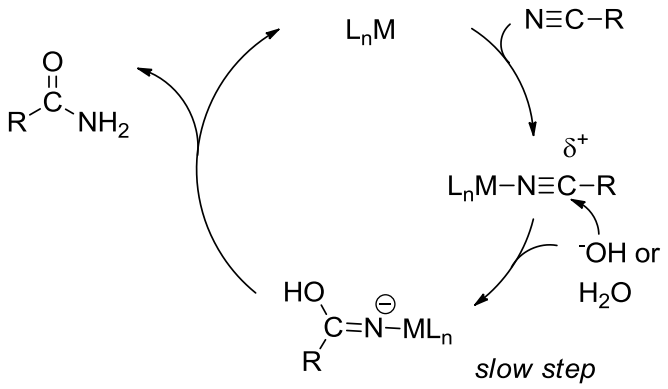

Scheme 6. General mechanism for metal catalyzed nitrile hydration. The rate limiting step involves a nucleophilic attack by a water or hydroxide on the activated nitrile carbon. R groups that are electron withdrawing further activate this carbon, accelerating the rate of the reaction.

Heteroaromatic nitriles were hydrated in excellent yields, with complete conversion taking pace at even higher rates than those for aromatic nitriles. These species were hydrated in under an hour at 140 ˚C, and the reaction went to completion at 40 ˚C (albeit in 48h, a greatly increased amount of time). This increased reactivity is unusual due to the strong coordination of heteroaromatic nitriles to metals. The stronger coordination generally resulted in slower reactions by slowing the release of the nitrile from the catalyst metal center. It is possible that the higher electron density of the metallic NPs results in weaker nitrile coordination and thus increases the rate of this final step in the catalytic cycle.

Microwave dielectric studies of water on the AgHAP surface indicate dissociation occurs to form OH^-, which can then perform a nucleophilic attack on the nitrile carbon.

The Ag NP surface is able to act as a bifucntional catalyst, (similar to mechanism proposed for Pd NPs with adsorbed oxygen (Scheme 5)) activating both the nitrile and water concurrently.

Kim and coworkers prepared unsupported AgNPs with a PVP stabilizing ligand.[74] The resulting particles had an average diameter of 100 nm. Tests with benzonitrile at 150 ˚C resulted in quantitative conversion in 1h (TOF of 333 h^{-1}). Several substituted aromatic nitriles were hydrated as well. Nitriles with a halogen in the *para* position were hydrated in a lower yield than those with an electron donating group *para* (e.g. $–CH_3$). The authors attribute this loss of activity to the electron withdrawing nature of the halogens, positing that electron donating groups accelerate the reaction, which is contrary mechanistically to most published nitrile hydration catalysts (Scheme 6). This is disproved, however, by the complete conversion of *4*-nitro benzonitrile, under the same conditions as were used to achieve quantitative yields of *4*-methyl benzonitrile. NO_2 has a Hammett σ value of 0.81, as compared to 0.24 and 0.26 for Cl and Br, respectively, and -0.14 for a $–CH_3$ group.[88] Thus NO_2 is much more electron withdrawing than either of the halogens, and its complete conversion indicates that electron withdrawing effect does not inhibit hydration. Instead, the low conversion of the halogen substituted benzonitriles was most likely a matter of their low solubility in water. Further, a claim of side on nitrile binding was made, but the IR spectrum does not support such a claim. The catalyst was recycled several times with no loss in activity, and TEM images taken after catalysis showed the particles remain roughly the same size and shape after use.

Acetonitrile and acrylonitrile were also hydrated, but with greatly reduced yields. Although the increased electron density of the NP catalysts as compared to molecular

catalysts results in faster hydration of extremely activated heteroaromatic nitriles, the reverse is true for aliphatic nitriles. The alkyl groups are excellent electron donors, and thus effectively deactivating towards nucleophilic attack on the nitrile carbon. A recurring theme with NP nitrile hydration catalysts is difficulty in hydrating these species.

Satsuma and co-workers also tested a SiO_2 supported Ag NP catalyst with oxygen atoms adsorbed to the surface, in the mode of their palladium nanoparticle catalyst on carbon.[81] Ag NPs with sizes ranging from 17 to 30 nm were prepared by H_2 reduction at different temperatures and exposed to air to generate the O_{ad} sites. The most active of these catalysts, the Ag/SiO_2 NPs of approximately 17 nm, was tested for hydration of a variety of nitriles. Unlike previous Ag NP catalysts, Ag/SiO_2 was able hydrate less reactive aliphatic nitriles in reasonable quantities (90% conversion of pentanonitrile), although a higher catalyst loading was required. As with other NP catalysts, heteroaromatic nitriles were hydrated in excellent yields with high turnover frequencies (667 h^{-1}) at 160 ˚C, most likely due to the strong coordinating ability of these species. The catalyst was similarly very active towards the hydration of aromatic nitriles; the TOF for benzonitrile was 35 h^{-1} with a catalyst loading of 0.05 mol%.

Like the Pd/C catalyst previously reported by the same group, the increased reactivity of Ag/SiO_2 is suggested to be due to the bifucntional mechanism that occurs at the Ag surface (Scheme 6). The metal acts as a Lewis acid and activates the nitrile, while the O_{ad} site acts as a Brønsted base, generating the more nucleophilic hydroxide ion. After recycling, the catalyst showed a decrease in activity, which was attributed to an increase in NP size and polydispersity after catalysis.

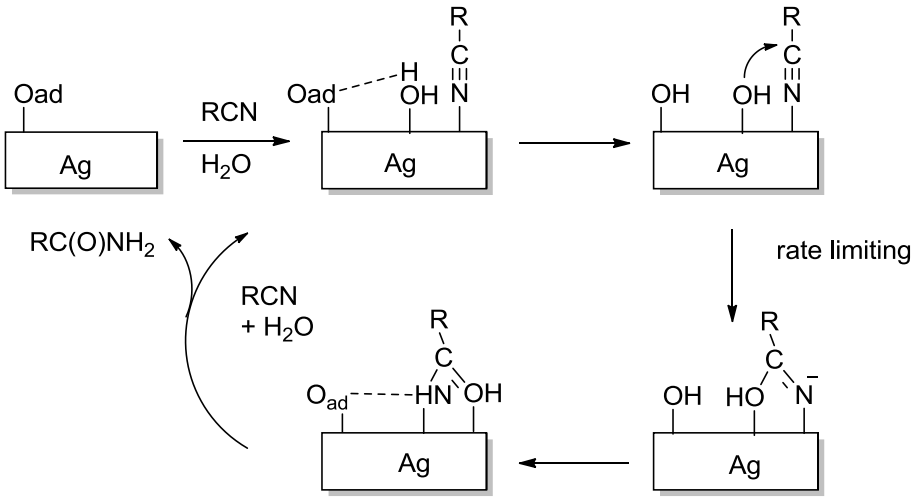

Scheme 7. Proposed nitrile hydration mechanism for Ag/SiO_2 NPs with adsorbed oxygen.

Our group prepared Ag NPs stabilized by a 1,3,5-triaza-7-phosphaadamantane (PTA) (Figure 3) ligand using a sodium borohydride reduction of $AgNO_3$. This straightforward synthesis was completed at 0 ˚C. TEM images showed that the nanoparticles had an average size of 4 nm with reasonable dispersion. This catalyst, in comparison to other silver nanoparticle catalysts, was active under mild conditions, in air and water and at temperatures under 100 ˚C. At 90 ˚C, benzonitrile was hydrated with a TOF of 0.86 h^{-1}, which is comparable to TOFs for other Ag NP catalysts at much higher temperatures. A variety of aromatic nitriles and one heteroaromatic nitrile were hydrated in good yields, but aliphatic nitriles proved unreactive with this catalyst. TEM images taken after catalysis showed that the particles underwent little structural change.

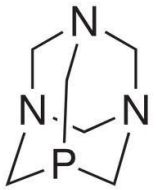

Figure 3. 1,3,5-triaza-7-phosphaadamantane (PTA), a common water soluble phosphine ligand.

The Ag/PTA NP catalyst was tested for the hydration of cyanohydrins, which have not been hydrated with a nanoparticle catalyst. Cyanohydrins are particularly difficult to hydrate in the conditions under which most nitrile hydration catalysts are active (e.g. high pH). However some success has been seen with bifucntional catalysts that are able to activate both the nitrile and the nucleophilic water at the same time. With such a catalyst, $[RuCl_2(\eta^6\text{-}p\text{-cymene})\{P(NMe_2)_3\}]$, ACH was successfully hydrated an unprecedented 15% before catalytic function was shut down by cyanide poisoning.[26] Thus it was hypothesized that AgNP catalysts might display similar reactivity towards cyanohydrins, as they have been proposed to operate via similar bifucntional mechanisms.

Ag/PTA NPs were also tested for the hydration of ACH, and surprising results were observed. The cyanide released by the cyanohydrin equilibrium (Scheme 3) resulted in the disassembly of the silver nanoparticles, as evidenced by the disappearance of the LSPR absorbance at 400 nm in the UV-vis spectrum. This Ag/PTA solution was nonetheless active for the hydration of cyanohydrins, achieving a 9.7 % yield before the ACH substrate decomposed entirely. However the resulting catalyst was still active upon

the addition of a second aliquot of ACH, and remained unpoisoned for a third catalytic cycle. The active catalyst was shown to be a labile silver cyanide complex (Scheme 8).

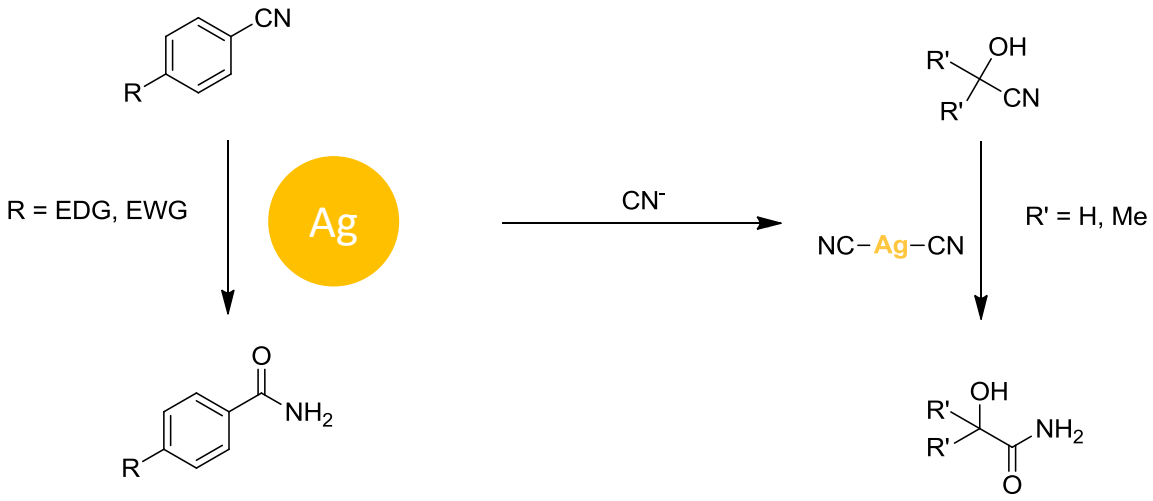

Scheme 8. Hydration reactions with Ag/PTA NPs as a catalyst.

Recently, Park *et.al* reported on the synthesis of Fe_3O_4 supported Ag nanoparticles and their use for the hydration of nitriles to amides.[75] (This catalyst was also usable for the reduction of nitro compounds.)Fe_3O_4 microspheres were prepared through reduction with sodium acetate in ethylene glycol. The material was treated with $AgNO_3$ and the sodium cations were exchanged for silver cations, which were then reduced with $NaBH_4$ to generate the active catalyst. The average diameters of the Ag nanoparticles and Fe_3O_4 microspheres were 12 and 150 nm, respectively, as determined from TEM images (Figure 4).

The hydration of benzonitrile was used as a test reaction. Quantitative conversion was observed in six hours at 150 ˚C and a 3 mol% catalyst loading (TOF = 6 h^{-1}). The catalyst required high temperatures to function, as dropping the temperature even to

100˚C resulted in a significant decrease in conversion (2% in two hours). The catalyst was also tested towards the hydration of other aromatic nitriles with a variety of electron donating and withdrawing groups. No significant trend was observed. With Br, Cl, and CH_3 in the *para* position with respect to the nitrile group, quantitative conversion occurred. The yield was lowered to 40 and 60 percent, however, when NH_2 and NO_2 were the substituents. This is unexpected, as NO_2 is extremely electron withdrawing and further activates the nitrile carbon towards nucleophilic attack, generally the slow step in the nitrile hydration mechanism (Scheme 6).[11,13] It is likely that this result reflects the low solubility of those particular nitriles in water rather than an unusual mechanism. When the substituent was in the *ortho* position with respected to the nitrile, the yield was greatly reduced (13%), likely as a result of steric hindrance.

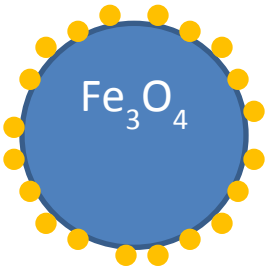

Figure 4. Diagram of the Ag/Fe_3O_4 catalyst. The blue circle represents the iron oxide support and the orange circles represent the Ag NPs.

Heteroaromatic nitriles were not tested, but the catalyst was successfully used to hydrate aliphatic and unsaturated nitriles (acetonitrile and acrylonitrile). After magnetic separation, the catalyst was reused three times for the hydration of benzonitrile with no loss in activity.

1.3.2.2. Gold

Fan and coworkers synthesized a heterogeneous gold nitrile hydration catalyst, with Au NPs of approximately 1.7 nm decorating a support.[80] This catalyst had unprecedented reactivity as an NP nitrile hydration catalyst, with activities under air and at temperatures of 60 ˚C. Benzonitrile was completely converted under these conditions in 15 h for a TOF of 25 h^{-1}. The catalyst was active towards for a variety of aromatic, heteroaromatic, and even aliphatic nitriles. As with other NP catalysts, heteroaromatic nitriles were hydrated with greater rates, while aliphatic species were more recalcitrant and required longer reaction times (TOF 50 h^{-1} for 2-furanylnitrile vs. 4.2 for acetonitrile). Nitriles containing alkenes such as acrylonitrile and cinnamonitrile were hydrated selectively at the nitrile bond in quantitative yields. The catalyst was active at temperatures as low as 25 ˚C.

Catalysis was attempted with Au NPs on a variety of solid supports such as Al_2O_3, SiO_2, and CeO_2, however these were found to be less active than NPs supported on TiO_2. At 140 ˚C, a larger scale synthesis (100 mmol) of pyrazinecarbonamide from pyrazinecarbonitrile was completed, and repeated with the same catalyst 10 times.

Mechanistic studies were also undertaken with this catalyst. When hydration trials were run in D_2O, a significant kinetic isotope effect (k_H/k_D = 1.43) was observed, suggesting that water dissociation could be part of the rate determining step. A bifucntional mechanism with the gold surface or the TiO_2 support facilitating the O-H bond cleavage of water was suggested. A Hammett plot had a positive ρ value of 0.76.[80] Although unsubstantiated claims of side-on nitrile binding were again made, other data

were consistent with the commonly proposed mechanism for catalytic nitrile hydration where the nucleophilic attack on the nitrile carbon is the rate limiting step.

1.3.3. Group 8

1.3.3.1. Ruthenium

One of the main benefits to nanoparticle catalysis is the possibility of catalyst recycling for increased TON, but for well-dispersed colloidal nanoparticles, separation can pose difficulties. Although magnetic nanoparticles allow for the possibility of easy catalyst separation, magnetic materials such as iron oxides are not known for being catalytically active towards nitriles.[2] Varma and coworkers developed ruthenium hydroxide nanoparticles on magnetic silica in a one-step synthesis (Figure 4).[76] $Ru(OH)_x$ NPs and SiO_2 are dispersed over the Fe_3O_4 NP surface. The resulting particles had a size range of 15-30 nm, with a 3.96 weight percent of Ru. The TOF for benzonitrile at 100 ˚C under microwave radiation was 33 h^{-1} and a variety of nitriles were hydrated, although no hydration of unsaturated or aliphatic nitriles was reported. This catalyst was reusable at least three times after magnetic separation from the amide product.

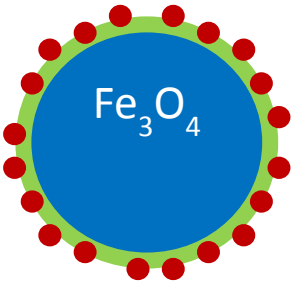

Figure 5. Diagram of the Ru/Fe_3O_4 catalyst. The blue circle represents the iron oxide support, the green represents the SiO_2 layer, and the red circles represent the $Ru(OH)_x$ NPs.

1.3.3.2. NP Supports for Ru Catalysts

This group also prepared amine functionalized magnetic nanoferrite (Fe_3O_4) particles, which were then decorated with $[Ru(OH)]_x$ to form the active catalyst (Scheme 9).[77] The particles had a size range of 11-16 nm. The $Ru(OH)/Fe_3O_4$ catalyst was tested for hydration under microwave irradiation at 130 ˚C. Benzonitrile was hydrated with a TOF of 56.6 h^{-1}. Aromatic, heteroaromatic, and aliphatic nitriles were all hydrated in good yields under these conditions. The catalyst was separated magnetically and reused three times without change in activity.

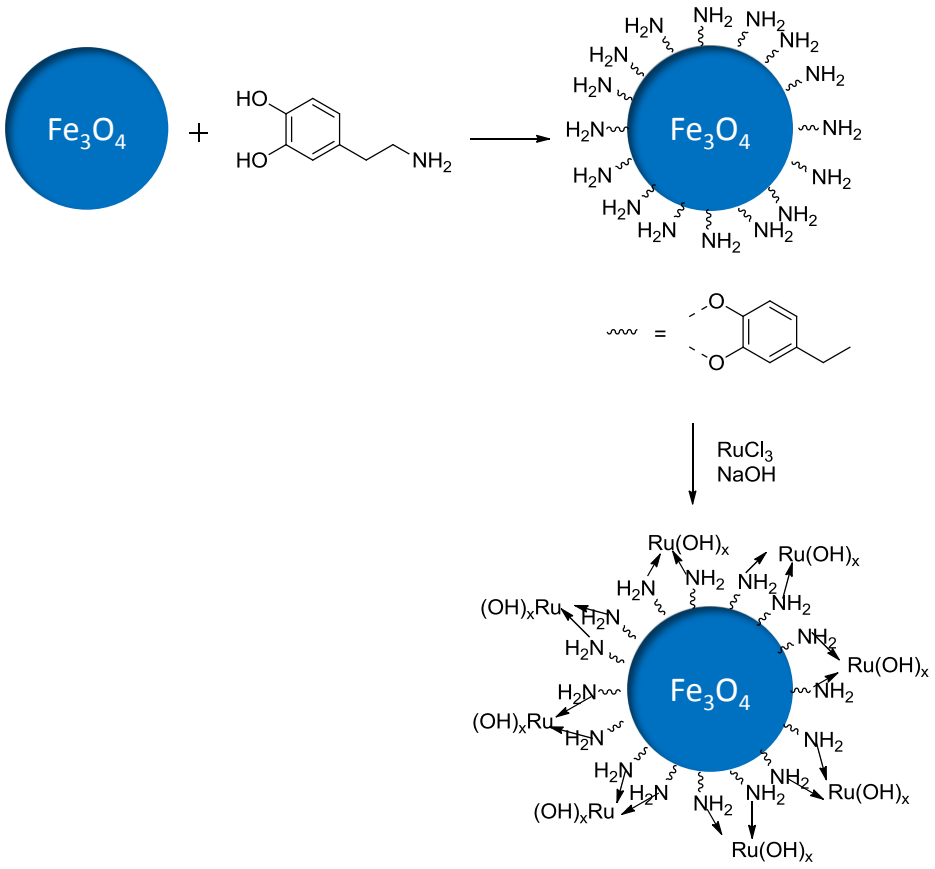

Scheme 9. Synthesis of nanoferrite-$[Ru(OH)_x]$.

While other examples involve the decoration of a magnetic nanoparticle with $Ru(OH)_x$, Cadierno *e. al*. prepared Fe_3O_4 particles with a water soluble ruthenium phosphine complex tethered to the surface.[89] Alkylated PTA was tethered to the surface of the nanoferrites and treated with [{RuCl(μ-Cl){(η-6-*p*-cymene)}$_2$] to generate the Ru functionalized nanoparticles (Figure 5). These were observed to have a size range of 12-20 nm by TEM.

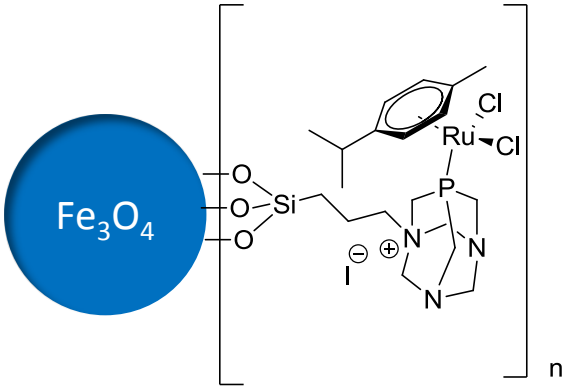

Figure 6. Generic structure of a nanoferrite supported Ru-PTA complex.

Catalytic tests with benzonitrile resulted in a TOF of 42 h^{-1} at 150 ˚C under microwave irradiation, and an extensive list of other nitriles were successfully hydrated as well. Recycling trials were undertaken with the catalyst, but appreciable loss of catalytic activity was observed with five subsequent cycles (TOF drops from 42 to 5 h^{-1}), which was attributed to an unidentified transformation of the Ru complex.

1.4. Thoughts on the Use of NP Catalysts for Cyanohydrin Hydration

Though there are many excellent examples of both heterogeneous and homogeneous nitrile hydration catalysts, no industrially viable catalyst for cyanohydrin

hydration has yet been developed. This is partly due to the drawbacks inherent in each type of catalysis, for example difficulty with recyclability and consequent low TONs for homogeneous catalysts, and the low TOFs of heterogeneous catalyst that are in part a result of the reduced contact between catalyst and substrate.[13] Nanocatalysis is a third option that combines many of the advantages of each of its competitors.

The field of nanocatalysis is quite new, and the use of NPs as catalysts for nitrile hydration even more so. The first example of the formation of amides from nitriles catalyzed by nanoparticles was reported less than a decade ago. Though there are limited examples of such reactions, a few conclusions can be drawn from a thorough study.

Nearly all of the NP nitrile hydration catalysts studies were recyclable, so that even in cases where the TOFs were lower, very reasonable TONs were achieved. This property is very promising for industrial applications. However, many of the catalysts still require relatively high temperatures to be functional.

NPs on solid supports appear to be more active for nitrile hydration than those protected by a ligand shell. This enhanced activity could be a result of the larger amount of surface area available for the nitrile substrate to bind when the particles are not covered by a stabilizing ligand. Or, as this effect seems particularly pronounced with NPs supported on metal oxides, electronic effects of the support could also play a role in the hydration. The support could also play a role in water activation, in a similar fashion to the adsorbed oxygen atoms do in several proposed mechanisms.

In depth reviews of homogeneous nitrile hydration catalysts have suggested the most active catalysts for this reaction able to activate the nitrile and water simultaneously

(Figure 3).[1,2,28] The only known examples of homogeneously catalyzed hydration of cyanohydrins are hypothesized to proceed through this type of mechanism.[20,26,27] A similar mechanism has been proposed for several of the NP catalysts discussed in this review, however instead of requiring a ligand to activate water, the multiple active sites available on the catalyst surface, are able to activate the water in tandem with the nitrile. (These active sites could be additional metal atoms, adsorbed oxygen atoms, or even the support.) The need for phosphine ligands, which are often difficult to synthesize and require special conditions or organic solvents, is thus removed. The potential for such a mechanism makes this class of catalysts look promising for cyanohydrin hydration.

Perhaps the most intriguing aspect of these catalysts, however, is the weaker metal binding that results from the increased electrons density of the metal(0) surfaces (as compared to homogeneous catalysts, which most often contain metals in higher oxidation states). Nearly all of the NP catalysts discussed were able to hydrate heteroaromatic nitriles, a class of molecules that are often problematic in catalysis due to their strong binding, which can cause product inhibition. Furthermore, the rates of hydration for these nitriles were often faster compared even to the very activated aromatic nitriles. This suggests the binding of common nitrile substrates to the metal surfaces is weaker, resulting in a slowing of the first step of the nitrile hydration mechanism and thus the rate of catalysis. The lability of binding to the metal surface suggests that even cyanide may bind reversibly; therefore avoiding the catalyst poisoning that has rendered even the best homogeneous catalysts unusable. This factor makes them excellent candidates for cyanohydrin hydration catalysts.

Choosing the best NP catalyst to test this theory is challenging, however. As Ag NPs are the most studied and best characterized, this would be a reasonable starting point. Yet our group has shown that even the small amounts of cyanide present from the cyanohydrin equilibrium result in the dissolution of AgNPs (Chapter IV). The Au/TiO_2 NPs were the most active towards nitrile hydration, so would be the most likely candidate; nonetheless gold particles have also been shown to fall apart in the presence of cyanide. Pt and Pd NPs were significantly less active than NPs of other metals. Of those already reported NP nitrile hydration catalysts Ni and Ru NPs remain to be studied as catalysts for this difficult reaction. However there are many metals shown to be active for nitrile hydration not yet tested as NPs; it is possible that one of these will be an excellent cyanohydrin hydration catalyst.

The choice of the best candidate for a cyanohydrin hydration catalyst is rendered even more difficult by the lack of characterization of many of these catalysts. In particular, characterization after catalysis is a key to understanding the function of the materials. The harsh reaction conditions used for many of the hydration reactions reported here could result in changes in the NP surfaces or the whole particle, and in order to fully understand the mechanism of catalysis and thus design improved

In conclusion, hydration of nitriles with nanocatalysts is a field with vast unexplored potential. In particular, this new class of nitrile hydration catalysts offers a potentially interesting solution to the challenge of cyanohydrin hydration. The production of α-hydroxy amides and their subsequent transformation to methacrylate monomers using NP catalysts would be of great interest to industry, offering large economic and environmental benefits.

1.5. Summary

This dissertation describes efforts made to catalytically hydrate cyanohydrins using different styles of catalysis. Chapter II describes the synthesis of and catalytic trials with platinum complexes with secondary coordination sphere modifications. Chapter III describes another modified platinum complex and the formation of nanoparticle catalysts from that species under catalytic conditions. Chapters IV and V examine silver and nickel nanoparticle catalysts, respectively. These studies are part of the emerging field of nanocatalysis, which is at the interface of homogeneous and heterogeneous catalysis.

1.6. Co-author Acknowledgements

This dissertation contains published and unpublished co-authored material. David Tyler, my advisor, contributed intellectually to all of the chapters contained in this dissertation. Jerrick Juliette, an industrial partner formerly with Dow Chemical, also contributed to the intellectual development of the project.

Chapter III is co-authored by Richard Sayler, who synthesized some of the platinum complexes. Dr. Richard Glover collected the XPS data.

Authorship of Chapter IV is shared with Tobias Sherbow, who contributed some of the content of the chapter. Richard Sayler synthesized some of the initial nanoparticles tested. Joshua Razink collected the TEM images in this chapter.

Chapter V is co-authored with Trenton Peters-Clark, who synthesized materials under my supervision.

CHAPTER II

NITRILE HYDRATION WITH PLATINUM COMPLEXES: EXPLORING SECONDARY COORDINATION SPHERE EFFECTS

2.1. Introduction

Methyl methacrylate (MMA) and other derivatives of methacrylic acid are important in the production of various commercial polymers, including polymethylmethacrylate (PMMA), which is commonly known as Plexiglass™. The industrial processes used for these materials often include harsh reagents and reaction conditions. For example, the industrial process currently used to produce MMA, the acetone cyanohydrin (ACH) process, uses concentrated sulfuric acid and produces many byproducts (Scheme 1). The most problematic of these is ammonium hydrogen sulfate (AHS) which is produced in large quantities (up to 2.5 kg for each 1 kg of MMA produced). The AHS is recycled to sulfuric acid; however that process requires pyrolysis at temperatures of greater than 1000 ˚C. A synthesis that could achieve hydration of acetone cyanohydrin without the use of sulfuric acid would be beneficial from both industrial and environmental standpoints.

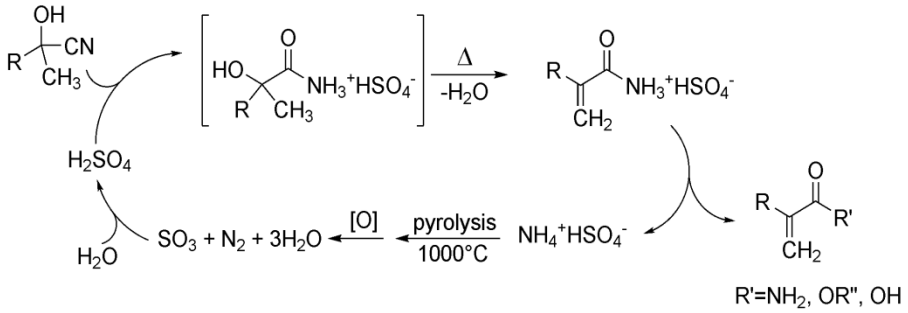

Scheme 1. The ACH process for the production of methyl methacrylate.

A possible method for eliminating sulfuric acid from the production of MMA is catalytic hydration of α-hydroxy nitriles (cyanohydrins) to amides, which can then be converted to the desired ester, amine, or acid. There are a wide range of nitrile hydration catalysts, but in previous studies by our lab, these were shown to be ineffective for cyanohydrin hydration.[1,2] This difficulty is due to the nature of cyanohydrins. In water, cyanohydrins are in equilibrium with their corresponding aldehyde or ketone and HCN (Scheme 2). Upon deprotonation, cyanide is produced and can bind irreversibly to the metal center, poisoning the catalyst.[3] In addition, cyanohydrins are destabilized by basic conditions (for the equilibrium of ACH shown in Scheme 2, $K = 7.16 \times 10^{-2}$ at pH = 3.78-4.68, and K = 68.5 at pH > 8.92.), and many of the best nitrile hydration catalysts are active only at high pH. [1]

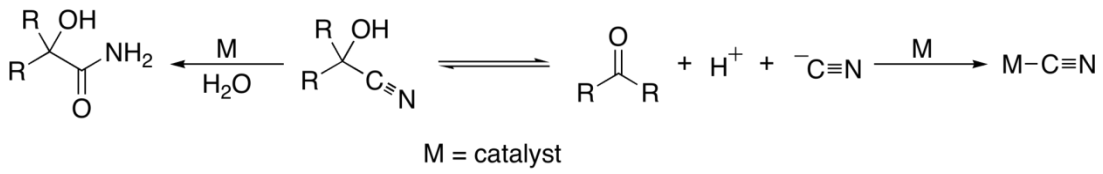

Scheme 2. Possible reactions of cyanohydrins in the presence of a metal catalyst.

One method to avoid base catalyzed degradation of cyanohydrins is to use a catalyst that activates both the nitrile and water simultaneously. Hydroxide is a much better nucleophile than water, thus the necessity for higher pH for most catalysts to be active for nitrile hydration. When the catalyst ligand is capable of hydrogen bonding, a similar effect can be achieved from the activation of water through hydrogen bonding interactions (Figure 1). Large rate accelerations in hydration reactions have been observed and attributed to this phenomenon, known as ligand assisted hydration or bifucntional catalysis(Figure 1).[4–6] Complexes with phosphines ligands containing hydrogen bonding moieties, in particular tris(dimethylamino)phosphine ($P(NMe_2)_3$), have achieved excellent results for nitrile hydration.

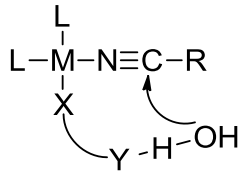

Figure 1. An example of a bifucntional nitrile hydration catalyst. The metal (M) activates the nitrile while the hydrogen bond acceptor on the ligand (Y) activates water.

Our group and others have observed excellent results for nitrile and hydration with ruthenium piano stool complexes using the tris(dimethylamino)phosphine ligand.[2,7–9] We have reported previously on one such homogeneous catalyst, [$RuCl_2(\eta^6$-*p*-cymene){$P(NMe_2)_3$}], that is also active for cyanohydrin hydrations.[2] Unlike related catalysts, this complex was active under acidic conditions (pH 3.5), and the improved stability of cyanohydrins in this environment yielded excellent results. Glycolonitrile (1) and lactonitrile (2) were hydrated fully to their corresponding amides and ACH (3) was

converted to 3-hydroxy-isobutyro nitrile (HIBAM) in 15% yield (Figure 2). The low yield was a result of catalyst poisoning by cyanide.

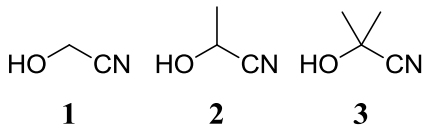

1 **2** **3**

Figure 2. Cyanohydrins tested for hydration.

We hypothesized that this technique could be used to modify other catalyst scaffolds, generating enhanced rates of hydration. The homogeneous catalyst $PtHCl(PMe_3)_2$ hydrated nitriles with a relatively high turnover frequency (TOF) of 90 h^{-1} using NaOH in quantities stoichiometric to the catalyst.[10,11] It had not been tested with cyanohydrins, but due to the basic conditions it would likely be poisoned by cyanide as the ACH degrades. Changing the phosphine ligand on this framework to $P(NMe_2)_3$ could activate the water enough to allow for hydration without the presence of a base. A similar dihydride complex, $PtH_2(P(NMe_2)_3)_2$, was also tested for catalytic activity.

Two novel platinum complexes, $PtHCl(P(NMe_2)_3)_2$ (**4**) and $PtH_2(P(NMe_2)_3)_2$ (**5**) (Figure 3), were synthesized and tested for activity for hydration of a variety of nitriles, including aromatic nitriles and aliphatic nitriles, and cyanohydrins.

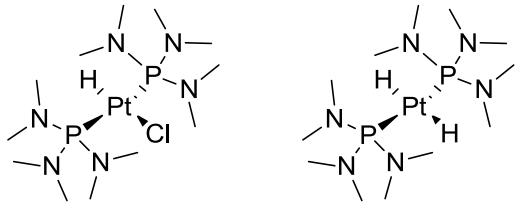

4 **5**

Figure 3. Platinum bis(tris(dimethylamino)phosphine) complexes tested as nitrile hydration catalysts.

2.2. Results and Discussion

2.2.1. Synthesis and Characterization

The complexes were prepared by adding two equivalents of $P(NMe_2)_3$ with Pt Cl_2(COD) to form the *cis* bisphosphine platinum dichloride complex, which was then reacted with sodium borohydride to form the desired complexes **4** and **5**. One equivalent of $NaBH_4$ afforded **4**, and addition of excess reagent resulted in the formation of **5**.

The compounds were isolated through a mixed solvent recrystallization in water and acetone and characterized with ^{1}H and ^{31}P NMR. The coordination of $P(NMe_2)_3$ to Pt was observed in the ^{31}P NMR spectrum through a shift from a single peak at 122 ppm for the free phosphine to a peak at 117 ppm for **4** or 132 ppn for **5** (Figure 4) . Both displayed platinum satellites as a result of coupling with the NMR active isotope ^{195}Pt, $J_{Pt\text{-}P}$ = 3,748 Hz for **4** and $J_{Pt\text{-}P}$ = 3782 Hz for **5** (Figure 4). The chemical shift and Pt-P coupling indicate that phosphorous atoms on **4** are more shielded than those on **5**.[12] Hydrides are very strong σ-donors; when two hydrides are *trans* to each other they are sharing the same orbitals, and thus their *trans* influence is not as strong, resulting in more electron density on the phosphorus atom.[12]

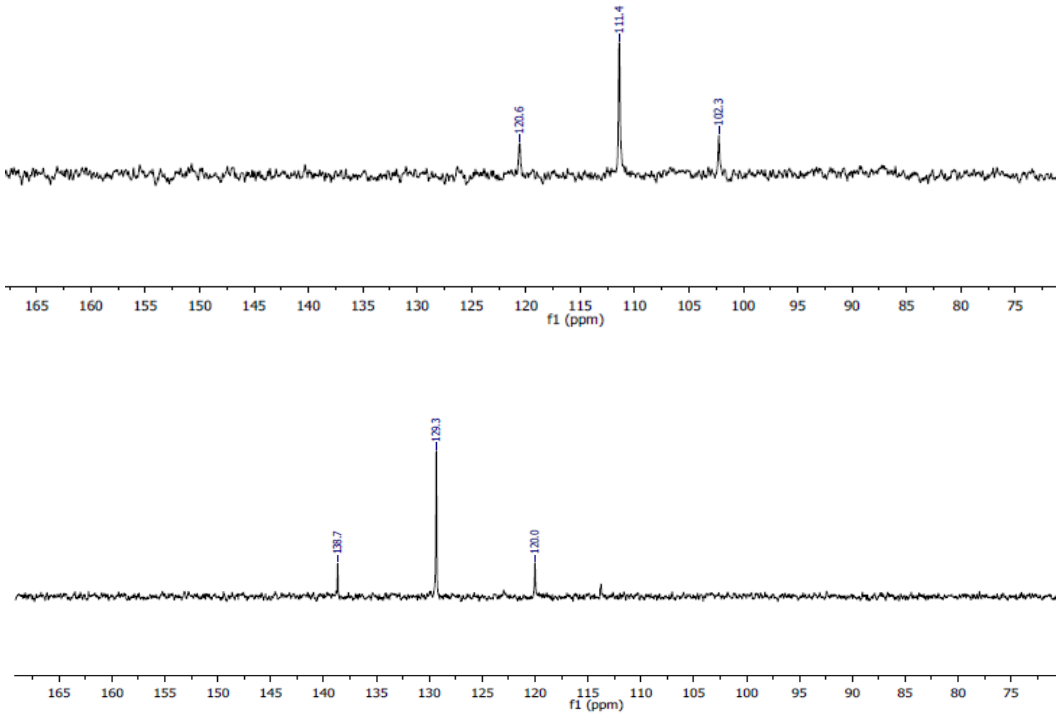

Figure 4. ^{31}P NMR spectra of complexes **4** (top) and **5** (bottom).

The trend is reversed in the ^{1}H NMR spectra (Figure 5). As the hydrides are sharing orbitals either with another hydride or a chloride, the increased π-donation of the chloride results in a larger downfield shift for **4**. The hydride peaks for **4** and **5** are observed at -18.6 and -3.5 ppm, respectively (Figure 3). The peaks are split into a triplet by the two phosphorous atoms, with coupling constants of $J_{P\text{-}H}$ = 14.5 Hz for **4** and $J_{P\text{-}H}$ = 17.5 Hz for **5**. They are further split by ^{195}Pt to form a satellite doublet of triplets. The platinum hydride coupling constants are $J_{Pt\text{-}H}$ = 656 and Hz $J_{Pt\text{-}H}$ = 405 Hz for the **4** and **5**, respectively. The larger coupling constant for complex **4** indicates a stronger Pt-H bond, which correlates with the decreased thermodynamic *trans* influence of the chloride compared to the hydride.[13]

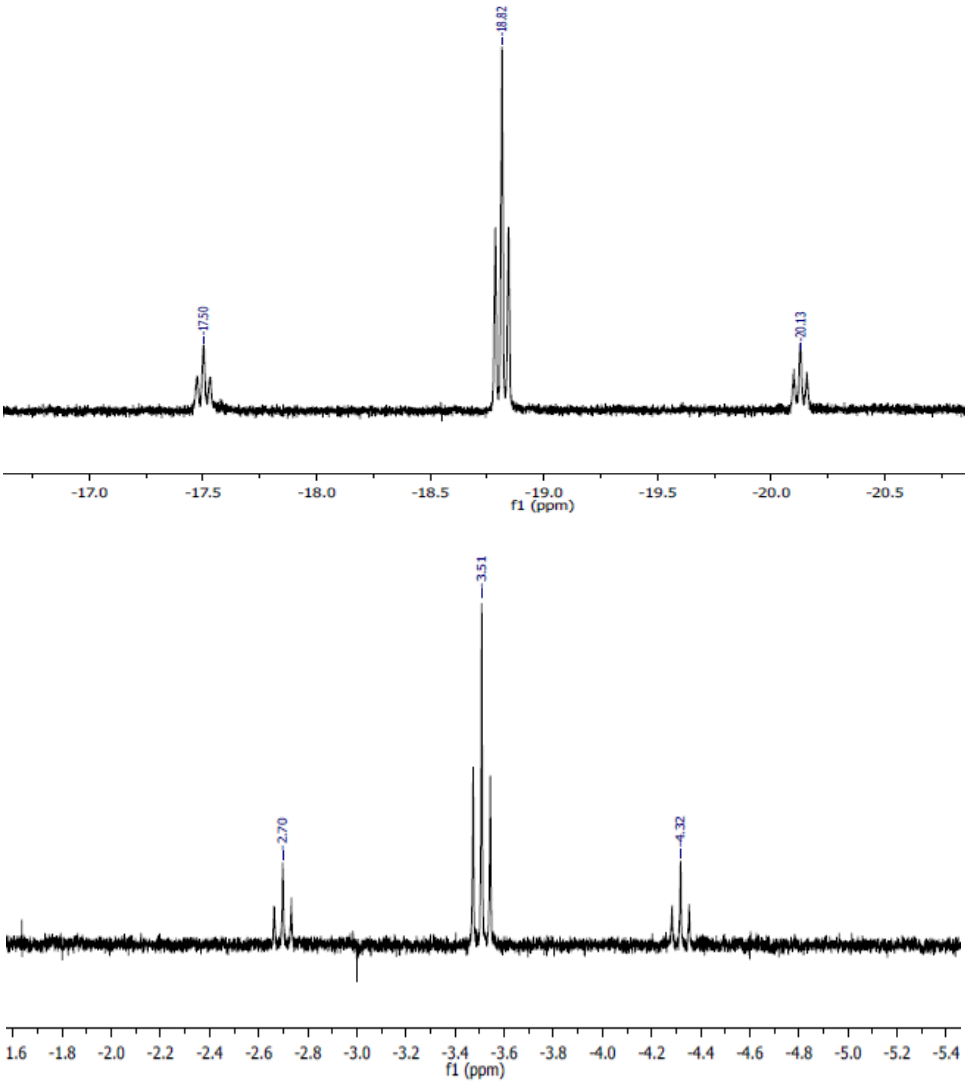

Figure 5. ^{1}H NMR spectra of the hydride regions of complexes **4** (top) and **5** (bottom).

In addition, a high quality x-ray crystal structure was obtained of complex **5** (Figure 6). The Pt-P bond lengths (2.25 Å) were comparable to other dihydride Pt complexes.[11]

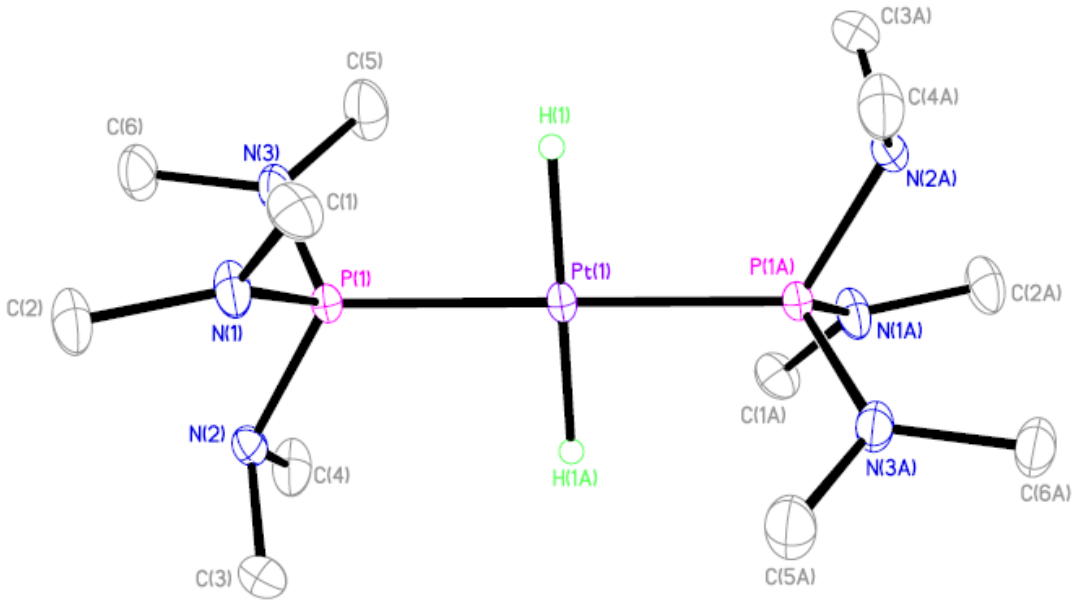

Figure 6. X-ray crystal structure of complex **5**. Ellipsoids are drawn at 50% probability. Hydrogen atoms (except the hydrides) have been omitted for clarity.

2.2.2. Nitrile Hydration Studies

Initial tests for the catalytic activity of complexes **4** and **5** used an aliphatic and an aromatic nitrile (4-nitrobenzonitrile and acetonitrile) as model substrates (Table 1). Both catalysts had reasonable TOFs, although lower than observed with the original complexes with trimethyl phosphine ligands. However, both **4** and **5** were active as catalysts without the addition of base, which promising for the use of these catalysts to hydrate cyanohydrins. The low conversions are most likely due to catalyst degradation. The dihydride complexes in particular have been shown to be unstable under catalytic conditions.[11,14] The conversion of nitrobenzonitrile was lower due to the poor solubility of that substrate in water.

Table 1. Hydration of acetonitrile to acetamide catalyzed by **4** and **5**.[a]

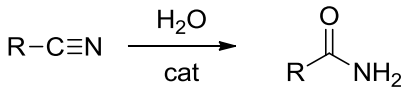

Catalyst	Substrate	Catalyst loading (mol%)	Temperature (˚ C)	% Hydration	TOF (h^{-1})
4	acetonitrile	0.05	80	58	40
4	4-nitrobenzonitrile	0.05	80	40	45
5	acetonitrile	0.05	80	36	26
5	4-nitrobenzonitrile	0.05	80	30	32

[a] Trials were conducted under air in water over 117 h.

2.2.3. Cyanohydrin Hydration

Complexes **4** and **5** were also tested as catalysts for cyanohydrin hydration using **1**, **2**, and **3** as substrates. Minimal hydration (< 5%) was detected in all cases. We hypothesized that this lack of reactivity was due to cyanide poisoning, as had been observed with previous Pt catalysts.[3] When hydration of acetonitrile was attempted with the catalysts in the presence of two equivalents of KCN, no acetamide formation occurred. This suggests that the cyanide resistance of the catalyst previously used successfully for cyanohydrin hydration, $[RuCl_2(\eta^6\text{-}p\text{-cymene})\{P(NMe_2)_3\}]$, was due in part to its second active site. That complex was fully active in the presence of up to one equivalent of KCN.[2]

2.3. Experimental

2.3.1. Instrumentation and Methods

Nuclear magnetic resonance spectra were recorded on a Varian Unity/Inova 500 MHz (^{1}H, 500.10 MHz; ^{31}P, 202.45 MHz; ^{13}C, 151 MHz) spectrometer, or on a Bruker Biospin 600 MHz (^{1}H, 600.02 MHz; ^{31}P, 242.83 MHz) spectrometer. The ^{1}H chemical shifts were referenced to the solvent peak or TMS (0.00ppm) and the ^{31}P chemical shifts were referenced to H_3PO_4 (0.00 ppm). Hydration trials were monitored with ^{1}H NMR. The solvent used for all NMR trials was D_2O. All hydration reaction samples were prepared in 1-dram screwcap vials fitted with septum caps, using 10.86 M NMe_4PF_6 as an internal standard.

Platinum starting materials were acquired from Strem. $P(NMe_2)_3$ was acquired from TCI.

2.3.2. Synthesis of $PtHCl(P(NMe_2)_3)_2$

In an inert atmosphere, $PtCl_2$(COD) (0.1 g, 0.27 mmol) was dissolved in 10 mL dichloromethane. Two equivalents $P(NMe_2)_3$ (0.1 mL, 0.54 mmol) was added drop-wise with stirring, and the solution turned from colorless to light yellow. The mixture was stirred overnight. ^{31}P NMR confirmed the formation of the *cis*-$PtCl_2(P(NMe_2)_3)_2$ as the free phosphine peak at 122 ppm had disappeared and a peak with platinum satellites at 65 ppm had appeared ($J_{Pt\text{-}P}$ = 2532 Hz). The solvent and COD were removed *in vacuo* and the resulting light yellow powder was redissolved in acetonitrile. One equivalent (0.01 g, 0.27 mmol) $NaBH_4$ was added with stirring. The solution was stirred for two hours and became bright yellow-orange, and solids began to precipitate. The mixture was run over a

celite plug to remove solids, and the solvent removed. The brown solid was redissolved in minimal acetone and layered on top of water to precipitate brown crystals. ^{31}P NMR: 111 ppm, Pt satellites at 102, 120 ppm. $J_{Pt\text{-}P}$ = 1,874 Hz. ^{1}H NMR: *t* , 2.6 ppm ($J_{P\text{-}H}$ = 5.4 Hz), *tt*, -18.6 ($J_{P\text{-}H}$ = 14.5 Hz, $J_{Pt\text{-}H}$ = 656).

2.3.3. Synthesis of $PtH_2(P(NMe_2)_3)_2$

In an inert atmosphere, $PtCl_2$(COD) (0.1 g, 0.27 mmol) was dissolved in 10 mL dichloromethane. Two equivalents $P(NMe_2)_3$ (0.1 mL, 0.54 mmol) was added drop-wise with stirring, and the solution turned from colorless to light yellow. The mixture was stirred overnight. ^{31}P NMR confirmed the formation of the *cis*-$PtCl_2(P(NMe_2)_3)_2$ as the free phosphine peak at 122 ppm had disappeared and a peak with platinum satellites at 60 ppm had appeared. The solvent and COD were removed *in vacuo* and the resulting light yellow powder was redissolved in acetonitrile. Two equivalents (0.02 g, 0.54 mmol) $NaBH_4$ was added with stirring. The solution was stirred for two hours and became bright orange, and solids began to precipitate. The mixture was run over a celite plug to remove solids, and the solvent removed. The brown solid was redissolved in minimal acetone and layered on top of water to precipitate brown crystals. ^{31}P NMR: 129 ppm, Pt satellites at 138, 120 ppm. $J_{Pt\text{-}P}$ = 1,891 Hz. ^{1}H NMR: *t* , 2.8 ppm ($J_{P\text{-}H}$ = 5.5 Hz), *tt*, -3.5 ($J_{P\text{-}H}$ = 17.5 Hz, $J_{Pt\text{-}H}$ = 405).

*2.3.4. General Procedure for Nitrile Hydration Catalyzed by **4** and **5***

Nitriles (0.5 mmol) were placed in a 1 dram vial with 2 mL water under air. 100 μL of a 1.6 mM solution of the catalyst was added and the vial was sealed and heated to 80 ˚C. Aliquots of 100 μL were taken periodically and the reaction followed by ^{1}H NMR

using an internal standard (500 μL 10.86 mmol NMe_4PF_6). Details for specific nitriles are as follows.

Acetonitrile. The progress of the reaction was monitored by observing the disappearance of the acetonitrile resonance at 2.01 ppm (*s*, C*H*$_3$CN) and the appearance of the acetamide at 1.93 ppm (*s*, C*H*$_3$C(O)NH_2).

4-Nitrobenzonitrile. This nitrile is minimally soluble in water, and a 0.2 M stock solution was prepared in acetone. The progress of the reaction was monitored by observing the disappearance of the aromatic *4*-nitrobenzonitrile resonances at 8.32 ppm (*d*, 2H, J = 8.5 Hz) and 7.96 ppm (*d*, 2 H, J = 8.7 Hz) and the appearance of the amide resonances at 8.27 (*d*, 2H, J = 8.6 Hz) and 7.92 ppm (*d*, 2H, J = 8.9 Hz) in the ^{1}H NMR spectrum.

Acetone Cyanohydrin. The progress of the reaction was monitored by observing the disappearance of the methyl resonance of acetone cyanohydrin at 1.57 ppm (*s*, 6H, HO(C*H*$_3$)$_2$CCN), and the appearance of the amide resonance at 1.34ppm (*s*, HO(C*H*$_3$)$_2$CC(O)NH_2) .

Lactonitrile. The progress of the reaction was monitored by observing the disappearance of the methyl resonance of lactonitrile at 1.45 ppm (*d*, J = 6.8 Hz, 3H, HOCHC*H*$_3$CN), and the appearance of the amide resonance at 1.23 ppm (*d*, J = 6.8 Hz, 3H, HOCHC*H*$_3$C(O)NH_2) .

Glycolonitrile. The progress of the reaction was monitored by observing the disappearance of the methyl resonance of glycolonitrile at 4.31 ppm (*s*, 2H, HOC*H*$_2$CN), and the appearance of the amide resonance at 1.23 ppm (*s*, 2H, HOC*H*$_2$C(O)NH_2) .

*2.3.5. Procedure for Poisoning Studies with **4** and **5***

4-Nitrobenzonitrile (0.5 mmol, 500 μL of a 0.2 M solution in acetone) was placed in a 1 dram vial with 2 mL water under air. KCN (500 μL of a 0.02 M solution in water) and 100 μL of a 1.6 mM solution of the catalyst was added and the vial was sealed and heated to 80 ˚C. Aliquots of 100 μL were taken periodically and the reaction followed by ^{1}H NMR using an internal standard (500 μL 10.86 mmol NMe_4PF_6). The progress of the reaction was monitored by observing the disappearance of the aromatic *4*-nitrobenzonitrile resonances at 8.32 ppm (*d*, 2H, J = 8.5 Hz) and 7.96 ppm (*d*, 2 H, J = 8.7 Hz) and the appearance of the amide resonances at 8.27 (*d*, 2H, J = 8.6 Hz) and 7.92 ppm (*d*, 2H, J = 8.9 Hz) in the ^{1}H NMR spectrum.

2.4. Summary

Two Pt complexes, $[PtHCl(P(NMe_2)_3)_2]$ and $[PtH_2(P(NMe_2)_3)_2]$ were synthesized and tested as catalysts for nitrile and cyanohydrin hydration. It was hypothesized that these complexes would be more active than similar complexes used previously due to the hydrogen bonding capability of the ligands and thus their ability to activate water. In contrast to previous catalysts, **4** and **5** were active with no base present. Nonetheless, the modest TOFs and susceptibility to cyanide poisoning of these catalysts render them unusable for cyanohydrin hydration.

2.5. Bridge

This chapter described the synthesis of the complexes $[PtHCl(P(NMe_2)_3)_2]$ and $[PtH_2(P(NMe_2)_3)_2]$ and the investigation of their reactivity towards nitriles and

cyanohydrins. Chapter III discusses the synthesis of a similar complex, $[PtH_2(P(OMe)_3)_2]$, and its transformation to nanoparticles under catalytic conditions. Characterization of these nanoparticles and tests of their reactivity towards nitriles and cyanohydrins are also reported.

CHAPTER III

NITRILE AND CYANOHYDRIN HYDRATION WITH NANOPARTICLES FORMED *IN SITU* FROM A PLATINUM COMPLEX

This chapter contains unpublished co-authored work. Under my direction, Richard Sayler synthesized platinum complexes and conducted hydration trials, andDr, Richard Glover collected the XPS data. The writing is entirely mine.

3.1. Introduction

Acrylate polymers are used to produce a wide variety of commercial products such as paints, diapers, detergents, and hard glass substitutes.[1] These materials are prepared from the polymerization of acrylic amides, esters, and acids. While the polymerization reactions proceed through efficient and well developed processes, the production of the monomers offers an opportunity for employment of greener practices.[2] For example, the production of methylmethacrylate (MMA) (the monomer of poly(methylmethacrylate) (PMMA), commonly known as Plexiglas) through the hydration of acetone cyanohydrin (ACH) with concentrated sulfuric acid generates approximately 7 million metric tons of waste per year. This is in comparison to the 2.8 million metric tons of the desired MMA product produced annually.[3] The imbalance is due to the formation of ammonium hydrogen sulfate (AHS) as a byproduct of the hydration reaction. Although the AHS can be recycled to sulfuric acid, this process requires pyrolysis at 1000 ˚C and consumes a large amount of energy.[2]

A process which eliminates sulfuric acid, and thus the byproducts and need for subsequent recycling, from the industrial production of MMA could have huge effects on the environmental and retail costs of the products it is utilized for.[2] One promising route involves using a transition metal catalyst to hydrate ACH to α-hydroxyisobutyronitrile (HIBAM) , which can then be dehydrated and treated with methanol to produce MMA (Scheme 1).

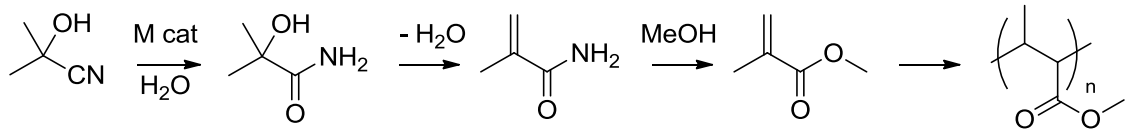

Scheme 1. Synthesis of PMMA using a transition metal catalyst.

There are a wide variety of catalysts able to transform nitriles to amides in water.[2,4,5] However this reaction becomes more difficult when the nitriles in question are α-hydroxy nitriles (cyanohydrins).[2,4,5] Cyanohydrins are in a delicate equilibrium with HCN and the corresponding aldehyde or ketone (Scheme 2, Chapter II).[6] When the equilibrium shifts away from the cyanohydrin and cyanide is generated, it can bind irreversibly to a transition metal catalyst and stop catalytic function (Scheme 2, Chapter II). Moreover, many of the best nitrile hydration catalysts require basic conditions to function, which further destabilize cyanohydrins.[2,6] (For the equilibrium of ACH shown in Scheme 3, $K = 7.16 \times 10^{-2}$ at pH = 3.78-4.68, and K = 68.5 at pH > 8.92). [2]

Our group and others have successfully developed catalysts that function under neutral and acidic conditions by utilizing phosphine ligands with hydrogen bonding capabilities.[7–19] These catalysts are able to activate both the nitrile and water simultaneously, with the metal acting as a Lewis acid and the ligand as a Brønsted base and thus eliminating the need for a higher pH (Figure 1).[12] In particular, the complex $[RuCl_2(\eta^6\text{-}p\text{-cymene})\{P(NMe_2)_3\}]$, was able to successfully hydrate nitriles under acidic conditions.[7,8,10] Because of this robustness, this catalyst was able to convert glycolonitrile and lactonitrile fully to their corresponding amides and ACH was hydrated to 3-hydroxy-isobutyro nitrile (HIBAM) in an unprecedented 15% yield.[7] The low yield was a result of catalyst poisoning by cyanide.[7]

We have examined using this technique of ligand assisted hydration with other catalyst scaffolds, including the dihydride bis(phosphine) platinum(II) complexes reported by Trogler and co-workers.[20,21] This chapter reports on a $PtH_2(P(OMe)_3)_2$ complex used for nitrile hydration. The complex was active towards the hydration of acetonitrile, however surprising kinetics were observed. Upon closer examination, the active catalyst was identified as a platinum nanoparticle species. This nanoparticle catalyst was active for the hydration of cyanohydrins, and other platinum nanoparticle species were examined as nitrile hydration catalysts.

3.2. Results and Discussion

3.2.1. Synthesis

The complex was synthesized in the manner of previous platinum dihydride complexes, by generating the *cis* intermediate through treatment of $PtCl_2(COD)$ with

trimethylphosphite ($P(OMe)_3$) and subsequent treatment with excess sodium borohydride to produce the desired complex (Scheme 2). The ^{1}H and ^{31}P NMR spectra were consistent with those of previous platinum dihydride complexes.[21]

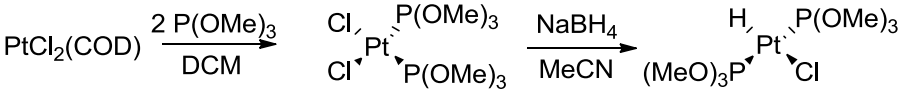

Scheme 2. Synthesis of the dihydridobis(trimethylphosphite)platinum(II) complex

3.2.2. Initial Hydration Trials.

Initial kinetic trials were performed hydrating acetonitrile to acetamide with a 0.05% catalyst loading at 80 ˚C. The turnover frequency (TOF) was 17.8 h^{-1}, which is reasonable but slower than the premier nitrile hydration catalysts.[22] However, unusual kinetics led to a surprising realization. Rather than the expected exponential hydration curve, an s-shaped curve with an induction period was observed (Figure 2, Trial 1). These sigmoidal kinetics are representative of an autocatalytic reaction (Equation 1) where the initial catalyst (A) is not the active one, but instead a second species (B) is formed, usually a heterogeneous material such as nanoparticles.[23,24] The formation of the active catalyst before the reaction begins results in an induction period.

$$A \rightarrow B \qquad (1)$$

$$A + B \rightarrow 2B$$

A classic test for heterogeneous catalyst formation is to examine the kinetics of the already formed catalyst.[23] In this case, a solution of the active catalyst was prepared by fully hydrating acetonitrile under the previous reaction conditions. The first trial displayed sigmoidal kinetics as in previous trials. When a second equivalent of

acetonitrile was added, however, the reaction began immediately with no induction period (Figure 2, Trial 2), suggesting the species formed during the induction period is the active catalyst. Trial 2 had a slower TOF (7.5 h^{-1}) than the initial trial, which was attributed to agglomeration of the particles over time. Solids forming in the reaction vessel corroborated this hypothesis.

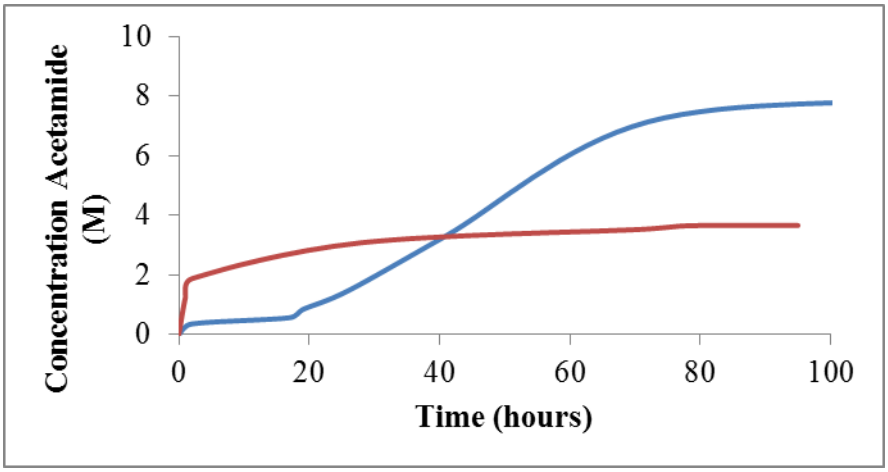

Figure 1. Hydration trials with acetonitrile at 50 ˚C and 0.05 mol % catalyst loading. Trial 1 (blue) shows the initial kinetics of the Pt complex (10 M acetonitrile). Trial 2 (red) shows the kinetics when a second aliquot of acetonitrile (3.8 M) is added.

3.2.3. Catalyst Characterization.

To test for the presence of a heterogeneous species a sample of the reaction mixture after the hydration of acetonitrile was analyzed with transmission electron microscopy (TEM). TEM images showed platinum nanoparticles around 2 nm in size, confirming the presence of a heterogeneous species (Figure 2). The nanoparticles were also characterized with x-ray photoelectron spectroscopy (XPS) and ^{31}P NMR.

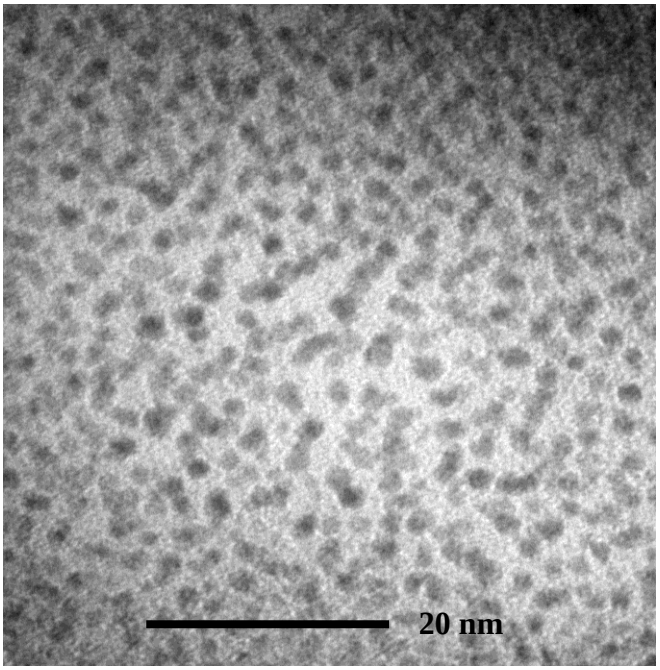

Figure 2. TEM images of the hydration reaction mixture. Pt nanoparticles of approximately 2-4 nm are observed.

Because there is literature precedent for water soluble platinum nanoparticles passivated by phosphine containing ligands, we hypothesized the nanoparticles would have a ligand shell of $P(OMe)_3$.[25–27] This hypothesis was examined with NMR and XPS. In the ^{31}P NMR spectrum, the peak at 130 ppm (with satellites indicating Pt coordination) corresponding to the complex disappeared, while a single sharp peak appeared upfield at 8 ppm, the shift expected for $(O)P(OMe)_3$, the oxidation product (Figure 2). The resulting peak had no platinum satellites, confirming the absence of a platinum complex. However this did not rule out the possibility of a phosphorous containing ligand on the nanoparticle surface, as nuclei bound to metal surfaces often cannot be observed.[25] Furthermore, the P 2p region of the XPS spectrum (Figure 3 B) contained P $2P_{3/2}$ peak at 132 eV , which is

in the range for either $P(OMe)_3$ or its oxide bound to a metal surface (Table 1).[29–31] Thus a phosphorous species could not be ruled out as the nanoparticle ligand.

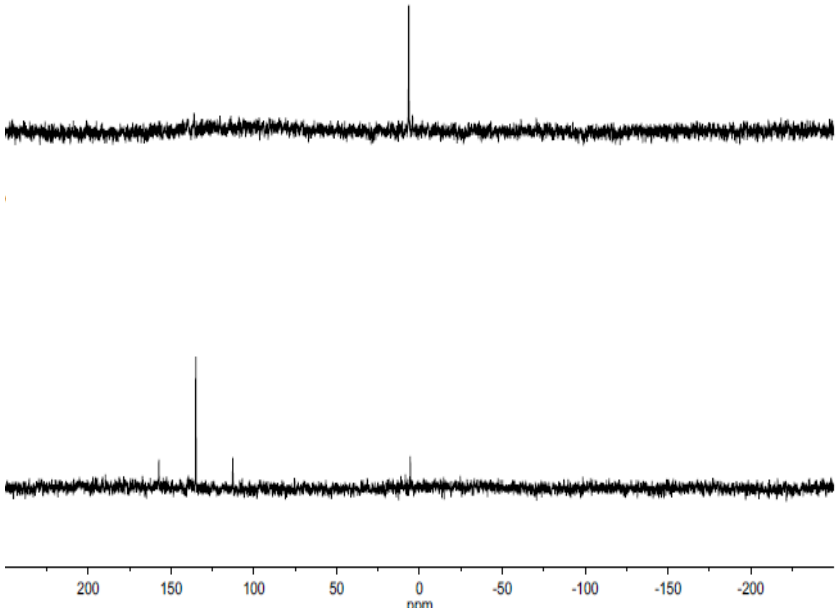

Figure 3. ^{31}P NMR spectrum of the $PtH_2(P(OMe)_3)_2$ complex at 50 ˚C in water and acetonitrile after 6 hours (bottom) and 48 hours (top).

Table 1. XPS P $2p_{3/2}$ Binding Energies for selected $P(OMe)_3$ and $(O)P(OMe)_3$ species

Entry	Species	P $2p_{3/2}$ Binding Energy (eV)	Reference
1	$(O)P(OMe)_3$	133.4	(28)
2	$Ru(0)\text{-}P(OMe)_3$	129.9	(29)
3	$(O)P(OMe)_3\text{-}Fe_2O_3$	133.6	(30)
4	$Co_4(CO)_9(P(OCH_3)_3(PC_6H_5)_2)$	133.0	(31)
5	$Fe_3(CO)_8(P(OCH_3)_3(PC_6H_5)_2)$	132.5	(31)

In addition, the XPS spectrum of the Pt 4f region showed Pt binding energies at 72 and 76 eV, which are common values for Pt(0). This confirmed that Pt had been

reduced (Figure 3A). The N 1s region of the XPS spectrum yielded an interesting observation as well (Figure 3C). Two peaks were present in the spectrum, at binding energies of 399 and 400.5 eV. The former could correspond to either residual acetonitrile or acetamide present in the sample (Table 2, Entries 1 and 2), while the latter was consistent with the binding energy of weakly adsorbed acetonitrile (Table 2, Entry 3).[32–34] This observation could offer further evidence that Pt nanoparticles were the catalyst, as the nitrile must bind to the surface to be activated for hydration.

Table 2. XPS N 1s Binding Energies for Selected Species.

Entry	Species	N 1s Binding Energy (eV)	Reference
1	$CH_3(O)NH_2$	399.6	(34)
2	CH_3CN	399.1	(33)
3	Pt(0)-CH_3CN	400.1	(32)
4	[Pt($CH_3CONH)_2$] · H_2)	399.3	(34)

Trogler and coworkers observed reductive elimination of dihydride complexes to form Pt(0) and H_2 in similar dihydridobis(trimethyl)phosphine Pt(II) complexes.[35,36] A similar reductive mechanism seems plausible in this case, as bubbling is observed when water is added to the dihydride complex. The $P(OMe)_3$ then oxidizes on dissociation.

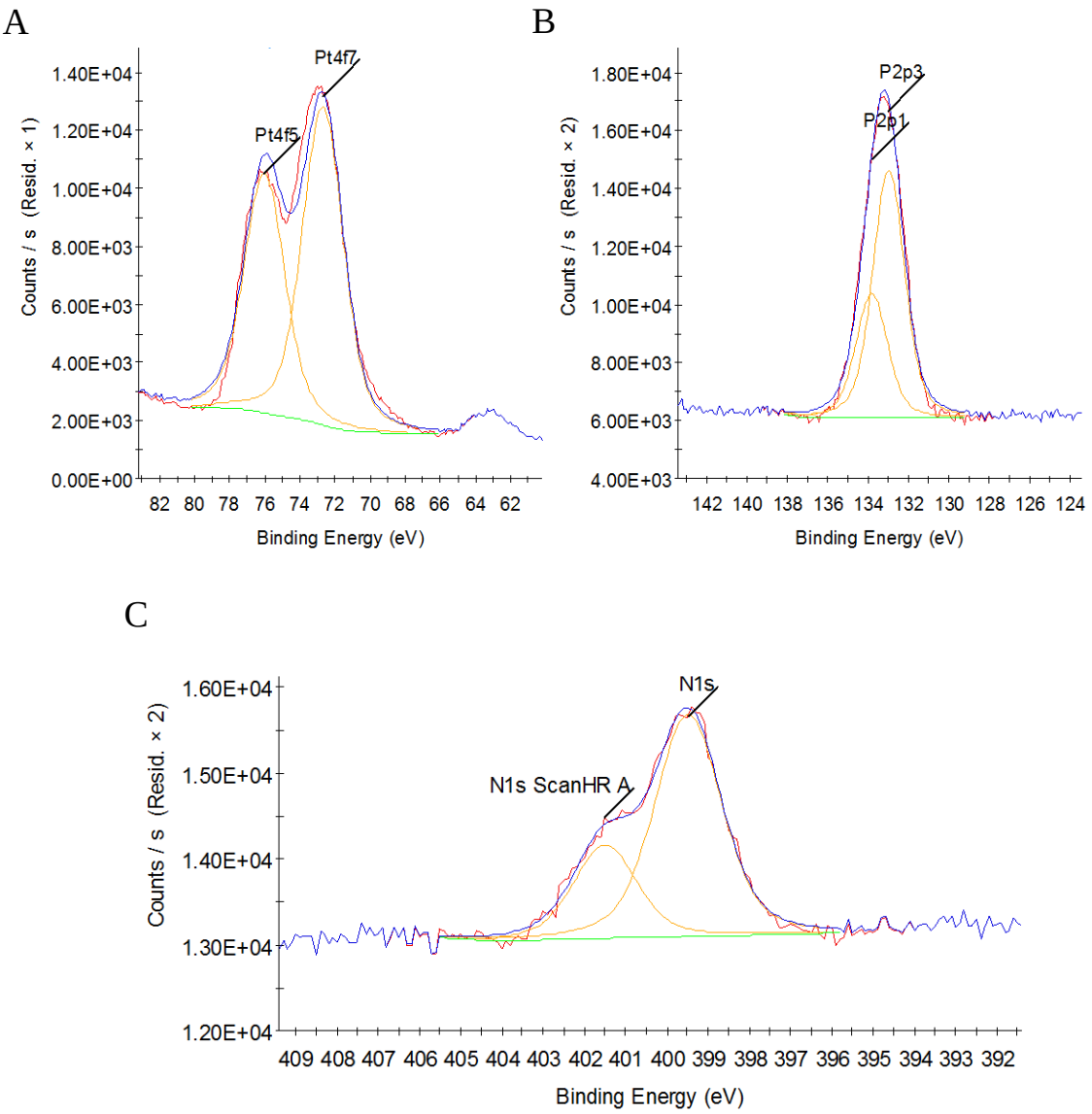

Figure 4. XPS spectra of platinum nanoparticles. A) Pt 4f spectrum B) P 2p spectrum C) N 1s spectrum. (Red, XPS scan; Blue, fitted envelope; Orange, fitted peak; Green, background).

3.2.4. Implications for Cyanohydrin Hydration and Poisoning Studies.

There are a handful of examples of NPs as catalysts for nitrile hydration,[37–43] including NPs composed of silver, gold, palladium, nickel, and ruthenium hydroxide. To the best of our knowledge, however, no NP catalysts have been used to hydrate cyanohydrins. We hypothesized that nanoparticles might be more resistant to cyanide poisoning than homogeneous complexes due to differences in electronic structure. Nanoparticles are generally M(0), and thus have more electron density than metal complexes in higher oxidation states. Furthermore, it is possible that cyanide would bind more weakly (possibly reversibly) to the nanoparticle surface, resulting in a longer lasting catalyst.

To test this theory, hydration trials of acetonitrile were performed in the presence of KCN. The acetonitrile was completely hydrated in all samples, but the rate of hydration decreased as more equivalents of cyanide (up to 5) were added (Table 3). Nonetheless, the catalysts from all samples were successfully reused for another acetonitrile hydration in recycling studies. Thus while cyanide poisoning did take place with this nanoparticle catalyst, a much larger amount of cyanide was required to kill function than with analogous homogeneous Pt complexes, where 3 equivalents of cyanide rendered the catalyst completely inactive.[6]

Table 3. Poisoning studies for the hydration of acetonitrile with platinum nanoparticles. [a]

Entry	Eq KCN (per Pt atom)	Time (h)	iTOF (h^{-1})
1	0	71	7.67
2	0.5	78	5.67
3	1	80	5.61
4	2	95	5.21
5	5	250	3.35

[a] Trials were conducted under air with 5 mmol acetonitrile and 0.05 mol% Pt

3.2.5. Cyanohydrin Hydration Trials.

The observed resistance to cyanide poisoning indicated the platinum nanoparticles might catalyze the hydration of cyanohydrins. The catalysts were tested at room temperature for the hydration of glycolonitrile, lactonitrile, and acetone cyanohydrin. (While the catalyst was more active at higher temperatures, heat drives the cyanohydrin equilibrium towards cyanide.) All three were converted successfully to the corresponding amides. Glycolonitrile and lactonitrile were completely converted (Table 4, Entry 1 and 2). After seven weeks, 30% of ACH was converted to HIBAM. No ACH was present in the sample, however, as much of the ACH had irreversibly degraded into acetone and cyanide before it could be hydrated. This degradation was confirmed by a growing acetone peak in the ^{1}H NMR spectrum. This was the first reported hydration of cyanohydrins by a nanoparticle catalyst, and the highest conversion of ACH by a transition metal catalyst to date.

Table 4. Cyanohydrin hydration with a platinum nanoparticle catalyst [a]

Entry	Nitrile	Structure	% Hydration	Time (weeks)
1	Glycolonitrile	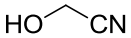	100	1
2	Lactonitrile	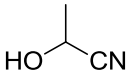	100	3
3	Acetone Cyanohydrin	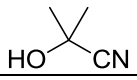	30	7

[a] Trials were conducted under air in a 50:50 water: acetonitrile mixture, 5 mmol nitrile and 0.05 mol% Pt

Despite the presence of cyanide, however, the catalyst from the ACH hydration mixture was reused at least twice for the hydration of acetonitrile. This result indicates that catalyst poisoning is not responsible for the low conversion of ACH, but rather that

the rate of hydration is too slow for complete conversion to occur before the substrate has degraded. Because acetonitrile was present in the solution, and likely also bound to the surface of the particle, there was the potential for a competitive reaction as acetamide was produced, further reducing the conversion of ACH. Thus several syntheses of platinum nanoparticles with no nitrile present were attempted to generate an improved catalyst.

3.2.6. Synthesis of Platinum Nanoparticles from Literature Preparations

There is only one previously reported example of nitrile hydration by platinum nanoparticles, where the catalyst was platinum nanoparticles stabilized by poly(vinyl)pyrollidone (PVP).[40] PVP is a water soluble polymer commonly used in nanoparticle synthesis. This catalyst required high temperatures (150 ˚C) as well as an the presence of an oxygen containing copper salt ($CuSO_4$, $Cu(acac)_2$, CuO) to be active. This catalyst was synthesized according to literature preparations and tested for the hydration of several nitriles.[44] Activated nitriles (benzonitrile and *p*-nitrobenzonitrile), an aliphatic nitrile (acetonitrile), and a cyanohydrin (ACH) were tested in the presence of $CuSO_4$. Trials were conducted at 80 ˚C, as higher temperatures increase the rate of cyanohydrin degradation. After five days, minimal hydration was observed for the activated nitriles only, and none of the acetonitrile or ACH was converted. Oshiki and coworkers had similar difficulty hydrating aliphatic nitriles with this catalyst, which could be a result of the coverage of the PVP ligand on the particle surface. [40] With the strong interaction between the metal and the polymer, it would be more difficult for the substrate to interact with the metal surface of the catalyst. In addition, plating on the reaction vessel indicated that the Pt/PVP nanoparticles were degrading in a similar fashion to the previous Pt nanoparticles.

Other syntheses of platinum nanoparticles using 1,3,5-7-triazaphosphaadamantane (PTA) as a stabilizer were also attempted, since this water soluble and air stable ligand has been used previously in nanoparticle synthesis.[25,45] However these nanoparticles underwent similar degradation under catalytic conditions as previously attempted species.

3.3. Experimental

3.3.1 Instrumentation and Procedures

Nuclear magnetic resonance spectra were recorded on a Varian Unity/Inova 500 MHz (^{1}H, 500.10 MHz; ^{31}P, 202.45 MHz; ^{13}C, 151 MHz) spectrometer, or on a Bruker Biospin 600 MHz (^{1}H, 600.02 MHz; ^{31}P, 242.83 MHz) spectrometer. The ^{1}H chemical shifts were referenced to the solvent peak or TMS (0.00ppm) and the ^{31}P chemical shifts were referenced to H_3PO_4 (0.00 ppm). Hydration trials were monitored with ^{1}H NMR. The solvent used for all NMR trials was D_2O. All hydration reaction samples were prepared in 1-dram screwcap vials fitted with septum caps, using 10.86 M NMe_4PF_6 as an internal standard. TEM images were acquired with a FEI Titan 80-300 kV transmission electron microscope equipped with a spherical aberration (C_s) image corrector, an EDAX energy dispersive spectrometer, and a Tridiem 863 Gatan imaging filter and electron energy loss spectrometer. All images were acquired at 300 kV.

Platinum starting materials were acquired from Strem. $P(OMe)_3$ was acquired from Sigma Aldrich. PTA was synthesized from literature methods.

3.3.2. Synthesis of $PtH_2(P(OMe)_3)_2$

Under an inert atmosphere, $PtCl_2$(COD) (0.31 g, 0.85 mmol) was dissolved in 10 mL dichloromethane at room temperature with stirring, and $P(OMe)_3$ (0.2 mL, 1.69 mmol) was added. The reaction mixture turned from clear to yellow, and the mixture was stirred overnight. Reaction progress was monitored with ^{31}P NMR, following the disappearance of the $P(OMe)_3$ peak at 112 ppm and the appearance of the *cis* complex with Pt satellites at 65 ppm. After complete conversion, the solvent was removed *in vacuo* and the resulting white powder was redissolved in 10 mL acetonitrile. 2 equivalents $NaBH_4$ were added. The resulting mixture, which turned orange over 30 min, was stirred for 2h. The reaction mixture was run through a celite plug to remove excess $NaBH_4$ and NaCl. The solvent was removed and the resulting brown solid was dissolved in a minimal amount of acetone, then added dropwise to 20 mL hexanes. A fine white powder crashed out, which was again filtered over celite, rinsed with hexanes and dissolved in DCM. This yielded a white powder. The ^{31}P NMR spectrum contained a single peak at 132 ppm with Pt satellites ($J_{P\text{-}Pt}$ = 2701). The ^{1}H NMR had a peak at 3.2 ppm corresponding to the methyl groups on the phosphines (*t*, $J_{P\text{-}H}$ = 9.5 Hz) and a hydride peak at -4 ppm with Pt satellites (*t*, $J_{P\text{-}H}$ = 15.2, $J_{Pt\text{-}H}$ = 705 Hz).

3.3.3. Hydration of Acetonitrile with $PtH_2(P(OMe)_3)_2$

0.02 g of the complex was dissolved in 2 mL D_2O. 500 μL of this solution was added to a 1 dram vial along with 500 μL water and 250 μL (4.8 mmol) acetonitrile. The mixture was heated to 80 ˚C. The reaction was monitored by observing the disappearance of the acetonitrile resonance at 2.0 ppm (*s*, 3H, C*H*$_3$CN) and the appearance of the acetamide resonance at 1.9 ppm (*s*, 3H, C*H*$_3$(O)NH_2).

3.3.4. Hydration of Acetonitrile with Pt NPs

0.02 g of the complex was dissolved in 2 mL D_2O. 500 μL of this solution was added to a 1 dram vial along with 500 μL water and 250 μL (4.8 mmol) acetonitrile. The mixture was heated to 80 ˚C overnight to form the Pt nanoparticles. A second aliquot of 250 μL (4.8 mmol) acetonitrile was added and the mixture was heated to 80 ˚C again. The reaction was monitored by observing the disappearance of the acetonitrile resonance at 2.0 ppm (*s*, 3H, C*H*$_3$CN) and the appearance of the acetamide resonance at 1.9 ppm (*s*, 3H, C*H*$_3$(O)NH_2).

3.3.5. KCN Poisoning Studies with Pt NPs

0.02 g of the complex was dissolved in 2 mL D_2O. 500 μL of this solution was added to a 1 dram vial along with 500 μL water and 250 μL (4.8 mmol) acetonitrile. The mixture was heated to 80 ˚C overnight to form the Pt nanoparticles. A second aliquot of 250 μL (4.8 mmol) acetonitrile and varying amounts of a 45 mM KCN solution in H_2O were added and the mixture was heated to 80 ˚C again. The reaction was monitored by observing the disappearance of the acetonitrile resonance at 2.0 ppm (*s*, 3H, C*H*$_3$CN) and the appearance of the acetamide resonance at 1.9 ppm (*s*, 3H, C*H*$_3$(O)NH_2).

3.3.6. Hydration of Glycolonitrile with Pt NPs

0.02 g of the complex was dissolved in 2 mL D_2O. 500 μL of this solution was added to a 1 dram vial along with 500 μL water and 250 μL (4.8 mmol) acetonitrile. The mixture was heated to 80 ˚C overnight to form the Pt nanoparticles. The progress of the reaction was monitored by observing the disappearance of the methyl resonance of acetone glycolonitrile at 4.3 ppm (*s*, 2H, HO(C*H*$_2$)CN), and the appearance of the amide resonance at 3.8 ppm (s, 2H, HO(C*H*$_2$)C(O)NH_2) .

3.3.7. Hydration of Lactonitrile with Pt NPs

0.02 g of the complex was dissolved in 2 mL D_2O. 500 μL of this solution was added to a 1 dram vial along with 500 μL water and 250 μL (4.8 mmol) acetonitrile. The mixture was heated to 80 ˚C overnight to form the Pt nanoparticles. The progress of the reaction was monitored by observing the disappearance of the methyl resonance of acetone lactonitrile at 1.25 ppm (*d*, 1 H, HO(C*H*)CN), and the appearance of the amide resonance at 3.8 ppm (*d*, 1H, $HO(CH)C(O)NH_2$) .

3.3.8. Hydration of ACH with Pt NPs

0.02 g of the complex was dissolved in 2 mL D_2O. 500 μL of this solution was added to a 1 dram vial along with 500 μL water and 250 μL (4.8 mmol) acetonitrile. The mixture was heated to 80 ˚C overnight to form the Pt nanoparticles. The progress of the reaction was monitored by observing the disappearance of the methyl resonance of ACH at 1.5 ppm (*s*, 6H, $HO(CH_3)_2CCN$), and the appearance of the amide resonance at 1.3 ppm (s, 6 H, $HO(CH_3)_2\ CC(O)NH_2$) .

3.3.9. Preparation of PVP Stabilized Pt NPs

H_2PtCl_4 (0.012 g) and PVP (0.067 g) were dissolved in 25 mL water in a 100 mL round bottom flask. The mixture was brought to reflux and 14 mL ethanol was added. The solution was refluxed for 3 hours and turned from yellow to brown.

3.3.10. General Procedure for Hydration Trials with PVP Stabilized Pt NPs

1 mmol nitrile (the appropriate volume of the neat substrate, or in the case of 4-nitrobenzonitrile a 0.2 M solution in acetone) was added to 2 mL Pt NP solution (0.2

mM) in a 1 dram screw cap vial, which was heated in an oil bath at 80 ˚C. The reaction went for five days and aliquots were taken daily.

3.4. Summary

Cyanohydrins are difficult to hydrate catalytically, however nanoparticle catalysis offers a new path forward for this challenging reaction. Using a platinum nanoparticle catalyst prepared *in situ* from $PtH_2(P(OMe)_3)_2$, unprecedented conversion of ACH to HIBAM was achieved, and the reaction was halted only by the degradation of the substrate. Although the rate of hydration was slowed by added cyanide, the catalyst remained active even in the presence of five equivalents of cyanide. Two other cyanohydrins, lactonitrile and glycolonitrile, were also hydrated completely. Attempts at hydration with other Pt nanoparticle catalysts (Pt/PVP and Pt/PTA) resulted in some hydration, but the particles degraded too quickly to be a viable catalyst. However a catalyst that is faster at ambient temperatures is required to circumvent the natural degradation of the ACH.

3.5. Bridge

This chapter described the synthesis of $PtH_2(P(OMe)_3)_2$, its conversion into a catalytically active nanoparticle species under reaction conditions, and investigations into the activity of those nanoparticles towards the hydration of nitriles and cyanohydrins. The catalytic activity of other platinum nanoparticles for these reactions was also examined. Chapter IV describes the synthesis and characterization of silver nanoparticles stabilized by a water soluble phosphine ligand, and the investigation of the reactivity of this catalyst

with nitriles and cyanohydrins. The degradation of these particles in the presence of cyanide, and the catalytic activity of the resulting silver complex was also examined.

CHAPTER IV

INVESTIGATION OF PTA STABILIZED SILVER NANOPARTICLES AS CATALYSTS FOR THE HYDRATION OF NITRILES AND CYANOHYDRINS

This chapter contains co-authored material. With my intellectual input, Tobias Sherbow synthesized the nanoparticles and conducted initial catalytic trials. He also contributed to the writing of the material. Joshua Razink collected the TEM images.This chapter has been submitted for publication to the journal *ACS Catalysis*.

4.1. Introduction

In an industrial setting, the hydration of nitriles to amides is typically performed under extreme conditions.[1] For example, the industrial route for the hydration of acetone cyanohydrin (α-hydroxyisobutyronitrile, ACH), the industrial precursor to methylmethacrylate (MMA), uses concentrated sulfuric acid. A major byproduct of this reaction is ammonium hydrogen sulfate (AHS), 2.5 kg of which are formed for every 1 kg of MMA produced.[2] This byproduct poses a significant environmental problem and economic disadvantage. To dispose of the 7 million metric tons of AHS produced annually, it is pyrolyzed at 1000 °C to reform sulfuric acid .[2,3] This process is energy intensive, and alternate synthetic routes are therefore sought.[1] A transition metal catalyzed hydration reaction run under mild conditions would potentially be more economically and environmentally favorable.

Our group and others have shown that nitriles can be successfully hydrated to their corresponding amides in high yields and under mild conditions with various transition metal catalysts.[1] Accordingly, we tested many of these same homogeneous catalysts to see if they could be used for the hydration of acetone cyanohydrin. Although the hydration of cyanohydrins would seem to be relatively straightforward, there were complications. Cyanohydrins are in equilibrium with hydrogen cyanide and the corresponding aldehyde or ketone (Scheme 1). When cyanide is present, it can poison a homogeneous catalyst by irreversibly binding to one or more active sites.[4] We previously reported on cyanohydrin hydration with a number of known nitrile hydration catalysts, but only minimal hydration was observed in these cases because of cyanide poisoning.[4,5]

In an effort to find cyanide-resistant catalysts, we turned our attention to nanocatalysts. Nanoparticles are capable of catalyzing a wide variety of reactions,[6] including hydrogenation, dehalogenation, oxidation, and photocatalytic reactions. However, only a handful of investigations have focused on hydration reactions and specifically on nitrile hydration.[7–16] To the best of our knowledge, no examples of cyanohydrin hydration using nanoparticle catalysts have been reported.

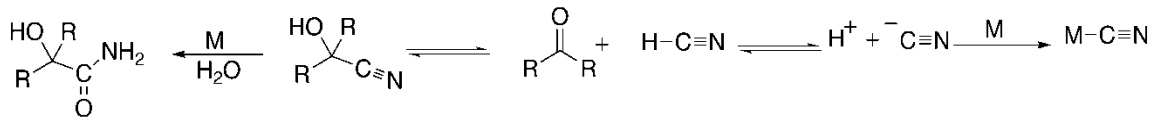

Scheme 1. Equilibrium between a cyanohydrin and the corresponding aldehyde/ketone and hydrogen cyanide. When cyanide is present, it typically binds irreversibly to the metal catalyst, poisoning it.

These studies show that nanoparticles have comparable activity to homogeneous transition metal catalysts for nitrile hydration. However, no nanoparticle catalysts have

been tested for cyanohydrin hydration. In this paper, we report on our investigation of nitrile and cyanohydrin hydration using silver nanoparticles. Because hydration reactions are typically carried out in aqueous solution, the nanoparticles in this study incorporated a water-soluble stabilizing ligand shell of 1,3,5-triaza-7-phosphaadamantane (PTA), which has been used previously to produce water soluble nanoparticle catalysts.[17] These catalysts are usable under air and at fairly mild temperatures (90 ˚C).

The catalyst hydrated nitriles in a similar fashion to previously reported Ag NP nitriles hydration catalyst. However when in the presence of even the small amounts of cyanide generated by the cyanohydrin equilibrium, the nanoparticles disassembled. The resulting AgCN species was nonetheless active for cyanohydrin hydration, and displayed excellent cyanide resistance, as discussed below.

4.2. Synthesis and Characterization of Ag-PTA Nanoparticles.

4.2.1. Nanoparticle Synthesis

The Ag-PTA nanoparticles were synthesized by the reduction of silver nitrate with sodium borohydride in cold water (Equation 1). As the $AgNO_3$ was added slowly to the $NaBH_4$ over 10 minutes, the solution in the reaction flask turned from colorless to yellow. The yellow color is attributed to the localized surface plasmon resonance (LSPR) of the nanoparticles (λ_{max} = 398 nm) and is evidence that a silver nanoparticle surface is present.[18–20] In the absence of added ligand, Solomon *et al.* showed that the silver nanoparticles are stabilized for a short time by excess borohydride that is adsorbed to the surface of the particles.[21] However, over a period of 30 minutes, the borohydride

decomposed,[21] and the nanoparticles precipitated from solution as bulk metal. In this study, PTA was added to the solution in order to stabilize the particles. (The addition took place immediately after all of the $AgNO_3$ solution had been added.) Experiments showed that a 1.1:1 ratio (PTA:$AgNO_3$) gave the maximum nanoparticle stability with respect to decomposition or unwanted precipitation. (More than 1.1 equivalents of PTA resulted in the decomposition of the nanoparticles and the formation of Ag-PTA complexes, while too little ligand led to the formation of bulk metal.) In contrast to the BH_4^- stabilized particles, the nanoparticles stabilized by PTA remained dispersed in aqueous solution for several weeks. The PTA-stabilized silver nanoparticles are a slightly darker orange color than the yellow borohydride-stabilized particles. The UV-vis spectrum showed a broadening and decrease in intensity of the LSPR peak at λ_{max} = 398 nm in the PTA-stabilized particles (Figure 1) compared to the borohydride stabilized particles. In other studies, the broadening and decrease in intensity of the LSPR peak has been attributed to modification of the electronic properties of the nanoparticle surface by the ligand shell.[18,19] A similar explanation is likely applicable here.

$$AgNO_3 + NaBH_4 \xrightarrow{H_2O,\ 0^\circ C} Ag^0 + 1/2H_2 + 1/2\ B_2H_6 + NaNO_3 \qquad (1)$$

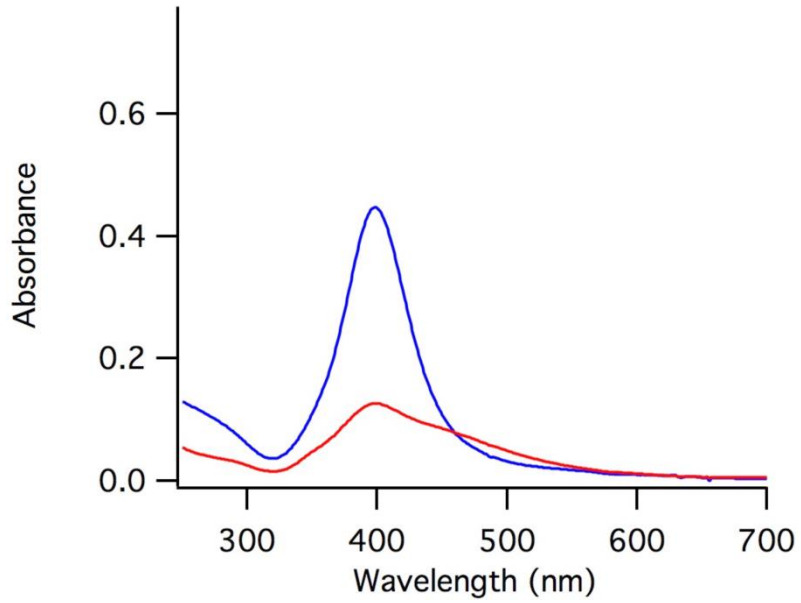

Figure 1. UV-vis spectrum of the surface plasmon resonance band of the Ag-PTA nanoparticles before (blue) and after (red) the addition of 1.1 equivalents of PTA.

4.2.2. NMR Characterization

The ^{31}P NMR spectrum of the Ag-PTA nanoparticles showed a peak at -85.6 ppm, assigned to the coordinated PTA ligand. This resonance is shifted downfield and broadened compared to that of uncoordinated PTA, which has a sharp peak at -98.3 ppm (Figure 2). Prior work showed that broadening and downfield shifts in the ^{31}P NMR spectra of phosphine-stabilized nanoparticles are due to the induced shielding on ligands that are bound to nanoparticles.[23,24] Thus, the broadening and changes in the chemical shift of the Ag-PTA nanoparticles indicate that PTA is bonded to the metal through the phosphorus atom. Note that no resonance for uncoordinated PTA ligand was observed in the ^{31}P NMR spectrum of the nanoparticles, indicating that all the PTA present is bound to the surface.

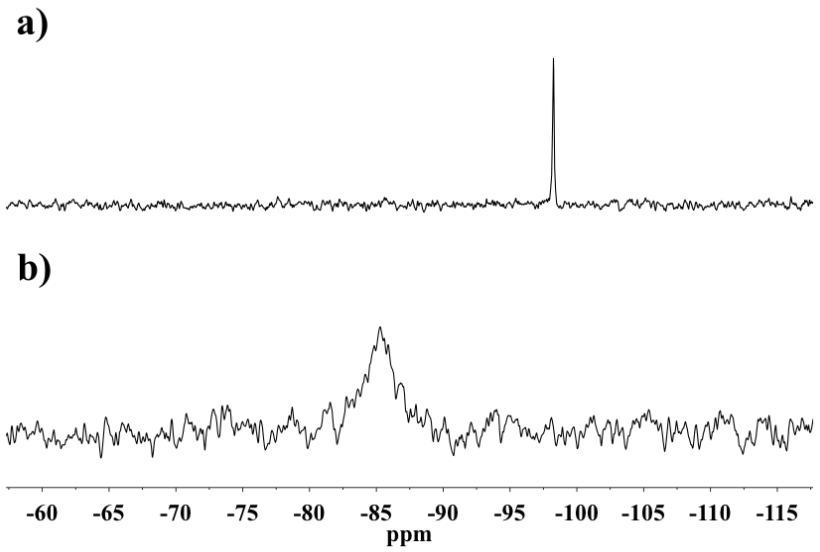

Figure 2. ^{31}P NMR spectrum of a) free PTA ligand at δ -98.3 ppm and b) bound PTA ligand on the surface of the Ag-PTA nanoparticles at δ -85.6 ppm.

4.2.3. TEM Characterization

The size distribution of the Ag-PTA nanoparticles was analyzed by TEM/HRTEM (Transmission Electron Microscopy/High Resolution Transmission Electron Microscopy). Prior research showed that $NaBH_4$ reduction of $AgNO_3$ yielded nanoparticles with diameters between 10-14 nm. In contrast, TEM images of the Ag-PTA nanoparticles prepared in this study (Figures 3 and 4) showed an average diameter of 3.5 ± 2 nm. The smaller size of the nanoparticles reported here (as compared to those in the original preparation) is attributed to the PTA ligand. In the preparation reported here, PTA was added after the addition of all the $AgNO_3$ to the $NaBH_4$. Previous literature preparations did not use a stabilizing ligand other than excess borohydride. Borohydride does not stabilize the nanoparticles as well as PTA, and the absence of that ligand, the nanoparticles precipitate as bulk metal.[25,26] When PTA is added, further

growth is prevented by coordination of the stronger-binding PTA ligand. The particles were also examined with energy dispersive spectrometry (EDX), which confirmed that the nanoparticles were composed of silver.

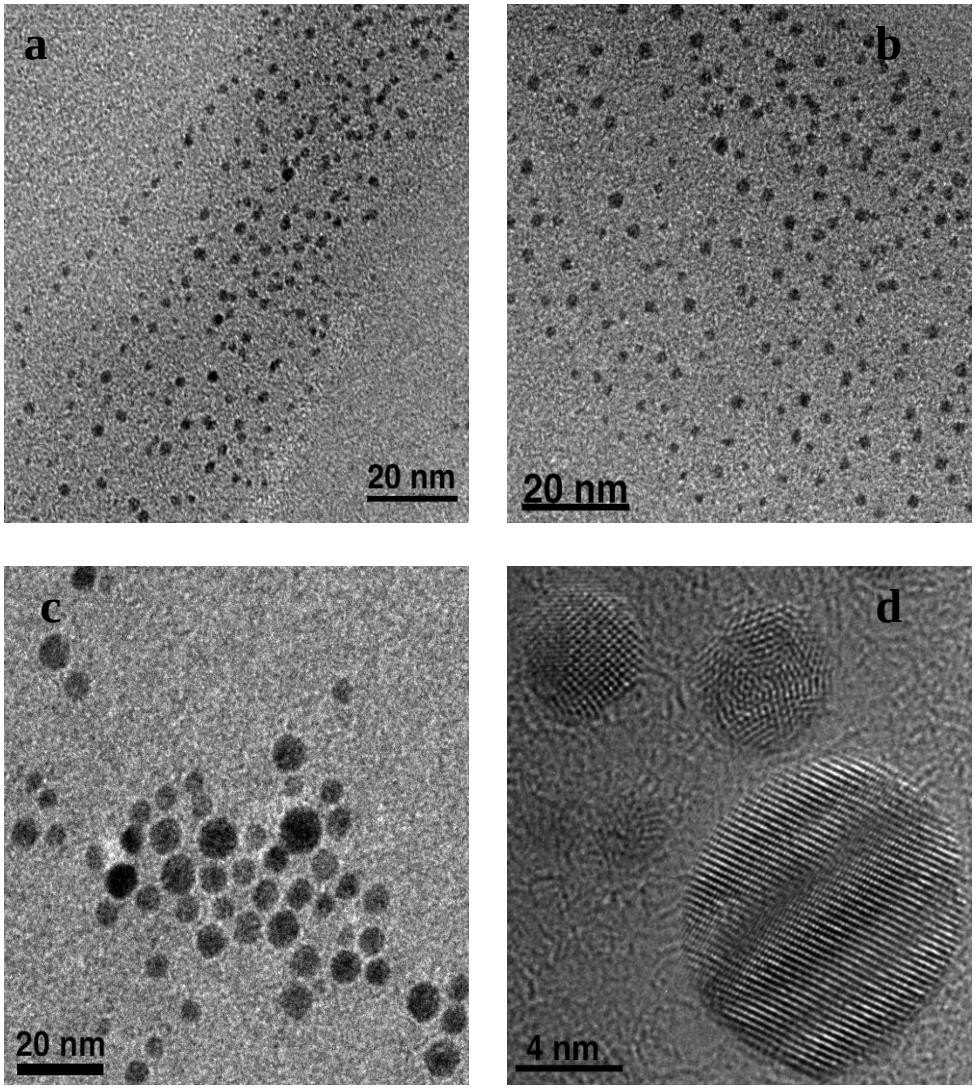

Figure 3. TEM images of 2 nm particles (a-b), and 4-10 nm particles (c). HRTEM image of 4-10 nm particles (d).

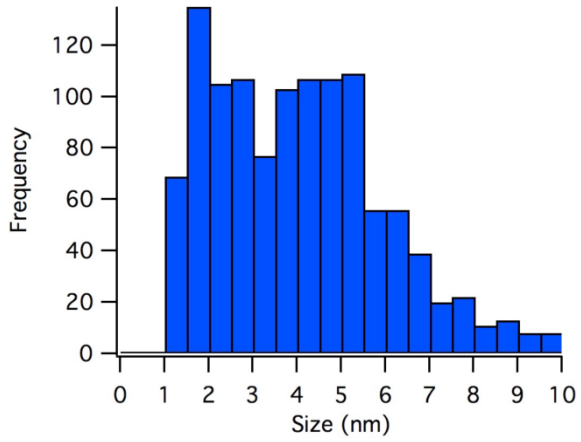

Figure 4. Size-distribution histogram of Ag-PTA nanoparticles. 1,175 nanoparticles were analyzed.

4.3. Catalysis Studies

4.3.1. Hydration of Aromatic Nitriles

A variety of activated and deactivated benzonitriles were hydrated to test the catalytic properties of the Ag-PTA nanoparticles (Table 1). Benzonitrile, a common substrate for testing nitrile hydration,[10,13] was hydrated to benzamide with 90% yield. We were pleased to find that the Ag-PTA nanoparticles catalyst was active in air and at fairly mild temperatures (90 ˚C), as previously reported Ag nanoparticle catalysts have required air-free conditions and temperatures in excess of 150 ˚C.[10,13,15]

Initial turnover frequencies (iTOF) for a range of *p*-substituted benzonitriles followed the trend that hydration goes faster as the electron-withdrawing ability of the substituent increases, as indicated by the Hammett plot in Figure 5.[4] As shown in prior studies,[1,4,27] the correlation between faster initial turnover frequency and increased

substituent electron withdrawing ability is attributed to the increased electrophilicity of the carbon atom in the nitrile as electron withdrawing ability increases. Similar results were found in this study. Thus, a Hammett plot for the hydration of substituted benzonitriles gave a positive slope ($\rho = 1.8$), indicating that electron withdrawing groups facilitate the reaction (Figure 5). Overall, these data suggest that nucleophilic attack of hydroxide or water is the rate limiting step, as has been shown previously with homogeneous nitrile hydration catalysts.[1,4]

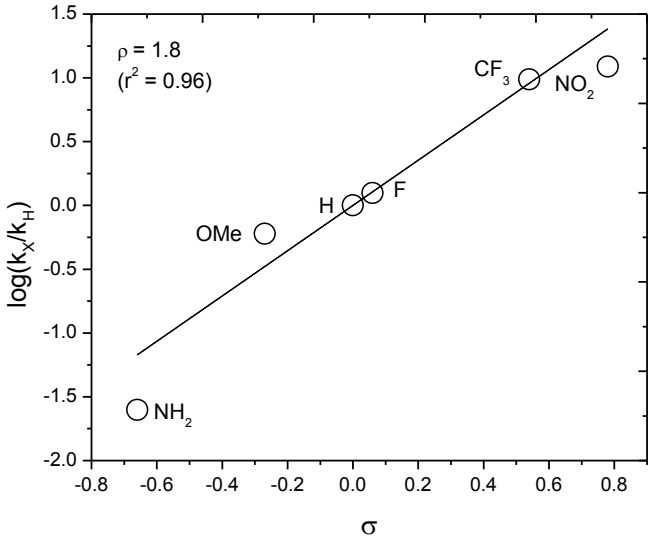

Figure 5. Hammett plot for hydration of *p*-substituted benzonitriles.

Hydration of several aliphatic nitriles was also examined with the Ag-PTA nanoparticles. Acetonitrile, propionitrile, and methoxyacetonitrile were not hydrated appreciably. It was hypothesized that this lack of activity is due to the increased electron density of the nitrile carbon in these aliphatic systems compared to the benzonitriles, making the nucleophilic attack on the nanoparticle-bound substrate less favorable.

Table 1. Selected Nitrile Hydration Results Using Ag-PTA nanoparticles [a]

Entry	Nitrile	[Nitrile] (M)	[Catalyst] (mM)	Catalyst Loading (mol %)	Temperature (°C)	iTOF (h^{-1})	Hammett sigma value(σ)[2] [8,29]	% Hydration	Ttime (h)
1	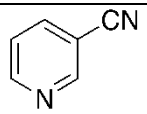	0.053	0.22	0.42	90		NA	48	282
2	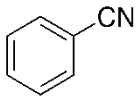	0.049	0.21	0.39	90	0.86	0.00	90	260
3	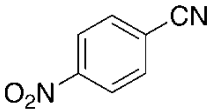	0.049	0.21	0.38	90	21.7	0.78	60	260
4	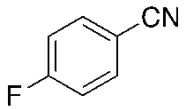	0.050	0.21	0.38	90	1.6	0.06	90	337
5	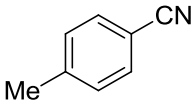	0.050	0.21	0.39	90	0.46	-0.27	44	337
6	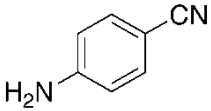	0.050	0.21	0.39	90	0.038	-0.66	3.7	337

Entry	Nitrile	[Nitrile] (M)	[Catalyst] (mM)	Catalyst Loading (mol %)	Temperature (°C)	iTOF (h^{-1})	Hammett sigma value(σ)$^2_{8,29}$	% Hydration	Ttime (h)
7	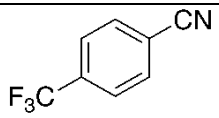	0.050	0.21	0.41	90	7.18	0.54	90	66

[a]Several other aromatic nitriles were tested (*p*-bromobenzonitrile, *p*-chlorobenzonitrile) but had poor solubility in water

This is a common issue with nanoparticle catalysts, as they are more electron rich than many homogeneous complexes and thus do not provide as much activation to the nitrile carbon.

4.3.2 Recycling Studies

Recycling studies were conducted for the hydration of benzonitrile. When the initial reaction was complete, the catalyst solution was cooled to 0 ˚C, causing the benzamide to crystalize out. The product was easily removed by filtration, and an additional aliquot of benzonitrile was added. This was also completely converted, and the catalyst was able to be reused at least three times total. The catalyst was also examined by scanning transmission electron microscopy (STEM) before and after the first hydration reaction (Figure 6). While the particles were several weeks old, and larger than when freshly prepared (Figure 1), they remained nearly the same size before and after catalysis

4.3.3. Cyanohydrin Hydrations

The catalytic activity of the Ag-PTA nanoparticles toward cyanohydrin hydration resulted in several observations. Addition of either acetone cyanohydrin or glycolonitrile (Figure 7) to the Ag-PTA nanoparticle solution produced an unexpected result: in less than 30 seconds, the orange nanoparticle solution became colorless. The UV-vis spectrum of the colorless solution showed the disappearance of the LSPR band at 400 nm, indicating that the nanoparticles had dissolved. Although the Ag-PTA nanoparticles were no longer present, the resulting solution was monitored to see if hydration would occur.

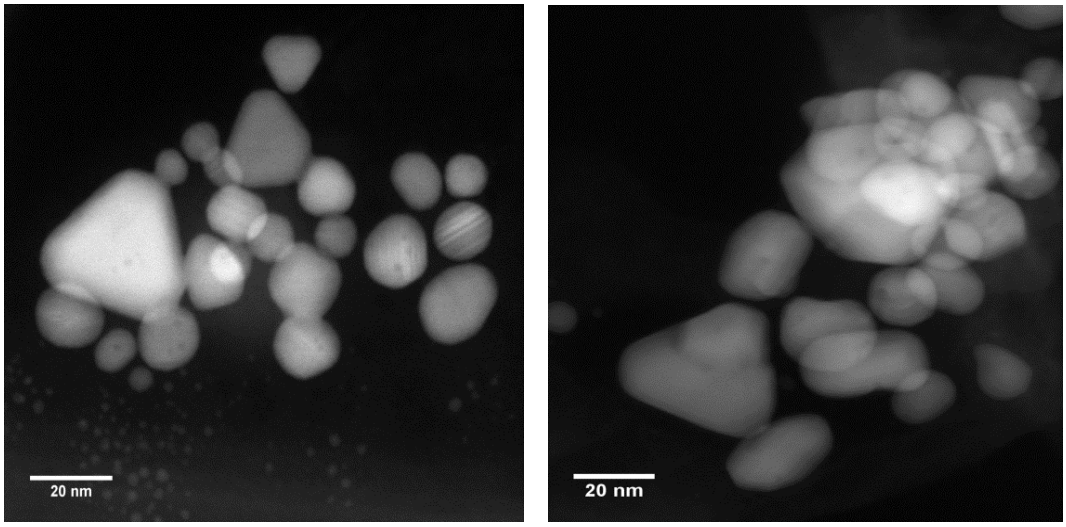

Figure 6. STEM images of Ag-PTA nanoparticles before (left) and after (right) catalyzing the hydration of benzonitrile. The particles do not undergo drastic changes under catalytic conditions.

Figure 7. Molecular structures of acetone cyanohydrin (**1**) and glycolonitrile (**2**).

After 504 hours, 9.7% of the ACH was hydrated to 2-hydroxyisobutyramide (HIBAM) (Table 2, entry 7). No further conversion was possible because the ACH had decomposed completely to acetone and HCN. In comparison, the best homogeneous catalyst for hydration of ACH, [Ru(η^6-cymene)Cl_2P($N(Me_2)_3$)], showed a maximum of 15% conversion of ACH to HIBAM in 22 hours.[27] (The catalyst was completely poisoned at this point so no further conversion was possible.) Thus, the catalyst resulting

from the nanoparticle dissolution that occurs when either ACH or glycolonitrile is added to the solution is reasonably active for the hydration of cyanohydrins.

Although other homogeneous catalysts became inactive due to cyanide poisoning after ACH degradation, the colorless solution generated from the dissolution of the Ag nanoparticles remained active. Addition of more ACH to the solution (after the first 504 hours of reaction) resulted in conversion of the added ACH to HIBAM, indicating that the solution was still catalytically active despite the presence of cyanide. As with the original solution, not all of the additional ACH was hydrated because some of it degraded to acetone and HCN. The solution, however, remained catalytically active, because addition of yet a third aliquot of ACH leads to more HIBAM.

4.3.4. Ag-PTA Nanoparticle Dissolution Studies

Studies were conducted to determine what caused the nanoparticle dissolution in the presence of cyanohydrins. As discussed previously, some cyanide is present in these cyanohydrin substrate solutions due to the equilibrium between the cyanohydrin, the aldehyde or ketone, and HCN (Scheme 2).[4] It has been shown in the literature that silver nanoparticles can disassemble to form $Ag(CN)_n$-type complexes in the presence of cyanide and dissolved oxygen.[20,30] It is proposed that this reactivity is also occurring in the Ag-PTA nanoparticle system. Addition of as little as 0.17 equivalent of cyanide to the Ag-PTA nanoparticle solution resulted in the solution becoming colorless almost immediately accompanied by the disappearance of the LSPR band in the electronic spectrum. Under an inert atmosphere, the nanoparticles persisted for several hours but

dissolution eventually occurred. Hydration of ACH proceeded at a similar rate to those trials conducted in air.

4.3.5. Cyanohydrin Hydration with a Silver Cyanide Solution

Experiments showed that the colorless solution formed by exposure of the Ag-PTA nanoparticles to an oxidant and cyanide was catalytically active. Table 2 (entries 8-13) has five separate ACH hydration trials with varying amounts of cyanide to show the effect of cyanide concentration on the catalyst

Unusually, the rate of hydration increased as the amount of added cyanide increased. In previous work from our lab, several ruthenium catalysts were found to increase in efficacy with small amounts (< 1 equivalent) of added cyanide.[5,27,31] In previously studied homogeneous catalysts, up to one equivalent of cyanide was found to increase the rate of hydration. This change was attributed to the electron-withdrawing ability of coordinated cyanide, a feature that facilitates nucleophilic attack of water or hydroxide ion on the coordinated nitrile.[27] However, as the amount of added cyanide increased above 1 equivalent, the rate of hydration significantly decreased because cyanide irreversibly bonded to both active sites in the complex. The result of adding cyanide to the nanoparticles is inconsistent with this trend. When 0.17 equivalents of cyanide were added to the reaction mixture, the rate of hydration increased compared to the case in which no cyanide was added (Table 2, Entry 10). As further cyanide was added to the reaction mixture (up to 9.3 equivalents), the rate of hydration was not affected.

Table 2. Hydration of acetone cyanohydrin (ACH) using a catalytically active colorless solution of cyanide and Ag-PTA nanoparticles

Entry	Nitrile	[Nitrile] (mM)	[KCN] (mM)	[Catalyst] (mM)	Catalyst Loading	Temperature (°C)	Eq CN^- to Ag atoms	% Hydration	Time (h)	iTOF (h^{-1})
8	Glycolonitrile	68.8	0.0	0.27	0.40	90	0	4.1	336	
9	ACH	65.3	0.0	0.27	0.41	90	0	9.7	504	0.078
10	ACH	65.2	0.05	0.27	0.41	90	0.2	13.8	504	0.087
11	ACH	64.6	0.26	0.27	0.41	90	1.0	17.1	504	0.09
12	ACH	61.8	1.26	0.25	0.41	90	5.0	14.5	843	0.1
13	ACH	61.5	2.26	0.24	0.39	90	9.3	17.1	843	0.093

4.3.6. Catalysis with Silver Cyanide Complexes

A control reaction showed that a solution of $AgNO_3$ and KCN hydrated ACH, which suggests that a $Ag(CN)_n^{1-n}$ type complex is capable of hydrating cyanohydrins. Thus, ACH was hydrated to HIBAM with a yield of 6.5% (Table 3). This result supports the hypothesis that, when the Ag-PTA nanoparticles become oxidized in the presence of oxygen and cyanide, they form an $Ag(CN)_n^{1-n}$ -type complex that is capable of hydrating nitriles. Further studies were conducted to determine the specific identity of the active catalyst.

AgCN is known to form insoluble linear coordination polymers in the solid state, and this species was observed as a precipitate in the solution of $AgNO_3$ and KCN.[32–34] Therefore this polymer is unlikely to be the active catalyst. It is more likely that a water soluble anionic complex such as $[Ag(CN)_2]^-$ catalyzes the hydration reaction. To test this hypothesis, the commercially available salt $K[Ag(CN)_2]$ was tested as a catalyst for nitrile and cyanohydrin hydration. Benzonitrile and ACH were tested as substrates and hydration of both species was observed (Table 4, Entries 15 and 16). Addition of PTA to the catalyst solution did not affect the rate of hydration (Table 4, Entry 17). Furthermore, the presence of additional CN^- did not change the rate significantly (Table 4, Entry 18).

Thus, the increase in rate of hydration in the presence of larger quantities of cyanide in the initial trials using the nanoparticle solution as catalyst was not due to the cyanide itself. Rather, as more cyanide was added, a more active catalyst $[AgCN_2^-]$, formed. The increased catalyst loading allowed the hydration reaction to proceed at a faster rate.

The resistance of the [$Ag(CN)_2^-$] complex to cyanide poisoning likely results from the lability of bonds to the d^{10} Ag(I) metal center. Thus, although cyanide is generated in the ACH equilibrium, it binds to the Ag center reversibly. Binding sites therefore remain available for the substrate. The greater activity of the anionic complex compared to Ag(I) alone can mostly likely be attributed to the greater electron deficiency of the metal center when cyanide is present.[1] This result offers a promising route forward for the hydration of cyanohydrins.

4.3.7. Control Reactions

Control experiments showed that aqueous $AgNO_3$ does act as a catalyst by itself; however the rate of hydration is quite slow and the activity of the $AgNO_3$ does not compare to that of the Ag nanoparticles. In a solution containing $AgNO_3$, *p*-nitrobenzonitrile was hydrated in very low yields (Table 4, Entry 20).

Solutions of $AgNO_3$ and PTA have been shown to form coordination polymers in which PTA binds silver through both P and N sites.[35] This polymer was synthesized and the species it formed in solution was shown to have similar catalytic potential to aqueous $AgNO_3$. These observations confirm that in the presence of cyanide, the catalyst is not simple Ag(I) or an $Ag(PTA)_n^+$ but an $Ag(CN)_n^{1-n}$ complex.

Table 3. Hydration reactions with silver cyanide complexes.

Entry	Nitrile	Catalyst	[Nitrile] (M)	[Catalyst] (mM)	Catalyst loading (mol) %	Temperature °C	% Hydration	Time (h)	iTOF (h^{-1})
14	ACH	$AgNO_{3(aq)}$+ KCN(aq)	0.063	2.70	4.3	90	6.5	499	0.01
15	ACH	$KAgCN_{2(aq)}$	0.049	0.25	0.52	90	6.5	216	0.14
16	Benzonitrile	$KAgCN_{2(aq)}$	0.048	0.25	0.52	90	50	216	0.7
17	ACH	$KAgCN_{2(aq)}$ +$PTA_{(aq)}$	0.048	0.25	0.52	90	6.0	216	0.13
18	ACH	$KAgCN_{2(aq)}$ +$KCN_{(aq)}$	0.048	0.25	0.52	90	6.0	216	0.13

Table 4. Control reactions hydrating *p*-nitrobenzonitrile

Entry	Catalyst	[Nitrile] (M)	[Catalyst] (mM)	Catalyst loading (mol %)	Temperature °C	iTOF (hr^{-1})	% Hydration	Time (h)
19	Ag-PTA nanoparticles	0.052	0.21	0.40	90	23.5	48	22
20	$AgNO_{3\ (aq)}$	0.057	0.24	0.42	90	1.4	11	19
21	$AgNO_{3(aq)}$ + $4PTA_{(aq)}$	0.057	0.24	0.42	90	1.8	14	19

4.4. Experimental

4.4.1. Instrumentation and Procedures

Nuclear magnetic resonance spectra were recorded on a Varian Unity/Inova 500 MHz (^{1}H, 500.10 MHz; ^{31}P, 202.45 MHz; ^{13}C, 151 MHz) spectrometer, or on a Bruker Biospin 600 MHz (^{1}H, 600.02 MHz; ^{31}P, 242.83 MHz) spectrometer. The ^{1}H chemical shifts were referenced to the solvent peak or TMS (0.00ppm) and the ^{31}P chemical shifts were referenced to H_3PO_4 (0.00 ppm). The solvent used for all NMR trials was D_2O. UV-vis spectra were recorded on a HP 8453 spectrometer using 1 cm quartz cuvettes. All hydration reaction samples were prepared in 1-dram screwcap vials fitted with septum caps. (HR)TEM images were acquired with a FEI Titan 80-300 kV transmission electron microscope equipped with a spherical aberration (C_s) image corrector, an EDAX energy dispersive spectrometer, and a Tridiem 863 Gatan imaging filter and electron energy loss spectrometer. All images were acquired at 300 kV. PTA was synthesized from literature methods.[30]

4.4.2. Preparation of PTA Stabilized Silver Nanoparticles

A preparation from the S. D. Solomon group for uncapped silver nanoparticle synthesis was modified.[17] $NaBH_4$ (0.0082g, 0.217mmol) was dissolved in 90 ml water and placed in an ice bath with magnetic stirring. $AgNO_3$ (0.0059g, 0.035mmol) was dissolved in 30 mL water and added over 10 minutes to the cool $NaBH_4$ solution. The solution turned yellow, characteristic of silver nanoparticles. After the particles had been formed, PTA (0.0061g, 0.039mmol) dissolved in 10 mL of water was added to the solution as a stabilizer. Samples were prepared for TEM on a lacey carbon grid with an ultrathin (3nm) carbon support film supported by copper mesh. A dilute nanoparticle solution was dropped on the grid and allowed to evaporate.

4.4.3. General Procedure for the Hydration of Benzonitrile with PTA- Stabilized Ag NPs

Benzonitrile (10 μL, 0.09 mmol) was added to 1000μL of a 0.22 mM Ag NP solution and heated to 90°C with stirring. Aliquots (100 μL) were removed periodically using a gas-tight syringe and were combined in an NMR tube with 500 μL of a 2.28mM NMe_4PF_6 solution in D_2O as an internal standard. The progress of the reaction was monitored by observing the disappearance of the benzonitrile resonances at 7.70 ppm (*d*, J = 7.48 Hz), 7.65 ppm (*t*, J = 7.85 Hz), and 7.49 ppm (*t*, J = 7.87 Hz) and the appearance of the amide resonances at 7.78 ppm (*m*) and 7.15 ppm (*t*, J=7.97 Hz) in the ^1H NMR spectrum of the mixture.

4.4.4. General Procedure for the Hydration of p-Substituted Benzonitriles with PTA-Stabilized Ag NPs

The nitrile was dissolved in 2 mL acetone and added to the 0.22 mM catalyst solution to achieve a concentration of approximately 50 mM. This solution was heated to 90°C with stirring. Aliquots (100 μL) were removed periodically using a gas-tight syringe and combined in an NMR tube with 500μL of a 2.28 mM solution of NMe_4PF_6 in D_2O. Specific details for individual nitriles are as follows.

p-Fluorobenzonitrile. The progress of the reaction was monitored by observing the disappearance of the aromatic p-fluorobenzonitrile resonances at 7.78 ppm (*m*) and 7.24 ppm (*t*, J = 8.8 Hz) and the appearance of the amide resonances at 7.79 ppm (*m*) and 7.17 ppm (*t*, J = 9.1 Hz) in the ^{1}H NMR spectrum.

p-Nitrobenzonitrile. The progress of the reaction was monitored by observing the disappearance of the aromatic *p*-nitrobenzonitrile resonances at 8.32 ppm (*d*, J = 8.5 Hz) and 7.96 ppm (*d*, J = 8.7 Hz) and the appearance of the amide resonances at 8.27 (*d*, J = 8.6 Hz) and 7.92 ppm (*d*, J = 8.9 Hz) in the ^{1}H NMR spectrum.

p-Methoxybenzonitrile. The progress of the reaction was monitored by observing the disappearance of the aromatic *p*-methoxybenzonitrile resonances at 7.66 ppm (*d*, J = 8.7 Hz) and 7.02 ppm (*d*, J = 8.8 Hz) and the appearance of the amide resonances at 7.74 ppm (*d*, J = 8.6 Hz) and 7.01 ppm (*d*, J = 8.7 Hz) in the ^{1}H NMR spectrum.

p-Aminobenzonitrile. The progress of the reaction was monitored by observing the disappearance of the aromatic *p*-aminobenzonitrile resonance at 7.43 ppm (*d*, J = 8.5

Hz) and the appearance of the amide resonance at 7.57 ppm (*d*, 8.4 Hz) in the ^{1}H NMR spectrum.

p-Trifluoromethylbenzonitril.e The progress of the reaction was monitored by observing the disappearance of the aromatic *p*-trifluoromethylbenzonitrile resonances at 7.89 ppm (*d*, J = 8.4 Hz) and 7.82 ppm (*d*, J = 8.0 Hz) and the appearance of the amide resonances at 7.87 ppm (*d*, J = 8.3 Hz) and 7.77 ppm (*d*, J = 8.1 Hz) in the ^{1}H NMR spectrum.

4.4.5. Hydration of Nicotinonitrile with PTA-Stabilized Ag NPs

Nicotinonitrile (0.0493g, 0.474mmol) was added to 1 mL acetone. This solution (125μL) was added to 1000μL of a 0.22 mM AgNP solution. The mixture was heated to 90°C with stirring. Aliquots (100 μL) were removed periodically using a gas-tight syringe and were combined in an NMR tube with 450 μL D_2O and 50μL of a 10.86mM NMe_4PF_6 in D_2O internal standard solution. The progress of the reaction was monitored by observing the disappearance of the nicotinonitrile resonance at 8.81ppm and the appearance of the amide resonance at 8.73ppm.

4.4.6. Hydration of ACH with PTA-Stabilized Ag NPs

ACH (10μL, 0.109 mmol) was added to 1750μL of a 0.22 mM Ag NP solution. This solution was heated to 90°C with stirring. After 264 hours, an additional 0.082 mmol of ACH (7.5μL of a 10.95M solution) was added to the reaction vessel. Aliquots (100 μL) were removed periodically using a gas-tight syringe and were combined in an NMR tube with 450 μL D_2O and 50μL of a 10.86 mM NMe_4PF_6 in D_2O internal standard

solution. The progress of the reaction was monitored by observing the disappearance of the methyl resonance of acetone cyanohydrin at 1.57 ppm (*s*, 6H, $HO(CH_3)_2CCN$), and the appearance of the amide resonance at 1.34ppm (s, $HO(CH_3)_2CC(O)NH_2$) .

4.4.7. Hydration of p-Nitrobenzonitrile with $AgNO_3$

$AgNO_3$ (0.006g, 0.03 mmol) was dissolved in 10mL water. Nitrobenzonitrile (0.0408g, 0.275mmol) was dissolved in1 mL acetone-*d6*. The *p*-nitrobenzonitrile solution (400μL) and the $AgNO_3$ solution (130μL) were added to 1400μL water in a 1 dram screwcap vial capped with a septum. This mixture was heated to 90°C with stirring. Aliquots (100 μL) were removed periodically using a gas-tight syringe and were combined in an NMR tube with 450 μL D_2O and 50μL of a 10.86mM NMe_4PF_6 in D_2O internal standard solution. The progress of the reaction was monitored by observing the disappearance of the p-nitrobenzonitrile resonance at 8.32 ppm (*d*, J = 8.5 Hz) and the appearance of the amide resonance at 8.27 (*d*, 8.6 Hz) in the ^1H NMR spectrum.

4.4.8. Hydration of p-Nitrobenzonitrile with $AgNO_3$ and 4 equivalents PTA

Nitrobenzonitrile (0.0408g, 0.275mmol) was dissolved in 1 mL acetone-*d6*. $AgNO_3$ (0.006g, 0.0353mmol) was dissolved in 10mL water. PTA (0.0088g, 0.0566mmol) was added to 4mL of the $AgNO_3$ solution. The *p*-nitrobenzonitrile solution (400μL) and the $AgNO_3$/PTA solution (130μL) were added to 1400μL water. This mixture was heated to 90°C with stirring in a 1 dram screwcap vial capped with a septum. Aliquots (100 μL) were removed periodically using a gas-tight syringe and were combined in an NMR tube with 450 μL D_2O and 50 μL of a 10.86 mM NMe_4PF_6 in D_2O internal standard solution. The progress of the reaction was monitored by observing the

disappearance of the *p*-nitrobenzonitrile resonance at 8.32 ppm (*d*, J = 8.5 Hz) and the appearance of the amide resonance at 8.27 (*d*, 8.6 Hz) in the ^{1}H NMR spectrum.

4.4.9. Hydration of ACH with $AgNO_3$ and KCN

ACH (10 μL, 0.109 mmol) was added to a solution containing 100 μL of $AgNO_3$ (58.87 mM) and varying amounts of KCN (24.5 mM) which had been diluted to 1610 μL. This mixture was heated to 90°C with stirring in a 1 dram screwcap vial with a septum cap. Aliquots (100 μL) were removed periodically using a gas-tight syringe and were combined in an NMR tube with 500 μL of a 10.86mM NMe_4PF_6 in D_2O. The progress of the reaction was monitored by observing the disappearance of the methyl resonance of acetone cyanohydrin at 1.57 ppm (*s*, 6H, $HO(CH_3)_2CCN$), and the appearance of the amide resonance at 1.34ppm (*s*, $HO(CH_3)_2CC(O)NH_2$) .

4.4.10. General Procedure for the Hydration of ACH with $K[Ag(CN)_2]$

ACH (10 μL, 0.109 mmol) was added to 1000μL of a 5.03 mM solution of $KAg(CN)_2$ in water. In some cases a solution of PTA (100 μL of a 50 mM solution in H_2O) was added to the catalyst solution. This solution was heated to 90°C with stirring in a 1 dram screwcap vial capped with a septum. Aliquots (100 μL) were removed periodically using a gas-tight syringe and were combined in an NMR tube with 500 μL of a 2.28 mM NMe_4PF_6 internal standard solution in D_2O. The progress of the reaction was monitored by observing the disappearance of the methyl resonance of acetone cyanohydrin at 1.57 ppm (*s*, 6H, $HO(CH_3)_2CCN$) and the appearance of the amide resonance at 1.34ppm (s, $HO(CH_3)_2CC(O)NH_2$) .

4.4.11. Hydration of Benzonitrile with $K[Ag(CN)_2]$

Benzonitrile (10 μL, 0.0969 mmol) was added to 1000μL of a 5.03 mM solution of $KAg(CN)_2$ in water. This mixture was heated to 90°C with stirring in a 1 dram screwcap vial capped with a septum. Aliquots (100 μL) were removed periodically using a gas-tight syringe and were combined in an NMR tube with 500 μL of a 2.28 mM NMe_4PF_6 internal standard solution in D_2O. The progress of the reaction was monitored by observing the disappearance of the benzonitrile resonance at 7.49 ppm (*t*, J = 7.87 Hz) and the appearance of the amide resonance at 7.15 ppm (*t*, J=7.97 Hz) in the ^1H NMR spectrum of the mixture.

4.5. Summary

The catalytic hydration of cyanohydrins and of acetone cyanohydrin, in particular, is plagued by two major problems, low TOFs and catalyst poisoning by cyanide. The results presented in this paper suggest a strategy for overcoming the poisoning problem. Specifically, it was found that the $Ag(CN)_2^-$ complex will catalytically hydrate acetone cyanohydrin and glycolonitrile in the presence of cyanide without getting poisoned, although the TOFs are very low. The insensitivity of the $Ag(CN)_2^-$ catalyst to cyanide is attributed to the lability of the Ag(I) metal center, which suggests it will be worthwhile to examine the catalytic hydration abilities of other complexes with labile electronic configurations.

This study also showed that water-soluble Ag nanoparticles can be synthesized by preparing them with a PTA ligand shell, where PTA is a water-soluble phosphine ligand. The Ag-PTA nanoparticles are respectable nitrile hydration catalysts, as demonstrated by

their ability to hydrate a variety of nitriles with various steric and electronic properties at rates comparable to some of the better homogeneous catalysts.[21] Unfortunately, the Ag-PTA nanoparticles do not hydrate acetone cyanohydrin or other cyanohydrins because the nanoparticles are unstable in the presence of cyanide.

Finally, it is noted that the Ag-PTA and $Ag(CN)_2^-$ catalysts are not fast enough to be used on either a laboratory or industrial scale so the next step in finding a viable catalyst for ACH hydration must be to find a more active catalyst. Although standard methods are known for improving the TOFs of homogeneous catalysts, most of these methods rely on making changes to inert (non-labile) ligands. Thus, combining these methods with the strategy of using a labile metal center could prove problematic. An alternative strategy would be to develop a catalyst that operates under conditions that stabilize ACH and prevent it from forming HCN, namely strongly acidic medium. Both strategies are currently being investigated in our laboratory.

4.6. Bridge

This chapter described the synthesis and characterization of PTA stabilized silver nanoparticles and their reactivity towards nitriles, as well as their degradation in the presence of cyanide and the catalytic activity for the resulting labile silver complex for the hydration of cyanohydrins. The next chapter reports on the synthesis and activity of a nickel catalyst supported on hydrotalcite clay for the hydration of nitriles and cyanohydrins.

CHAPTER V

HYDRATION OF CYANOHYDRINS WITH A SOLID SUPPORTED NICKEL CATALYST

Chapter V is co-authored with Trenton Peters-Clark, who synthesized materials under my supervision.

5.1. Introduction

Methyl methacrylate (MMA) and other derivatives of methacrylic acid are important in the production of various commercial polymers, including polymethylmethacrylate (PMMA), which is commonly known as Plexiglass™.[1] The industrial processes used for these materials often include harsh reagents and reaction conditions. For example, the industrial process currently used to produce MMA, the acetone cyanohydrin (ACH) process, uses concentrated sulfuric acid and produces many byproducts . The most problematic of these is ammonium hydrogen sulfate (AHS) which is produced in large quantities (up to 2.5 kg for each 1 kg of MMA produced).[2] The AHS is recycled to sulfuric acid; however, that process requires pyrolysis at temperatures of greater than 1000 ˚C. A synthesis that could achieve hydration of ACH without the use of sulfuric acid would be beneficial both economically and environmentally.[3]

A promising route for an acid-free synthesis of acrylate monomers is through the transition metal catalyzed hydration of α-hydroxy-nitriles to amides, which can then be converted easily to the desired ester, acid or amine. There are a number of homogeneous

catalysts for the hydration of nitriles that are tolerant of for a range of functional groups and electronics.[3–5] Yet when hydration of cyanohydrins is attempted, minimal conversion is observed. These low yields are due to the natural equilibrium of cyanohydrins,[3,6] where the cyanohydrin is in equilibrium with the corresponding aldehyde or ketone and hydrogen cyanide (Scheme 1). When a transition metal catalyst is present, the cyanide can bind to the active site irreversibly, stopping catalytic function. Acidic conditions stabilize cyanohydrins, and by developing a catalyst that functions at low pH ([$RuCl_2(\eta^6$-*p*-cymene){$P(NMe_2)_3$}]), our lab was able to achieve 15% hydration of ACH.[7] Although this is the highest conversion of ACH with a homogeneous transition metal catalyst to date, the catalyst was nonetheless poisoned by cyanide, precluding complete hydration.

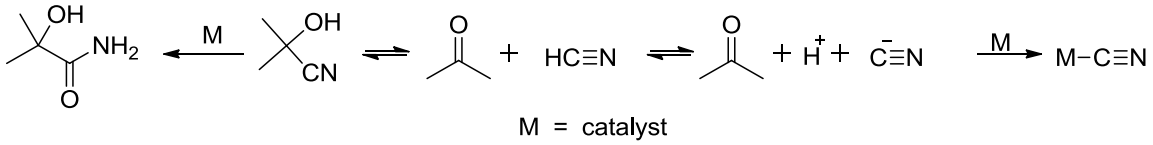

Scheme 1. ACH equilibrium and possible reactions with a metal catalyst.

Our lab has recently begun to investigate nanoparticles as catalysts for cyanohydrin hydration as well. There are reports of a variety of reactions catalyzed by nanoparticles, which present multiple advantages over traditional homogeneous catalysts, including ease of separation and robustness.[8–10] The literature offers a handful of examples of nitrile hydration.[11–19] Many of these, however, focus on silver nanoparticles,[13,14,18] which we recently showed were unsuitable for the hydration of cyanohydrins due to a propensity to disassemble in the presence of cyanide. The amount of cyanide generated by the ACH

equilibrium is enough to cause this degradation (see Chapter IV). Gold nanoparticles, which have the highest observed turnover frequency (TOF) among reported nanoparticle nitrile hydration catalysts, are similarly unstable when exposed to cyanide.[19] We have also had some success hydrating cyanohydrins with platinum nanoparticles. Using a nanoparticle catalyst generated *in situ* from a platinum complex, 30% hydration of ACH to HIBAM was achieved. Yet although these particles showed impressive cyanide resistance, they degraded under catalytic conditions, rendering them unusable from an industrial standpoint (see Chapter III).

Thus we turned our attention to nickel nanoparticles, which have been used for nitrile hydration by Subramian and Pitchumani.[17] They prepared Ni nanoparticles supported on hydrotalcite (HT) ($Mg_6Al_2(CO)_3OH$), which catalyzed the hydration of a range of nitriles.[17] This catalyst was promising from an industrial standpoint because it was easily prepared, used inexpensive Ni and clay, and could be separated from the reaction mixture.

HT is a layered material with interesting properties. The structure resembles that of brucite ($Mg(OH)_2$) where Mg cations are octahedrally coordinated by hydroxyl anions, but some of the Mg atoms are replaced with Al in the network. They have a lamellar structure, with interstitial anions (usually carbonate) and water molecules between the positively charged layers (Figure 1).[20] Both the metals in the layers and the interstitial anions are easily tunable, and many interesting materials have been generated through ion exchange of HT. These materials have been used as catalysts for various reactions such as Pd-cross coupling[21], olefin epoxidation[22], olefin dihydroxylation[23], depolymerization[24],

and H_2 production[25]. Furthermore, HT itself can be used as a solid base catalyst for reactions such as lipid transesterification.[26,27]

The catalyst was prepared by depositing Ni on the HT surface and reducing it to produce Ni nanoparticles (Ni/HT). This catalyst afforded unprecedented yields for the hydration of ACH, with 60 % conversion to HIBAM, however characterization of the active catalyst was difficult and inconclusive. Work towards elucidating the active species is ongoing.

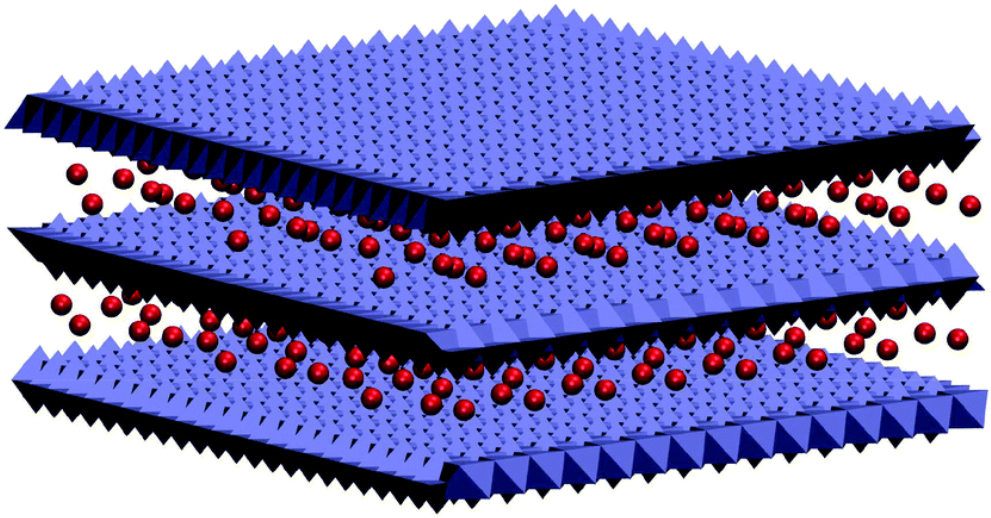

Figure 1. Illustration of hydrotalcite, a layered double hydroxide with carbonate anions (red balls) in the interstitial space. The brucite like layers composed of magnesium and aluminum are shown in blue.

5.2. Hydration Trials

5.2.1. Initial Trials

The catalyst was prepared according to the published procedure.[17] As the substrate scope of the catalyst had been thoroughly examined in previous investigations,[17]

our study focused mainly on the hydration of cyanohydrins. Initial trials before optimization were very promising, reaching 10 % hydration of ACH as well as good results for other nitriles tested (Table 1).

Table 1. Initial nitrile hydration trials with a solid supported nickel catalyst [a]

Entry	Nitrile	% Hydration	Time (h)
1	ACH	10	164
2	Glycolonitrile	58	164
3	Benzonitrile	100	168
4	Acetonitrile	4	168

[a] Trials were conducted under air and in water, with 0.55 mmol nitrile and 5 mg catalyst

5.2.2. Optimization Reactions

Because cyanohydrins are stabilized by lower pH and temperatures, hydration trials using benzonitrile as a model substrate were conducted to probe catalyst activity under these conditions (Table 2). An acetone co-solvent was also tested, as the presence of excess acetone can help drive the cyanohydrin equilibrium away from the ketone. The catalyst was found to be active at pHs as low as 4, although conversion was halted at pH 2 (Table 2, Entries 1 and 2). Lowering the pH resulted in decreased conversion and TOF, however. The use of acetone did not have any appreciable results on the conversion or turnover frequency (Table 2, Entry 4). As expected, the TOF was lowered along with the temperature (Table 2, Entry 5).

Table 2. Hydration of benzonitrile to benzamide with a solid supported nickel catalyst[a]

Entry	pH	Temperature (˚C)	% Hydration	TOF (h^{-1})
1	2	90	0	-
2	4	90	35	0.086
3	6	90	60	0.16
4[b]	6	90	58	0.15
5	6	50	33	0.083

[a] Trials were conducted over 209 h, under air and in water, with 0.55 mmol benzonitrile and 5 mg catalyst
[b] Conducted in 2:1 water: acetone.

5.2.3. Cyanohydrin Trials.

Cyanohydrin hydration trials were then conducted with better optimized conditions (Table 3). Using a lower temperature and acetone co-solvent, a range of catalyst loadings were tested. By increasing the catalyst loading to 16 mol %, (assuming all Ni is adsorbed to the support surface) a 60 % conversion of ACH to HIBAM was achieved. This is by far the best yield observed for the hydration of ACH using a transition metal catalyst under mild conditions.

5.3. Characterization

5.3.1. TEM Characterization

The catalyst was analyzed with transmission electron microscopy (TEM), and energy dispersive spectroscopy (EDX). The TEM images showed only solid support and no evidence of nanoparticles. However the EDX, which gives elemental analysis, did

show that there was nickel present in the material, along with magnesium and aluminum as expected.

Table 3. Hydration of cyanohydrins with a solid supported nickel catalyst [a]

Entry	Substrate	Weight Catalyst (mg)	Catalyst Loading[b] (mol %)	% Hydration	TOF (h^{-1})
1	ACH	5	1	31	0.05
2	ACH	10	8	48	0.04
3	ACH	20	16	63	0.02
4	Glycolonitrile	10	8	90	0.08

[a] Trials were conducted at 40 ˚C over 483 h, under air and in a 2:1 water: acetone mixture, 0.2 mmol nitrile

[b] Assumes all Ni has adsorbed to catalyst surface

The original paper contained characterization by XRD and SEM, though the images are difficult to resolve and the diffraction patterns are inconclusive.[17] It is certainly possible that the material obtained by those researchers was different from that obtained by our lab due to some difference in preparation or conditions. However the differences are not readily apparent based on the information reported.

5.3.2. Control Reactions

A range of control reactions were conducted to elucidate the makeup of the active catalyst. ACH hydration to HIBAM was tested with various catalyst components as well as the HT support with no Ni present (Table 4). Minimal hydration occurred with metal nitrate salts and Ni(0) (Table 4, Entries 4-7). Some hydration was observed with $NaBH_4$, however the substrate all degraded before conversion could take place, in contrast to the

reaction with the active catalyst (Table 4, Entry 3). This was most likely due to the high pH driving the equilibrium away from ACH. The HT support acted as a catalyst on its own, but the amount of conversion was not as much as with the Ni/HT catalyst.

Table 4. Control Reactions for the Hydration of ACH to HIBAM[a]

Entry	Catalyst	% Hydration
1	none	nil
2	HT	35
3	$NaBH_4$	20
4	$Ni(NO_3)_{2(aq)}$	nil
5	$Al(NO_3)_{3(aq)}$	nil
6	$Mg(NO_3)_{2(aq)}$	6
7	Ni^0	nil
8	NaOH (pH 8)	25

[a] Trials conducted at 40 ˚C over 260 h, under air and in water, 0.2 mmol ACH

The Ni/HT catalyst was tested directly for activity against the HT support, which was treated in the same manner as the catalyst but without the addition of Ni. Samples of HT were suspended in water with stirring and the pH adjusted to 8 with a solution of ammonium hydroxide. Aqueous $Ni(NO_3)_2$ was added to one, and they were stirred for 5 hours, filtered, and washed with excess water. The sample containing Ni had turned blue green, while the HT sample remained white. Both were then stirred for 1h at 80 ˚C with sodium borohydride.

When hydration of ACH was attempted with equal amounts of material, both materials were active towards ACH hydration, although the catalyst containing Ni achieved somewhat higher conversion (50% vs. 40%). This result suggests that although HT is active as a catalyst in its own right, the presence of nickel enhances the catalytic activity.

The pH of the reaction mixture was observed to rise over time from 6.5 to 8 as the catalyst was heated. This is possibly due to the deprotonation of water by the hydroxide linkers in the HT support. A similar alkalinity was seen with the HT alone under reaction conditions. However when catalysis was attempted at a similar pH in pure water, the conversion of ACH to HIBAM was less than that of HT or Ni/HT (Table 4, Entry 8).

5.3.3. Recycling Studies

Recycling studies were also undertaken with the Ni/HT catalyst. After the full conversion of all remaining ACH (Table 3, Entry 3), the solid supported catalyst was filtered from the reaction mixture, then washed and dried. The recovered catalyst (10 mg) was tested for catalytic activity along with the filtrate. Only the solid catalyst resulted in hydration, although the activity was significantly decreased compared to previous trials (10% conversion). The reduced activity is most likely a result of structural changes to the catalyst under the reaction conditions rather than cyanide poisoning. HT catalysts have previously displayed altered structures after heating.[26] Furthermore, UV-vis studies of the filtrate showed no Ni, Mg, or Al, indicating that metal leaching from the catalyst surface was not responsible for hydration (Figure 2).

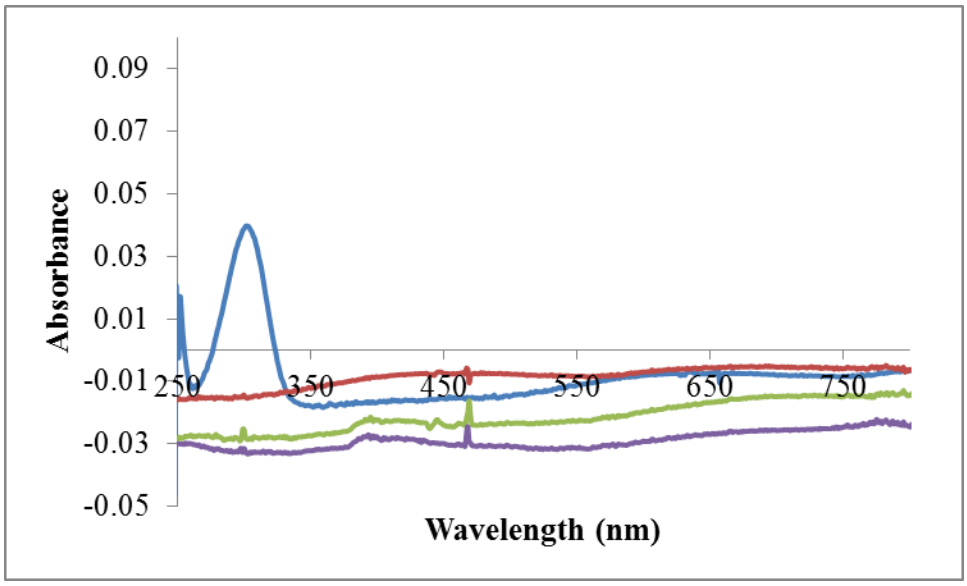

Figure 2. UV-vis spectra of metals Ni/HT is composed of: Ni(blue), Mg(red), and Al (green) as well as the filtrate of the recycled catalyst(purple).

5.4. Catalyst Hypothesis

Because the catalysts containing nickel were more active than those without, it seemed likely that Ni provided a better active site for nitrile binding than the support itself. Nonetheless, it was possible that either Al^{3+} or Mg^{2+} could act as a binding site, since hydration occurred with no Ni present. However this does not account for the high activity of the catalyst for cyanohydrin hydration. Sturgeon *et. al* suggested a synergistic effect between the hydroxides and metal centers for a similar HT supported Ni catalyst used for the depolymerization of lignin.[24] In a similar fashion to nitrile hydration, this reaction could be achieved with a simple base catalyst with mixed results, however the reaction was was much more selective when a metal center was involved. Yet they were unable to conclusively determine the exact species of Ni involved in the reaction, as Ni oxides and hydroxides were both possibly present.[24]

We hypothesized that a similar mechanism was responsible for the results observed with ACH. The proposed mechanism involved the binding of the nitrile on a Ni (or Mg where no Ni is present) active site, with a hydroxide from the HT deprotonating water for attack on the nitrile carbon to form the iminol intermediate and eventually the amide product (Scheme 2). The Ni/HT catalyst could thus behave in a similar manner to the successful bifucntional nitrile hydration catalysts, and activate the nitrile while simultaneously generating a hydroxide ion for nucleophilic attack.

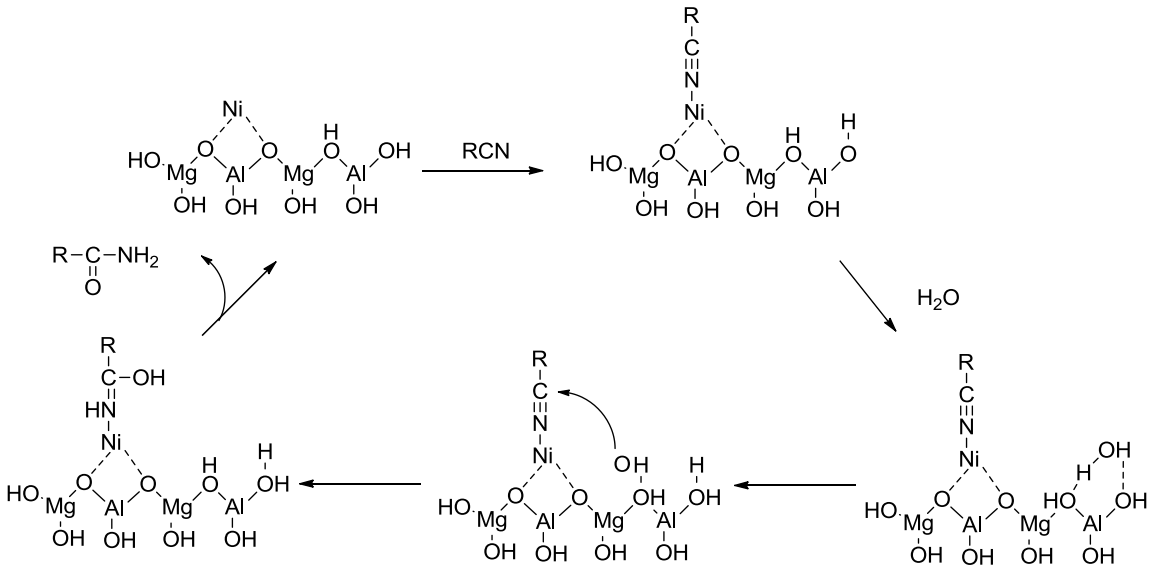

Scheme 2. Proposed mechanism for nitrile hydration with a HT supported Ni catalyst, where the OH ions contained in the support structure activate water for nucleophilic attack.

5.5. Experimental

5.5.1. Instrumentation and Procedures

Nuclear magnetic resonance spectra were recorded on a Varian Unity/Inova 500 MHz (^{1}H, 500.10 MHz; ^{31}P, 202.45 MHz; ^{13}C, 151 MHz) spectrometer. The ^{1}H chemical

shifts were referenced to the solvent peak or TMS (0.00ppm) and the ^{31}P chemical shifts were referenced to H_3PO_4 (0.00 ppm). The solvent used for all NMR trials was D_2O, and the internal standard was 10.86 mM NMe_4PF_6. UV-vis spectra were recorded on a HP 8453 spectrometer using 1 cm quartz cuvettes. All hydration reaction samples were prepared in 1-dram screwcap vials fitted with septum caps. (HR)TEM images were acquired with a FEI Titan 80-300 kV transmission electron microscope equipped with a spherical aberration (C_s) image corrector, an EDAX energy dispersive spectrometer, and a Tridiem 863 Gatan imaging filter and electron energy loss spectrometer. All images were acquired at 300 kV. All reagents and starting materials were obtained commercially and used without further purification.

5.5.2. Synthesis of Ni/HT

Hydrotalcite was synthesized by co-precipitation. $Al(NO_3)_3 \cdot 9\ H_2O$ (1 mmol) and $Mg(NO_3)_2 \cdot 6H_2O$ (5 mmol) were dissolved in DI water (100 mL) and added slowly to a solution (50 mL) of Na_2CO_3 (3 mmol) and NaOH (7 mmol) with stirring. The mixture was stirred for 18h at 65 ˚C. The resulting white slurry was cooled to room temperature, filtered, and washed with DI water. It was then dried overnight at 100 ˚C under vacuum.

The catalyst was prepared by suspending 0.2 g HT in 2 mL of a 0.08 mmol solution of nickel nitrate. The pH was adjusted to 8.0 with ammonium hydroxide and the mixture stirred for five hours at room temperature. The slurry was filtered washed and dried to yield a green powder. The supported Ni(II) was reduced with sodium borohydride (0.1 mmol) at 80 ˚C for 1h. The color changed from green to gray.

5.5.3. General Procedure for Nitrile Hydration with Ni/HT.

Ni/HT (10 mg in most cases) was placed in a 1 dram vial with a stir bar and 2 mL reagent grade water and 0.5 mmol nitrile. For cyanohydrin hydration trials, an additional 1 mL acetone was added. The vial was sealed and heated to 40 ˚C. Aliquots of 100 μL were taken periodically and the reaction followed by ^{1}H NMR using an internal standard (500 μL 10.86 mmol NMe_4PF_6). Details for specific nitriles are as follows.

Acetonitrile. The progress of the reaction was monitored by observing the disappearance of the acetonitrile resonance at 2.01 ppm (*s*, C*H*$_3$CN) and the appearance of the acetamide at 1.93 ppm (*s*, C*H*$_3$C(O)NH$_2$).

Benzonitrile. The progress of the reaction was monitored by observing the disappearance of the benzonitrile resonances at 7.70 ppm (*d*, J = 7.48 Hz), 7.65 ppm (*t*, J = 7.85 Hz), and 7.49 ppm (*t*, J = 7.87 Hz) and the appearance of the amide resonances at 7.78 ppm (*m*) and 7.15 ppm (*t*, J=7.97 Hz) in the ^{1}H NMR spectrum of the mixture.

Acetone Cyanohydrin. The progress of the reaction was monitored by observing the disappearance of the methyl resonance of acetone cyanohydrin at 1.57 ppm (*s*, 6H, HO(C*H*$_3$)$_2$CCN), and the appearance of the amide resonance at 1.34ppm (*s*, HO(C*H*$_3$)$_2$CC(O)NH$_2$) .

Glycolonitrile. The progress of the reaction was monitored by observing the disappearance of the methyl resonance of glycolonitrile at 4.31 ppm (*s*, 2H, HOC*H*$_2$CN), and the appearance of the amide resonance at 1.23 ppm (*s*, 2H, HOC*H*$_2$C(O)NH$_2$) .

5.5.4. Control Reactions

The hydration trials were conducted with ACH according to the general hydration procedure, in a 1 dram vial containing ACH (0.5 mmol) with 2 mL water and 1 mL acetone. The vials were sealed and placed in an oil bath at 40 ˚C. The progress of the reaction was monitored by observing the disappearance of the methyl resonance of acetone cyanohydrin at 1.57 ppm (*s*, 6H, $HO(CH_3)_2CCN$), and the appearance of the amide resonance at 1.34ppm (*s*, $HO(CH_3)_2CC(O)NH_2$) .

5.6. Summary

A nitrile hydration catalyst was prepared based on a literature report of Ni nanoparticles on a solid support. The Ni catalyst supported on HT, an LDH support, achieved 60 % hydration of ACH to HIBAM, unprecedented conversion for a transition metal catalyst. However the exact identity of the catalyst was not conclusively determined, as no nanoparticles were observed in the TEM images of the material, differentiating from literature reports.

A hypothesized mechanism involved a Ni active site for nitrile binding in conjunction with deprotonation of water by the hydroxides contained by the HT support in order to generate the nucleophile. In addition, the catalyst is active at relatively low temperatures. This allows for a relatively high conversion, because these conditions stabilize cyanohydrins.

LDH materials such as HT have tunable properties; the metal composition and interstitial anions can be changed with relative ease. Additionally, various metals have been deposited on HT as catalysts. This opens up a new and interesting class of nitrile and cyanohydrin hydration catalysts using HT as a solid base and supported metals as Lewis acids for nitrile activation.

5.7. Bridge

This chapter investigates the catalytic activity of a solid supported nickel catalyst for nitrile and cyanohydrin hydration. The material had unprecedented activity for the hydration of acetone cyanohydrin, but the specific identity of the catalyst could not be determined. The outlook for transition metal catalyzed cyanohydrin hydration is discussed in Chapter VI.

CHAPTER VI

SUMMARY AND OUTLOOK

Cyanohydrins are currently used industrially for the production of commercially important acrylic monomers. The first step in the production of these high value targets is the hydration of cyanohydrins, which is accomplished industrially using concentrated sulfuric acid. This inefficient process generates large amounts of useless byproducts and uses large amounts of energy. Therefore a more effective route to the hydration of cyanohydrins would be beneficial both economically and environmentally.

Ideally, cyanohydrin hydration would be done using a transition metal nitrile hydration catalyst, which would convert the cyanohydrin to its corresponding α-hydroxyamide in water under mild conditions, generating no byproducts. The catalytic conversion of cyanohydrins with metal catalysts has been difficult because cyanohydrins degrade to produce cyanide, which poisons most homogeneous transition metal catalysts. Recent work in the field has focused on designing catalysts that are active under conditions that stabilize cyanohydrins (e.g. low temperature and pH).

The initial investigations in this dissertation used this strategy, examining the use of secondary coordination sphere effects with modified platinum hydridochloride and dihydride bis(phosphine) complexes as nitrile and cyanohydrin hydration catalysts. Although these complexes were active under milder conditions than previously reported

catalysts of a similar structure, they were still poisoned by cyanide when the hydration of cyanohydrins was attempted.

Serendipitously, the transformation of one of these complexes to form nanoparticles generated an active catalyst with unprecedented cyanide resistance. The development of a catalyst that is able to reversibly coordinate cyanide, and thus remain active, would be the ideal route to catalytic cyanohydrin hydration. Because the metal atoms in nanoparticles have more electron density than those in most homogeneous complexes, they could potentially bind cyanide more reversibly and avoid poisoning.

Investigations of other nanoparticle nitrile hydration catalysts revealed the promise of this direction. Ag/PTA nanoparticles were reasonably active towards the hydration of aromatic nitriles, and though they dissolved in the presence of cyanide, the resulting silver cyanide complex was able to hydrate cyanohydrins and remained unpoisoned. We hypothesize that the lability of the cyanide bonds to Ag(I) allowed the complex to retain catalytic function. Furthermore, a solid supported Ni catalyst was able to achieve unprecedented hydration of cyanohydrins. (Ni is a first-row transition metal and forms labile bonds as well.)

The labile bonding of cyanide to these metals allows cyanide to act as a catalyst inhibitor rather than poisoner. However, the nitrile or cyanohydrin substrate also binds more weakly to the catalyst, which slows the first step of the catalytic mechanism and thus the rate of hydration. In the case of cyanohydrins, this means that although poisoning is avoided, the substrate may degrade before conversion can be completed. Therefore, in

order to be viable for cyanohydrin hydration, especially on an industrial scale, the rates for these catalysts must be improved.

There are several viable options to achieve this improvement. While this work examined several of the reported nanoparticle nitrile hydration catalysts for activity towards cyanohydrins, there are still several untested catalysts. The ruthenium nanoparticle systems are of particular interest, as a homogeneous ruthenium complex was previously used to hydrate cyanohydrins. New nanoparticle nitrile hydration catalysts of metals that are as yet untested in that form, such as cobalt, also have potential.

Another interesting route is the adjustment of the nanoparticle support. A cooperative effect between a metal and a basic support achieved excellent results for the hydration of ACH. Exploring new basic supports or tuning the composition of the hydrotalcite support, both the metals and the interstitial anions, could result in enhanced catalytic properties. Both these avenues are worthy of further exploratio

APPENDIX A

SUPPORTING INFORMATION FOR CHAPTER II

A.1. ^{31}P NMR of *cis* and *trans*-$PtCl_2(P(NMe_2)_3)_2$

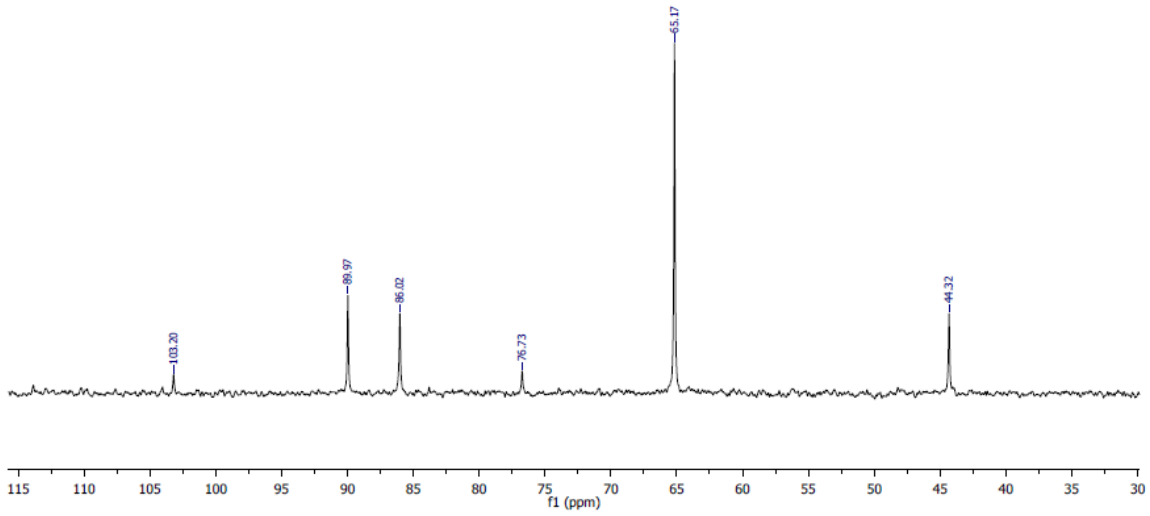

Figure A1. ^{31}P NMR spectrum of *cis* and *trans*-$PtCl_2(P(NMe_2)_3)_2$. The *cis* species appears at 65 ppm with Pt satellites at 44 and 86 ppm, and the *trans* species appears at 90 ppm with Pt satellites at 76 and 100 ppm.

A.2. Crystal data for $PtH_2(P(NMe_2)_3)_2$

Table A.2.1. Crystal data and structure refinement for $PtH_2(P(NMe_2)_3)$.

Identification code	dt8
Empirical formula	C12 H38 N6 P2 Pt
Formula weight	523.51
Temperature	173(2) K
Wavelength	0.71073 Å

Crystal system	Triclinic	
Space group	P-1	
Unit cell dimensions	a = 7.8871(19) Å	□= 76.807(4)°.
	b = 7.9499(19) Å	□= 73.241(4)°.
	c = 9.891(2) Å	□ = 60.652(3)°.
Volume	514.8(2) $Å^3$	
Z	1	
Density (calculated)	1.689 Mg/m^3	
Absorption coefficient	6.973 mm^{-1}	
F(000)	260	
Crystal size	0.08 x 0.06 x 0.03 mm^3	
Theta range for data collection	2.16 to 27.00°.	
Index ranges	-10<=h<=10, -10<=k<=10, -12<=l<=12	
Reflections collected	5813	
Independent reflections	2238 [R(int) = 0.0196]	
Completeness to theta = 27.00°	99.2 %	
Absorption correction	Semi-empirical from equivalents	
Max. and min. transmission	0.8181 and 0.6054	
Refinement method	Full-matrix least-squares on F^2	
Data / restraints / parameters	2238 / 0 / 173	
Goodness-of-fit on F^2	1.056	
Final R indices [I>2sigma(I)]	R1 = 0.0185, wR2 = 0.0417	
R indices (all data)	R1 = 0.0185, wR2 = 0.0417	
Largest diff. peak and hole	0.610 and -0.458 $e.Å^{-3}$	

Table A.2.2. Atomic coordinates (x 10^4) and equivalent isotropic displacement parameters ($Å^2$x 10^3) for $PtH_2(P(NMe_2)_3)$. U(eq) is defined as one third of the trace of the orthogonalized U^{ij} tensor.

	x	y	z	U(eq)
Pt(1)	5000	10000	5000	25(1)
P(1)	5809(1)	8075(1)	7012(1)	23(1)
N(1)	8019(4)	7593(4)	7245(3)	34(1)

N(2)	6132(4)	5758(3)	7203(3)	27(1)
N(3)	4049(4)	8931(4)	8436(3)	39(1)
C(1)	8860(5)	8927(5)	6638(4)	37(1)
C(2)	9100(6)	6069(6)	8245(4)	43(1)
C(3)	7764(6)	4524(5)	6166(4)	40(1)
C(4)	4315(6)	5651(6)	7251(4)	43(1)
C(5)	2226(6)	10659(7)	8351(5)	56(1)
C(6)	4172(7)	7935(7)	9862(4)	50(1)

Table A.2.3. Bond lengths [Å] and angles [°] for $PtH_2(P(NMe_2)_3)$.

Pt(1)-P(1)#1	2.2572(8)
Pt(1)-P(1)	2.2572(8)
Pt(1)-H(1)	1.53(4)
P(1)-N(3)	1.661(3)
P(1)-N(1)	1.666(3)
P(1)-N(2)	1.704(2)
N(1)-C(1)	1.448(4)
N(1)-C(2)	1.449(4)
N(2)-C(3)	1.460(4)
N(2)-C(4)	1.464(4)
N(3)-C(5)	1.429(5)
N(3)-C(6)	1.455(4)
C(1)-H(1A)	1.00(4)
C(1)-H(1B)	0.96(4)
C(1)-H(1C)	1.05(4)
C(2)-H(2A)	1.01(5)
C(2)-H(2B)	0.99(5)
C(2)-H(2C)	1.03(4)
C(3)-H(3A)	1.00(5)
C(3)-H(3B)	1.02(4)
C(3)-H(3C)	0.95(4)
C(4)-H(4A)	0.93(4)

C(4)-H(4B)	0.94(5)
C(4)-H(4C)	0.95(5)
C(5)-H(5A)	0.91(5)
C(5)-H(5B)	0.96(4)
C(5)-H(5C)	1.01(6)
C(6)-H(6A)	1.05(5)
C(6)-H(6B)	0.96(6)
C(6)-H(6C)	0.84(5)

P(1)#1-Pt(1)-P(1)	180.00(2)
P(1)#1-Pt(1)-H(1)	92.9(16)
P(1)-Pt(1)-H(1)	87.1(16)
N(3)-P(1)-N(1)	110.86(15)
N(3)-P(1)-N(2)	100.94(14)
N(1)-P(1)-N(2)	98.70(13)
N(3)-P(1)-Pt(1)	112.12(10)
N(1)-P(1)-Pt(1)	113.82(9)
N(2)-P(1)-Pt(1)	119.08(9)
C(1)-N(1)-C(2)	112.9(3)
C(1)-N(1)-P(1)	121.0(2)
C(2)-N(1)-P(1)	125.1(2)
C(3)-N(2)-C(4)	109.8(3)
C(3)-N(2)-P(1)	114.7(2)
C(4)-N(2)-P(1)	113.3(2)
C(5)-N(3)-C(6)	114.2(3)
C(5)-N(3)-P(1)	122.5(2)
C(6)-N(3)-P(1)	123.2(2)
N(1)-C(1)-H(1A)	110(2)
N(1)-C(1)-H(1B)	111(2)
H(1A)-C(1)-H(1B)	106(3)
N(1)-C(1)-H(1C)	113(2)
H(1A)-C(1)-H(1C)	104(3)
H(1B)-C(1)-H(1C)	112(3)
N(1)-C(2)-H(2A)	112(3)
N(1)-C(2)-H(2B)	111(3)
H(2A)-C(2)-H(2B)	103(4)

N(1)-C(2)-H(2C)	110(2)
H(2A)-C(2)-H(2C)	113(4)
H(2B)-C(2)-H(2C)	107(3)
N(2)-C(3)-H(3A)	112(3)
N(2)-C(3)-H(3B)	110(2)
H(3A)-C(3)-H(3B)	106(3)
N(2)-C(3)-H(3C)	110(2)
H(3A)-C(3)-H(3C)	108(3)
H(3B)-C(3)-H(3C)	110(3)
N(2)-C(4)-H(4A)	114(2)
N(2)-C(4)-H(4B)	110(3)
H(4A)-C(4)-H(4B)	104(3)
N(2)-C(4)-H(4C)	110(3)
H(4A)-C(4)-H(4C)	111(4)
H(4B)-C(4)-H(4C)	108(4)
N(3)-C(5)-H(5A)	113(3)
N(3)-C(5)-H(5B)	115(2)
H(5A)-C(5)-H(5B)	108(4)
N(3)-C(5)-H(5C)	110(4)
H(5A)-C(5)-H(5C)	97(4)
H(5B)-C(5)-H(5C)	113(4)
N(3)-C(6)-H(6A)	106(3)
N(3)-C(6)-H(6B)	112(3)
H(6A)-C(6)-H(6B)	102(4)
N(3)-C(6)-H(6C)	110(3)
H(6A)-C(6)-H(6C)	113(4)
H(6B)-C(6)-H(6C)	114(5)

Symmetry transformations used to generate equivalent atoms:

#1 –x+1,-y+2,-z+1

Table A.2.4. Anisotropic displacement parameters ($Å^2 x\ 10^3$) for $PtH_2(P(NMe_2)_3)$. The anisotropic displacement factor exponent takes the form: $-2\pi^2[h^2 a^{*2} U^{11} + \ldots + 2\ h\ k\ a^*\ b^*\ U^{12}]$

	U^{11}	U^{22}	U^{33}	U^{23}	U^{13}	U^{12}
Pt(1)	33(1)	21(1)	20(1)	5(1)	-11(1)	-11(1)
P(1)	29(1)	20(1)	20(1)	3(1)	-9(1)	-10(1)
N(1)	39(2)	32(1)	37(2)	13(1)	-22(1)	-21(1)
N(2)	35(1)	20(1)	27(1)	3(1)	-11(1)	-14(1)
N(3)	42(2)	32(1)	21(1)	1(1)	-4(1)	-3(1)
C(1)	37(2)	33(2)	47(2)	2(2)	-10(2)	-22(2)
C(2)	46(2)	41(2)	49(2)	16(2)	-30(2)	-23(2)
C(3)	49(2)	25(2)	40(2)	-4(1)	-11(2)	-11(2)
C(4)	52(2)	49(2)	41(2)	14(2)	-23(2)	-34(2)
C(5)	42(2)	49(2)	37(2)	-1(2)	-1(2)	5(2)
C(6)	54(2)	43(2)	25(2)	3(2)	-5(2)	-5(2)

Table A.2.5. Hydrogen coordinates ($x\ 10^4$) and isotropic displacement parameters ($Å^2 x\ 10^3$) for $PtH_2(P(NMe_2)_3)$.

	X	y	z	U(eq)
H(1)	4880(60)	11620(60)	5670(40)	62(12)
H(1A)	10280(70)	8210(60)	6150(40)	57(12)
H(1B)	8190(50)	9850(60)	5930(40)	40(10)
H(1C)	8940(60)	9600(60)	7410(40)	47(10)
H(2A)	9190(70)	6600(80)	9040(50)	78(15)
H(2B)	10510(70)	5320(70)	7790(50)	62(13)
H(2C)	8510(60)	5110(60)	8600(40)	57(12)
H(3A)	7960(70)	3160(70)	6370(50)	69(13)
H(3B)	7450(60)	4990(60)	5180(40)	46(10)
H(3C)	8970(60)	4520(50)	6170(40)	40(10)
H(4A)	3850(60)	6150(60)	6410(50)	51(11)
H(4B)	4560(60)	4350(70)	7380(40)	54(12)

H(4C)	3310(70)	6260(70)	8030(50)	67(14)
H(5A)	1940(70)	11500(70)	8970(50)	69(15)
H(5B)	2150(50)	11350(60)	7420(40)	44(10)
H(5C)	1060(100)	10360(90)	8790(70)	110(20)
H(6A)	2850(80)	7790(70)	10270(60)	82(16)
H(6B)	4060(80)	8740(80)	10510(60)	89(17)
H(6C)	5200(70)	6860(70)	9830(50)	60(13)

Table A.2.6. Torsion angles [°] for $PtH_2(P(NMe_2)_3)$.

P(1)#1-Pt(1)-P(1)-N(3)	-97(100)
P(1)#1-Pt(1)-P(1)-N(1)	136(100)
P(1)#1-Pt(1)-P(1)-N(2)	20(100)
N(3)-P(1)-N(1)-C(1)	-100.4(3)
N(2)-P(1)-N(1)-C(1)	154.3(3)
Pt(1)-P(1)-N(1)-C(1)	27.1(3)
N(3)-P(1)-N(1)-C(2)	67.6(3)
N(2)-P(1)-N(1)-C(2)	-37.7(3)
Pt(1)-P(1)-N(1)-C(2)	-164.9(3)
N(3)-P(1)-N(2)-C(3)	-174.2(2)
N(1)-P(1)-N(2)-C(3)	-60.8(3)
Pt(1)-P(1)-N(2)-C(3)	62.7(2)
N(3)-P(1)-N(2)-C(4)	58.7(3)
N(1)-P(1)-N(2)-C(4)	172.1(2)
Pt(1)-P(1)-N(2)-C(4)	-64.4(3)
N(1)-P(1)-N(3)-C(5)	130.2(4)
N(2)-P(1)-N(3)-C(5)	-126.0(4)
Pt(1)-P(1)-N(3)-C(5)	1.8(4)
N(1)-P(1)-N(3)-C(6)	-53.6(4)
N(2)-P(1)-N(3)-C(6)	50.2(4)
Pt(1)-P(1)-N(3)-C(6)	178.0(3)

Symmetry transformations used to generate equivalent atoms: #1 –x+1,-y+2,-z+1

APPENDIX B

SUPPORTING INFORMATION FOR CHAPTER III

B.1. ^{31}P NMR of $[PtH_2(P(OMe)_3)_2$

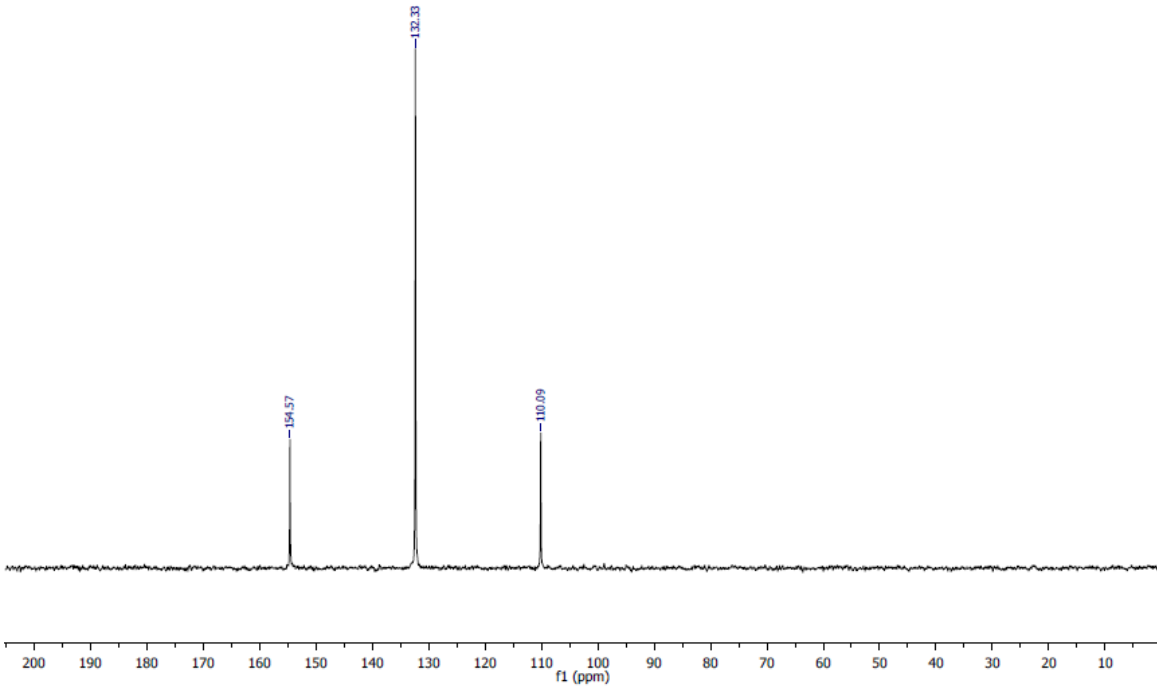

Figure B.1. ^{31}P NMR spectrum of $[PtH_2(P(OMe)_3)$

APPENDIX C

SUPPORTING INFORMATION FOR CHAPTER IV

C.1. EDX Spectrum of Ag-PTA

Nanoparticles

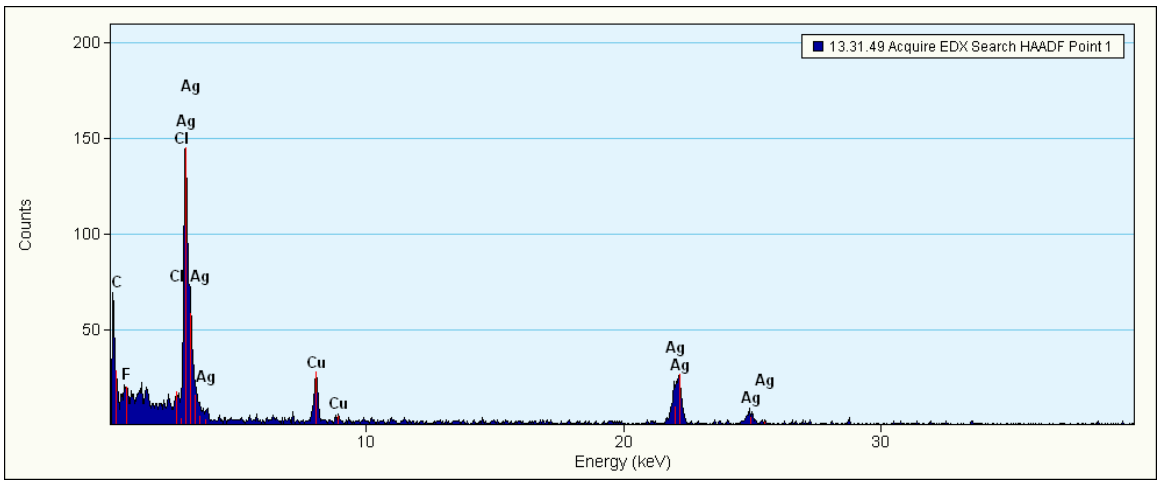

REFERENCES CITED

CHAPTER I

(1) García-Álvarez, R.; Crochet, P.; Cadierno, V. *Green Chemistry* **2013**, *15*, 46
.

(2) Ahmed, T. J.; Knapp, S. M. M.; Tyler, D. R. *Coord. Chem. Rev.* **2011**, *255*, 949–974.

(3) Chemical profile: acrylamide http://www.icis.com/resources/news/2008/07/21/9141553/chemical-profile-acrylamide/ (accessed Apr 21, 2014).

(4) Green, M. M. Wittcoff, H.A. In *Organic Chemistry Principles and Industrial Practice*; Wiley-VCH: Weinheim, Germany, 2003; pp. 137–155.

(5) Kukushkin, V. Y.; Pombeiro, A. J. L. *Inorg. Chim. Acta* **2005**, *358*, 1–21.

(6) Hayashi, H.; Nishi, H.; Watanabe, Y.; Okazaki, T. *J.Catal.***1981**, *69*, 44–50.

(7) Ravindranathan, M.; Kalyanam, N.; Sivaram, S. *J. Org. Chem.* **1982**, *47*, 4812–4813.

(8) Toshima, N.; Wang, Y. *Langmuir* **1994**, *10*, 4574–4580.

(9) Zheng, R.-C.; Zheng, Y.-G.; Shen, Y.-C.; Flickinger, M. C. In *Encyclopedia of Industrial Biotechnology*; John Wiley & Sons, Inc., 2009.

(10) W. Gruber, G. Schroeder. U.S. Patent, 4018829.

(11) Haefele. Canadian Patent, 5736385.

(12) M. Weschsberg R. Schoenbeck. German Patent, DE 2825267, 1980.

(13) Polshettiwar, V.; Varma, R. S. *Green Chem.* **2010**, *12*, 743–754.

(14) Jensen, C. M.; Trogler, W. C. *J. Am. Chem. Soc.* **1986**, *108*, 723–729.

(15) Ghaffar, T.; Parkins, A. W. *J. Molec. Catal. A* **2000**, *160*, 249–261.

(16) Ghaffar, T.; Parkins, A. W. *Tet. Lett.* **1995**, *36*, 8657–8660.

(17) Jiang, X.; Minnaard, A. J.; Feringa, B. L.; de Vries, J. G. *J. Org. Chem.* **2004**, *69*, 2327–2331.

(18) Ahmed, T. J.; Fox, B. R.; Knapp, S. M. M.; Yelle, R. B.; Juliette, J. J.; Tyler, D. R. *Inorg. Chem.* **2009**, *48*, 7828–7837.

(19) Knapp, S. M. M.; Sherbow, T. J.; Ahmed, T. J.; Thiel, I.; Zakharov, L. N.; Juliette, J. J.; Tyler, D. R. *J Inorg Organomet Polym* **2014**, *24*, 145–156.

(20) Knapp, S. M. M.; Sherbow, T. J.; Yelle, R. B.; Zakharov, L. N.; Juliette, J. J.; Tyler, D. R. *Organometallics* **2013**, *32*, 824–834.

(21) Cadierno, V.; Díez, J.; Francos, J.; Gimeno, J. *Chem. Eur. J.* **2010**, *16*, 9808–9817.

(22) Díez, J.; Gimeno, J.; Merino, I.; Rubio, E.; Suárez, F. J. *Inorg. Chem.* **2011**, *50*, 4868–4881.

(23) García-Álvarez, R.; Díez, J.; Crochet, P.; Cadierno, V. *Organometallics* **2010**, *29*, 3955–3965.

(24) García-Álvarez, R.; Díez, J.; Crochet, P.; Cadierno, V. *Organometallics* **2011**, *30*, 5442–5451.

(25) Lee, W.-C.; Sears, J. M.; Enow, R. A.; Eads, K.; Krogstad, D. A.; Frost, B. J. *Inorg. Chem.* **2013**, *52*, 1737–1746.

(26) Knapp, S. M. M.; Sherbow, T. J.; Juliette, J. J.; Tyler, D. R. *Organometallics* **2012**, *31*, 2941–2944.

(27) Knapp, S. M. M.; Sherbow, T. J.; Yelle, R. B.; Juliette, J. J.; Tyler, D. R. *Organometallics* **2013**, *32*, 3744–3752.

(28) García-Álvarez, R.; Francos, J.; Tomás-Mendivil, E.; Crochet, P.; Cadierno, V. *J. Organometallic Chem*.

(29) Muranaka, M.; Hyodo, I.; Okumura, W.; Oshiki, T. *Catal. Today* **2011**, *164*, 552–555.

(30) Lee, W.-C.; Frost, B. J. *Green Chem.* **2012**, *14*, 62.

(31) Oshiki, T.; Yamashita, H.; Sawada, K.; Utsunomiya, M.; Takahashi, K.; Takai, K. *Organometallics* **2005**, *24*, 6287–6290.

(32) Fung, W. K.; Huang, X.; Man; ManNg, S. M.; Hung, M. Y.; Lin, Z.; Lau, C. P. *J. Am. Chem. Soc.* **2003**, *125*, 11539–11544.

(33) Ahmed, T. J.; Zakharov, L. N.; Tyler, D. R. *Organometallics* **2007**, *26*, 5179–5187.

(34) Ahmed, T. J.; Tyler, D. R. *Organometallics* **2008**, *27*, 2608–2613.

(35) Breno, K. L.; Pluth, M. D.; Tyler, D. R. *Organometallics* **2003**, *22*, 1203–1211.

(36) Breno, K. L.; Ahmed, T. J.; Pluth, M. D.; Balzarek, C.; Tyler, D. R. *Coord. Chem. Rev.* **2006**, *250*, 1141–1151.

(37) Crestani, M. G.; Arévalo, A.; García, J. J. *Adv. Synth. Catal.* **2006**, *348*, 732–742.

(38) Crestani, M. G.; García, J. J. *J. Molec. Catal. A:* **2009**, *299*, 26–36.

(39) Crisóstomo, C.; Crestani, M. G.; García, J. J. *Inorg. Chim. Acta* **2010**, *363*, 1092–1096.

(40) Ramón, R. S.; Marion, N.; Nolan, S. P. *Chem. Eur. J.* **2009**, *15*, 8695–8697.

(41) Ramón, R. S.; Gaillard, S.; Poater, A.; Cavallo, L.; Slawin, A. M. Z.; Nolan, S. P. *Chem. Eur. J.* **2011**, *17*, 1238–1246.

(42) Buil, M. L.; Cadierno, V.; Esteruelas, M. A.; Gimeno, J.; Herrero, J.; Izquierdo, S.; Oñate, E. *Organometallics* **2012**, *31*, 6861–6867.

(43) Cariati, E.; Dragonetti, C.; Manassero, L.; Roberto, D.; Tessore, F.; Lucenti, E. *J. Molec. Catal. A,* **2003**, *204–205*, 279–285.

(44) Stepanenko, I. N.; Cebrián-Losantos, B.; Arion, V. B.; Krokhin, A. A.; Nazarov, A. A.; Keppler, B. K. *Eur. J. Inorg. Chem.* **2007**, *2007*, 400–411.

(45) Curtis, N. J.; Hagen, K. S.; Sargeson, A. M. *J. Chem. Soc., Chem. Commun.* **1984**, 1571–1573.

(46) Buckingham, D. A.; Morris, P.; Sargeson, A. M.; Zanella, A. *Inorg. Chem.* **1977**, *16*, 1910–1923.

(47) Heinrich, L.; Mary-Verla, A.; Li, Y.; Vaissermann, J.; Chottard, J.-C. *Eur. J. Inorg. Chem.* **2001**, *2001*, 2203–2206.

(48) Kim, J. H.; Britten, J.; Chin, J. *J. Am. Chem. Soc.* **1993**, *115*, 3618–3622.

(49) Pinnell, D.; Wright, G. B.; Jordan, R. B. *J. Am. Chem. Soc.* **1972**, *94*, 6104–6106.

(50) Goto, A.; Endo, K.; Saito, S. *Angew. Chem. Int. Ed.* **2008**, *47*, 3607–3609.

(51) M.C.K.B. Djoman, A.N. Ajjou. *Tet. Lett.* **2000**, *41*, 4845

.

(52) Bennett, M. A.; Yoshida, T. *J. Am. Chem. Soc.* **1973**, *95*, 3030–3031.

(53) Hirano, T.; Uehara, K.; Kamata, K.; Mizuno, N. *J. Am. Chem. Soc.* **2012**, *134*, 6425–6433.

(54) Kaminskaia, N. V.; Kostić, N. M. *J. Chem. Soc., Dalton Trans.* **1996**, 3677–3686.

(55) Kaminskaia, N. V.; Guzei, I. A.; Kostić, N. M. *J. Chem. Soc., Dalton Trans.* **1998**, 3879–3886.

(56) Crestani, M. G.; Steffen, A.; Kenwright, A. M.; Batsanov, A. S.; Howard, J. A. K.; Marder, T. B. *Organometallics* **2009**, *28*, 2904–2914.

(57) Kopylovich, M. N.; Kukushkin, V. Y.; Haukka, M.; Fraústo da Silva, J. J. R.; Pombeiro, A. J. L. *Inorg. Chem.* **2002**, *41*, 4798–4804.

(58) Roy, S. C.; Dutta, P.; Nandy, L. N.; Roy, S. K.; Samuel, P.; Pillai, S. M.; Kaushik, V. K.; Ravindranathan, M. *App. Catal. A* **2005**, *290*, 175–180.

(59) Miura, H.; Sugiyama, K.; Kawakami, S.; Aoyama, T.; Matsuda, T. *Chem. Lett.* **1982**, *11*, 183–186.

(60) Yamaguchi, K.; Wang, Y.; Kobayashi, H.; Mizuno, N. *Chem. Lett.* **2012**, *41*, 574–576.

(61) Khadilkar, B. M.; Madyar, V. R. *Synth. Commun.* **2002**, *32*, 1731.

(62) Battilocchio, C.; Hawkins, J. M.; Ley, S. V. *Org. Lett.* **2014**, *16*, 1060–1063.

(63) Gangarajula, Y.; Gopal, B. *Chemistry Letters* **2012**, *41*, 101–103.

(64) Tamura, M.; Satsuma, A.; Shimizu, K. *Catal. Sci. Technol.* **2013**, *3*, 1386–1393.

(65) Tamura, M.; Wakasugi, H.; Shimizu, K.; Satsuma, A. *Chem. Eur. J.* **2011**, *17*, 11428–11431.

(66) Yamaguchi, K.; Matsushita, M.; Mizuno, N. *Angew. Chem.* **2004**, *116*, 1602–1606.

(67) Mori, K.; Yamaguchi, K.; Mizugaki, T.; Ebitani, K.; Kaneda, K. *Chem. Commun.* **2001**, 461–462.

(68) Prakash, G. K. S.; Munoz, S. B.; Papp, A.; Masood, K.; Bychinskaya, I.; Mathew, T.; Olah, G. A. *Asian J. Org. Chem.* **2012**, *1*, 146–149.

(69) Kumar, S.; Das, P. *New J. Chem.* **2013**, *37*, 2987–2990.

(70) Varma, R. S. *Pure Appl. Chem.* **2013**, *85*, 1703–1710.

(71) Yan, N.; Xiao, C.; Kou, Y. *Coord. Chem. Rev.* **2010**, *254*, 1179–1218.

(72) Ishizuka, A.; Nakazaki, Y.; Oshiki, T. *Chem. Lett.* **2009**, *38*, 360–361.

(73) Mitsudome, T.; Mikami, Y.; Mori, H.; Arita, S.; Mizugaki, T.; Jitsukawa, K.; Kaneda, K. *Chem. Comm.* **2009**, 3258.

(74) Kim, A. Y.; Bae, H. S.; Park, S.; Park, S.; Park, K. H. *Catal Lett* **2011**, *141*, 685–690.

(75) Woo, H.; Lee, K.; Park, S.; Park, K. H. *Molecules* **2014**, *19*, 699–712.

(76) Baig, R. B. N.; Varma, R. S. *Chem. Commun.* **2012**, *48*, 6220–6222.

(77) Polshettiwar, V.; Varma, R. S. *Chem. Eur. J.* **2009**, *15*, 1582–1586.

(78) Shimizu, K.; Kubo, T.; Satsuma, A.; Kamachi, T.; Yoshizawa, K. *ACS Catal.* **2012**, 2467–2474.

(79) Subramanian, T.; Pitchumani, K. *Catal. Commun.* **2012**, *29*, 109–113.

(80) Liu, Y.-M.; He, L.; Wang, M.-M.; Cao, Y.; He, H.-Y.; Fan, K.-N. *ChemSusChem* **2012**, *5*, 1392–1396.

(81) Shimizu, K.; Imaiida, N.; Sawabe, K.; Satsuma, A. *Appl. Catal. A* **2012**, *421–422*, 114–120.

(82) Becica, J; Jackson, A.B.; Dougherty, W.G.; Kassel W.S.; West, N.W. *Dalton Transactions*.**2014 DOI:** 10.1039/C4DT00734D

(83) Meyer, F.; Hyla-Kryspin, I.; Kaifer, E.; Kircher, P. *Eur. J. Inorg. Chem.* **2000**, *2000*, 771–781.

(84) Chetcuti, P. A.; Knobler, C. B.; Hawthorne, M. F. *Organometallics* **1988**, *7*, 650–660.

(85) Eisch, J. J.; Ma, X.; Han, K. I.; Gitua, J. N.; Krüger, C. *Eur. J. Inorg. Chem.* **2001**, *2001*, 77–88.

(86) Sexton, B. A.; Avery, N. R. *Surf. Sci.* **1983**, *129*, 21–36.

(87) Eustis, S.; El-Sayed, M. A. *Chem. Soc. Rev.* **2006**, *35*, 209.

(88) Hansch, C.; Leo, A.; Taft, R. W. *Chem. Rev.* **1991**, *91*, 165–195.

(89) Garcia-Garrido, S.E.; Francos, J; Cadierno, V.; Basset, J.M.; Polshettiwar, V; *ChemSusChem*, **2011**, *4*, 104-111

CHAPTER II

(1) Ahmed, T. J.; Knapp, S. M. M.; Tyler, D. R. *Coord. Chem. Rev.* **2011**, *255*, 949–974.

(2) Knapp, S. M. M.; Sherbow, T. J.; Juliette, J. J.; Tyler, D. R. *Organometallics* **2012**, *31*, 2941–2944.

(3) Ahmed, T. J.; Fox, B. R.; Knapp, S. M. M.; Yelle, R. B.; Juliette, J. J.; Tyler, D. R. *Inorg. Chem.* **2009**, *48*, 7828–7837.

(4) Grotjahn, D. B.; Kragulj, E. J.; Zeinalipour-Yazdi, C. D.; Miranda-Soto, V.; Lev, D. A.; Cooksy, A. L. *J. Am. Chem. Soc.* **2008**, *130*, 10860–10861.

(5) Grotjahn, D. B. *Chem. Eur. J.* **2005**, *11*, 7146–7153.

(6) Grotjahn, D. B.; Miranda-Soto, V.; Kragulj, E. J.; Lev, D. A.; Erdogan, G.; Zeng, X.; Cooksy, A. L. *J. Am. Chem. Soc.* **2008**, *130*, 20–21.

(7) García-Álvarez, R.; Díez, J.; Crochet, P.; Cadierno, V. *Organometallics* **2011**, *30*, 5442–5451.

(8) Knapp, S. M. M.; Sherbow, T. J.; Yelle, R. B.; Zakharov, L. N.; Juliette, J. J.; Tyler, D. R. *Organometallics* **2013**, *32*, 824–834.

(9) Knapp, S. M. M.; Sherbow, T. J.; Yelle, R. B.; Juliette, J. J.; Tyler, D. R. *Organometallics* **2013**, *32*, 3744–3752.

(10) Jensen, C. M.; Trogler, W. C. *J. Am. Chem. Soc.* **1986**, *108*, 723–729.

(11) Packett, D. L.; Jensen, C. M.; Cowan, R. L.; Strouse, C. E.; Trogler, W. C. *Inorg. Chem.* **1985**, *24*, 3578–3583.

(12) Grim, S. O.; Keiter, R. L.; McFarlane, W. *Inorg. Chem.* **1967**, *6*, 1133–1137.

(13) Waddell, P. G.; Slawin, A. M. Z.; Woollins, J. D. *Dalton Trans.* **2010**, *39*, 8620–8625.

(14) Packett, D. L.; Trogler, W. C. *J. Am. Chem. Soc.* **1986**, *108*, 5036–5038.

CHAPTER III

(1) Green, M. M. Wittcoff, H.A. *Organic Chemistry Priciples and Industrial Practice*; Wiley-VCH: Weinheim, Germany, 2003.

(2) Ahmed, T. J.; Knapp, S. M. M.; Tyler, D. R. *Coord. Chem. Rev.* **2011**, *255*, 949–974.

(3) S. Bizzari. Chemical Economics Handbook, 2012.

(4) García-Álvarez, R.; Crochet, P.; Cadierno, V. *Green Chem.* **2013**, *15*, 46.

(5) Kukushkin, V. Y.; Pombeiro, A. J. L. *Inorg. Chim. Act.* **2005**, *358*, 1–21

.

(6) Ahmed, T. J.; Fox, B. R.; Knapp, S. M. M.; Yelle, R. B.; Juliette, J. J.; Tyler, D. R. *Inorg. Chem.* **2009**, *48*, 7828–7837.

(7) Knapp, S. M. M.; Sherbow, T. J.; Juliette, J. J.; Tyler, D. R. *Organometallics* **2012**, *31*, 2941–2944.

(8) Knapp, S. M. M.; Sherbow, T. J.; Yelle, R. B.; Zakharov, L. N.; Juliette, J. J.; Tyler, D. R. *Organometallics* **2013**, *32*, 824–834.

(9) Knapp, S. M. M.; Sherbow, T. J.; Yelle, R. B.; Juliette, J. J.; Tyler, D. R. *Organometallics* **2013**, *32*, 3744–3752.

(10) García-Álvarez, R.; Díez, J.; Crochet, P.; Cadierno, V. *Organometallics* **2011**, *30*, 5442–5451.

(11) Grotjahn, D. B.; Kragulj, E. J.; Zeinalipour-Yazdi, C. D.; Miranda-Soto, V.; Lev, D. A.; Cooksy, A. L. *J. Am. Chem. Soc.* **2008**, *130*, 10860–10861.

(12) Grotjahn, D. B. *Chem. Eur. J.* **2005**, *11*, 7146–7153.

(13) Grotjahn, D. B.; Miranda-Soto, V.; Kragulj, E. J.; Lev, D. A.; Erdogan, G.; Zeng, X.; Cooksy, A. L. *J. Am. Chem. Soc.* **2008**, *130*, 20–21.

(14) Muranaka, M.; Hyodo, I.; Okumura, W.; Oshiki, T. *Catal. Today* **2011**, *164*, 552–555.

(15) Daw, P.; Sinha, A.; Rahaman, S. M. W.; Dinda, S.; Bera, J. K. *Organometallics* **2012**, *31*, 3790–3797.

(16) Díez, J.; Gimeno, J.; Merino, I.; Rubio, E.; Suárez, F. J. *Inorg. Chem.* **2011**, *50*, 4868–4881.

(17) Lee, W.-C.; Sears, J. M.; Enow, R. A.; Eads, K.; Krogstad, D. A.; Frost, B. J. *Inorg. Chem.* **2013**, *52*, 1737–1746.

(18) Cadierno, V.; Díez, J.; Francos, J.; Gimeno, J. *Chem.Eur. J.* **2010**, *16*, 9808–9817.

(19) García-Álvarez, R.; Díez, J.; Crochet, P.; Cadierno, V. *Organometallics* **2010**, *29*, 3955–3965.

(20) Paonessa, R. S.; Trogler, W. C. *J. Am. Chem. Soc.* **1982**, *104*, 1138–1140.

(21) Packett, D. L.; Jensen, C. M.; Cowan, R. L.; Strouse, C. E.; Trogler, W. C. *Inorg. Chem.* **1985**, *24*, 3578–3583.

(22) Jensen, C. M.; Trogler, W. C. *J. Am. Chem. Soc.* **1986**, *108*, 723–729.

(23) Widegren, J. A.; Finke, R. G. *J. Molec. Catal. A* **2003**, *198*, 317–341.

(24) Stracke, J. J.; Finke, R. G. *ACS Catal.* **2014**, 909–933.

(25) Debouttière, P.-J.; Coppel, Y.; Denicourt-Nowicki, A.; Roucoux, A.; Chaudret, B.; Philippot, K. *Eur. J. Inorg. Chem.* **2012**, *2012*, 1229–1236.

(26) Kostelansky, C. N.; Pietron, J. J.; Chen, M.-S.; Dressick, W. J.; Swider-Lyons, K. E.; Ramaker, D. E.; Stroud, R. M.; Klug, C. A.; Zelakiewicz, B. S.; Schull, T. L. *J. Phys. Chem. B* **2006**, *110*, 21487–21496.

(27) Richter, M.; Karschin, A.; Spingler, B.; Kunz, P. C.; Meyer-Zaika, W.; Kläui, W. *Dalton Trans.* **2012**, *41*, 3407–3413.

(28) McCarty, W. J.; Yang, X.; Anderson, L. J. D.; Jones, R. A. *Dalton Trans.* **2012**, *41*, 13496–13503.

(29) K. Kouba, J.; Pierce, J. L.; Walton, R. A. *Journal of Organometallic Chemistry* **1980**, *202*, C105–C107.

(30) Aw, B. H.; Looh, K. K.; Chan, H. S. O.; Tan, K. L.; Hor, T. S. A. *J. Chem. Soc., Dalton Trans.* **1994**, 3177–3182.

(31) Mäkie, P.; Persson, P.; Österlund, L. *J. Colloid Interface Sci.* **2013**, *392*, 349–358.

(32) Sexton, B. A.; Avery, N. R. *Surf. Sci.* **1983**, *129*, 21–36.

(33) Barber, M.; Connor, J. A.; Guest, M. F.; Hillier, I. H.; Schwarz, M.; Stacey, M. *J. Chem. Soc., Faraday Trans. 2* **1973**, *69*, 551–558.

(34) Nefedov, V. I.; Salyn, Y. V. *Inorg. Chim. Act.* **1978**, *28*, L135–L136.

(35) Packett, D. L.; Trogler, W. C. *J. Am. Chem. Soc.* **1986**, *108*, 5036–5038.

(36) Packett, D. L.; Trogler, W. C. *Inorg. Chem.* **1988**, *27*, 1768–1775.

(37) Baig, R. B. N.; Varma, R. S. *Chem. Commun.* **2012**, *48*, 6220–6222.

(38) Shimizu, K.; Kubo, T.; Satsuma, A.; Kamachi, T.; Yoshizawa, K. *ACS Catal.* **2012**, 2467–2474.

(39) Subramanian, T.; Pitchumani, K. *Catal. Commun.***2012**, *29*, 109–113.

(40) Ishizuka, A.; Nakazaki, Y.; Oshiki, T. *Chem. Lett.* **2009**, *38*, 360–361.

(41) Mitsudome, T.; Mikami, Y.; Mori, H.; Arita, S.; Mizugaki, T.; Jitsukawa, K.; Kaneda, K. *Chem. Comm.* **2009**, 3258.

(42) Liu, Y.-M.; He, L.; Wang, M.-M.; Cao, Y.; He, H.-Y.; Fan, K.-N. *ChemSusChem* **2012**, *5*, 1392–1396.

(43) Kim, A. Y.; Bae, H. S.; Park, S.; Park, S.; Park, K. H. *Catal Lett* **2011**, *141*, 685–690.

(44) Narayanan, R.; El-Sayed, M. A. *J. Phys. Chem. B* **2003**, *107*, 12416–12424.

(45) Bravo, J.; Bolaño, S.; Gonsalvi, L.; Peruzzini, M. *Coord. Chem. Rev.* **2010**, *254*, 555–607.

CHAPTER IV

(1) Ahmed, T. J.; Knapp, S. M. M.; Tyler, D. R. *Coord. Chem. Rev.* **2011**, *255*, 949–974.

(2) Green, M. M. Wittcoff, H.A. *Organic Chemistry Priciples and Industrial Practice*; Wiley-VCH: Weinheim, Germany, 2003.

(3) Bizzari, S. *Chemical Economics Handbook* **2010**, *SRI Consulting*.

(4) Ahmed, T. J.; Fox, B. R.; Knapp, S. M. M.; Yelle, R. B.; Juliette, J. J.; Tyler, D. R. *Inorg. Chem.* **2009**, *48*, 7828–7837.

(5) Knapp, S. M. M.; Sherbow, T. J.; Juliette, J. J.; Tyler, D. R. *Organometallics* **2012**, *31*, 2941–2944.

(6) Yan, N.; Xiao, C.; Kou, Y. *Coord. Chem. Rev.* **2010**, *254*, 1179–1218.

(7) Shimizu, K.; Kubo, T.; Satsuma, A.; Kamachi, T.; Yoshizawa, K. *ACS Catal.* **2012**, *2*, 2467–2474.

(8) Subramanian, T.; Pitchumani, K. *Catal. Commun.* **2012**, *29*, 109–113.

(9) Ishizuka, A.; Nakazaki, Y.; Oshiki, T. *Chem. Lett.* **2009**, *38*, 360–361.

(10) Kim, A. Y.; Bae, H. S.; Park, S.; Park, S.; Park, K. H. *Catal Lett* **2011**, *141*, 685–690.

(11) Hirano, T.; Uehara, K.; Kamata, K.; Mizuno, N. *J. Am. Chem. Soc.* **2012**, *134*, 6425–6433.

(12) Liu, Y.-M.; He, L.; Wang, M.-M.; Cao, Y.; He, H.-Y.; Fan, K.-N. *ChemSusChem* **2012**, *5*, 1392–1396.

(13) Mitsudome, T.; Mikami, Y.; Mori, H.; Arita, S.; Mizugaki, T.; Jitsukawa, K.; Kaneda, K. *Chem. Commun.* **2009**, 3258–3260.

(14) Baig, R. B. N.; Varma, R. S. *Chem. Commun.* **2012**, *48*, 6220–6222.

(15) Shimizu, K.; Imaiida, N.; Sawabe, K.; Satsuma, A. *Appl. Cat. A* **2012**, *421–422*, 114–120.

(16) Polshettiwar, V.; Varma, R. S. *Chem, Eur. J.* **2009**, *15*, 1582–1586.

(17) Debouttière, P.-J.; Coppel, Y.; Denicourt-Nowicki, A.; Roucoux, A.; Chaudret, B.; Philippot, K. *Eur. J. Inorg. Chem.* **2012**, *2012*, 1229–1236.

(18) Hendrich, C.; Bosbach, J.; Stietz, F.; Hubenthal, F.; Vartanyan, T.; Troger, F. *Appl. Phys. B* **2003**, *76*, 869–875.

(19) Lismont, M.; Dreesen, L. *Mat. Sci. Eng. C* **2012**, *32*, 1437–1442.

(20) Hajizadeh, S.; Farhadi, K.; Forough, M.; Sabzi, R. E. *Anal. Methods* **2011**, *3*, 2599–2603.

(21) Mulfinger, L.; Solomon, S. D.; Bahadory, M.; Jeyarajasingam, A. V.; Rutkowsky, S. A.; Boritz, C. *J. Chem. Educ.* **2007**, *84*, 322.

(22) Debouttière, P.-J.; Coppel, Y.; Denicourt-Nowicki, A.; Roucoux, A.; Chaudret, B.; Philippot, K. *Eur. J. Inorg. Chem.* **2012**, *2012*, 1229–1236.

(23) Debouttière, P.-J.; Martinez, V.; Philippot, K.; Chaudret, B. *Dalton Trans.* **2009**, 10172–10174.

(24) Madras, G.; McCoy, B. J. *J. Chem. Phys.* **2002**, *117*, 8042–8049.

(25) Marqusee, J. A.; Ross, J. *J. Chem. Phys.* **1983**, *79*, 373–378.

(26) Knapp, S. M. M.; Sherbow, T. J.; Yelle, R. B.; Zakharov, L. N.; Juliette, J. J.; Tyler, D. R. *Organometallics* **2013**.

(27) Hammett, L. P. *J. Am. Chem. Soc.* **1937**, *59*, 96–103.

(28) Hansch, C.; Leo, A.; Taft, R. W. *Chem. Rev.* **1991**, *91*, 165–195.

(29) Ghosh, S. K.; Kundu, S.; Pal, T. *Bull. Mater. Sci.* **2002**, *25*, 581–582.

(30) Knapp, S. M. M.; Sherbow, T. J.; Yelle, R. B.; Juliette, J. J.; Tyler, D. R. *Organometallics* **2013**, *32*, 3744–3752.

(31) Bayse, C. A.; Ming, J. L.; Miller, K. M.; McCollough, S. M.; Pike, R. D. *Inorganica Chimica Acta* **2011**, *375*, 47–52.

(32) Bryce, D. L.; Wasylishen, R. E. *Inorg. Chem.* **2002**, *41*, 4131–4138.

(33) Bowmaker, G. A.; Kennedy, B. J.; Reid, J. C. *Inorg. Chem.* **1998**, *37*, 3968–3974.

(34) Mohr, F.; Falvello, L. R.; Laguna, M. *Eur. J. Inorg. Chem.* **2006**, *2006*, 3152–3154.

CHAPTER V

(1) Green, M. M. Wittcoff, H.A. In *Organic Chemistry Principles and Industrial Practice*; Wiley-VCH: Weinheim, Germany, 2003; pp. 137–155.

(2) S. Bizzari. Chemical Economics Handbook, 2012.

(3) Ahmed, T. J.; Knapp, S. M. M.; Tyler, D. R. *Coord. Chem. Rev.* **2011**, *255*, 949–974.

(4) García-Álvarez, R.; Crochet, P.; Cadierno, V. *Green Chem.* **2013**, *15*, 46.

(5) Kukushkin, V. Y.; Pombeiro, A. J. L. *Inorg. Chim. Act.* **2005**, *358*, 1–21.

(6) Ahmed, T. J.; Fox, B. R.; Knapp, S. M. M.; Yelle, R. B.; Juliette, J. J.; Tyler, D. R. *Inorg. Chem.* **2009**, *48*, 7828–7837.

(7) Knapp, S. M. M.; Sherbow, T. J.; Juliette, J. J.; Tyler, D. R. *Organometallics* **2012**, *31*, 2941–2944.

(8) Polshettiwar, V.; Varma, R. S. *Green Chem.* **2010**, *12*, 743–754.

(9) Varma, R. S. *Pure Appl. Chem.* **2013**, *85*, 1703–1710.

(10) Yan, N.; Xiao, C.; Kou, Y. *Coord. Chem. Rev.* **2010**, *254*, 1179–1218.

(11) Ishizuka, A.; Nakazaki, Y.; Oshiki, T. *Chem. Lett.* **2009**, *38*, 360–361.

(12) Baig, R. B. N.; Varma, R. S. *Chem. Commun.* **2012**, *48*, 6220–6222.

(13) Kim, A. Y.; Bae, H. S.; Park, S.; Park, S.; Park, K. H. *Catal Lett* **2011**, *141*, 685–690.

(14) Mitsudome, T.; Mikami, Y.; Mori, H.; Arita, S.; Mizugaki, T.; Jitsukawa, K.; Kaneda, K. *Chem. Commun.* **2009**, 3258.

(15) Polshettiwar, V.; Varma, R. S. *Chem, Eur. J.* **2009**, *15*, 1582–1586.

(16) Shimizu, K.; Kubo, T.; Satsuma, A.; Kamachi, T.; Yoshizawa, K. *ACS Catal.* **2012**, 2467–2474.

(17) Subramanian, T.; Pitchumani, K. *Catal. Commun.* **2012**, *29*, 109–113.

(18) Shimizu, K.; Imaiida, N.; Sawabe, K.; Satsuma, A. *Appl. Catal. A* **2012**, *421–422*, 114–120.

(19) Liu, Y.-M.; He, L.; Wang, M.-M.; Cao, Y.; He, H.-Y.; Fan, K.-N. *ChemSusChem* **2012**, *5*, 1392–1396.

(20) Wang, Q.; O'Hare, D. *Chem. Rev.* **2012**, *112*, 4124–4155.

(21) Choudary, B. M.; Madhi, S.; Chowdari, N. S.; Kantam, M. L.; Sreedhar, B. *J. Am. Chem. Soc.* **2002**, *124*, 14127–14136.

(22) Tyagi, B.; Sharma, U.; Jasra, R. V. *Appl. Catal. A* **2011**, *408*, 171–177.

(23) Choudary, B. M.; Chowdari, N. S.; Jyothi, K.; Kantam, M. L. *J. Am. Chem. Soc.* **2002**, *124*, 5341–5349.

(24) Sturgeon, M.R.; O'Brien, M.H.; Ciesielski, P.N.; Katahira, R; Kruger, J.S.; Chmely, S.C.; Hamlin, J.; Lawrence, K.; Hunsinger, G. B.; Foust, T.D.; Baldwin, R.D.; Biddy, M.J.; Beckham, G.T. *Green Chemistry*.**2014 DOI:** 10.1039/C3GC42138D

(25) Qi, C.; Amphlett, J. C.; Peppley, B. A. *Catal Surv Asia* **2009**, *13*, 16–21.

(26) Debecker, D. P.; Gaigneaux, E. M.; Busca, G. *Chem. Eur. J.* **2009**, *15*, 3920–3935.

(27) Liu, Y.; Lotero, E.; Goodwin Jr., J. G.; Mo, X. *Appl. Catal. A: General* **2007**, *331*, 138–148.